

Boston University

OpenBU

<http://open.bu.edu>

Boston University Theses & Dissertations

Boston University Theses & Dissertations

2018

Paradigm and paradox in power networks

<https://hdl.handle.net/2144/30724>

"Downloaded from OpenBU. Boston University's institutional repository."

BOSTON UNIVERSITY
COLLEGE OF ENGINEERING

Dissertation

PARADIGM AND PARADOX IN POWER NETWORKS

by

SHUAI WANG

B.S., Xi'an Jiaotong University, 2010
M.S., Xi'an Jiaotong University, 2013

Submitted in partial fulfillment of the
requirements for the degree of
Doctor of Philosophy

2018

© 2018 by
SHUAI WANG
All rights reserved

Approved by

First Reader

John Baillieul, PhD
Distinguished Professor of Mechanical Engineering
Distinguished Professor of Systems Engineering
Distinguished Professor of Electrical and Computer Engineering

Second Reader

Michael C. Caramanis, PhD
Professor of Mechanical Engineering
Professor of Systems Engineering

Third Reader

Hua O. Wang, PhD
Associate Professor of Mechanical Engineering
Associate Professor of Systems Engineering

Fourth Reader

Pablo A. Ruiz, PhD
Research Associate Professor of Mechanical Engineering

Fifth Reader

Na Li, PhD
Assistant Professor of Electrical Engineering
Assistant Professor of Applied Mathematics
Harvard University

*All models are wrong,
but some are useful.*
- George Box

Acknowledgments

Words cannot even begin to express the deep gratitude that I feel towards my family, mentors, friends and colleagues for their unconditional support, encouragement and guidance over the past five years. This thesis could not have been completed without all of you.

When I started my PhD studies at BU, I knew very little about my advisor, Prof. John Baillieul. All that I knew about Prof. Baillieul was that I enjoyed talking to him and that he always promised us a free drink when we solved a challenging problem, which I am still waiting for to this day. Five years later, I now realize how extremely fortunate I am to have had the opportunity to get to work with him. Prof. Baillieul is one of the most sincere and caring individuals that I have ever met in my life. He guided, mentored, and provided me with a wealth of opportunities that ultimately changed the direction of my life forever. I can never repay Prof. Baillieul for all that he has done for me.

I would like to express my gratitude to Prof. Michael Caramanis for the guidance and collaboration. It was Prof. Caramanis that taught me much of what I know in power systems and markets. Discussing problems with him was such an enjoyable experience, and his guidance has consistently been extremely helpful.

My sincere gratitude also goes to Prof. Hua Wang, Prof. Pablo Ruiz, and Prof. Na Li for serving on my dissertation committee.

Sharing the graduate school experience with my lab mates and fellow colleagues has given me a lifetime of fantastic memories. I would like to thank Bowen Zhang, Kayhan Ozcimder, Zhaodan Kong, Xi Yu, Trevor Ashley and Brian Maxwell for their help in my adaptation to the new environment at BU. I would also like to thank Nan Hu, Yufan Luo, and Laura Corvese for making the lab so much fun.

My family has been my pillar of strength for my entire life, especially during my

graduate studies. To Mom and Dad, you have given me so much over the years that I do not even know where to begin. You have always been there for me, cared for me and loved me. I love you with all my heart.

PARADIGM AND PARADOX IN POWER NETWORKS

SHUAI WANG

Boston University, College of Engineering, 2018

Major Professor: John Baillieul, PhD

Distinguished Professor of Mechanical Engineering
Distinguished Professor of Systems Engineering
Distinguished Professor of Electrical and Computer
Engineering

ABSTRACT

Well known in the theory of network flows, Braess paradox states that adding path(s) to a congested road network may increase overall journey time. In transportation networks, the phenomenon results from selfish routing. In power systems, an analogous increase in congestion can arise as a consequence of Kirchhoff's laws, suggesting opportunities to optimize grid topology.

The thesis starts with the discussion of Braess-like congestion phenomena in linear circuits. We prove that adding electrical path(s) always increases congestion in networks powered by voltage sources, while the opposite in networks driven by current sources. Although such predictability is not present in networks controlled by a mixture of voltage and current sources, our results offer a clean decomposition that completely separates the effect of current sources and voltage sources on total loss. The culmination of this research is a set of four equivalent methods of computing I^2R loss in mixed-source networks.

We go on to explore network decomposition in combination with greedy sequential line switching heuristics to address the NP-hardness of power grid topology control.

By means of some low order examples, it is shown that within a reasonably large class of greedy heuristics, none can be found that perform better than the others across all grid topologies. Despite this cautionary tale, statistical evidence indicates that, among three most representative heuristics, the global greedy heuristic is most computationally intensive but has the best chance of reducing generation cost while enforcing connectivity.

The final part of the thesis presents a new approach to grid decomposition using *vertex cut sets*. We show that each vertex cut set and corresponding grid decomposition establishes a natural upper bound on the interactions between subgrids as nodal injections are regulated within each. Using such decomposition, it becomes possible to isolate congestion effects to a relatively small subgrid. A fast grid decomposition heuristic based on vertex cut sets and *locational marginal prices* is then proposed and studied through simulations on IEEE 118-bus system. On average, the computational cost is significantly reduced and the generation cost saving is similar to what is obtained with a global greedy algorithm.

Contents

1	Introduction	1
1.1	Motivation	1
1.2	Prior Work	3
1.3	Contribution and Organization of the Thesis	6
2	Kirchhoff-Braess Phenomena in DC Electric Networks	9
2.1	Problem Formulation	10
2.2	Congestion Sensitivity to Small Changes in Circuit	13
2.3	Power Flow Sensitivity to Small Changes in Network Parameters	17
2.4	Embedded Wheatstone bridge and Biconnected Component	22
2.5	The NP-hardness of Topology Control	35
3	Paradigm of Topology Control	39
3.1	The Case of Current-Controlled Networks	40
3.2	The Case of Voltage-Controlled Networks	48
3.3	The Case of Mixed-Source Networks	55
3.4	Four Equivalent Loss Computing Methods for Mixed-Source Circuit	74
3.5	Summary	77
4	Heuristics of Topology Control	78
4.1	Paradox in Topology Control Heuristics	79
4.2	Paradigm in Topology Control Heuristics	86
4.3	Grid Decomposition Heuristics Based on Vertex Cut Sets	91
4.3.1	Vertex Cut Sets & Pseudo Biconnected Components	93

4.3.2	Embedded Wheatstone Bridge & LODF	94
4.3.3	Shift Factors & LMPs	96
4.3.4	The Optimality of Vertex Cut Sets	98
4.3.5	Grid Decomposition Heuristic	108
4.3.6	Simulation Results	109
4.4	Summary	110
5	Conclusions	112
5.1	Contributions	112
5.2	Future Work	114
A	Proof of Remark 1	116
	References	118
	Curriculum Vitae	123

List of Tables

2.1	The equivalence between current driven circuits and DC power flow models of transmission grids.	35
4.1	Performance comparison 1.	90
4.2	Performance comparison 2.	110

List of Figures

2·1	The classic Braess paradox of congested network flows.	11
2·2	Distribution grids of the future will feature increased amounts of local generation involving power sources with widely varying capacities and increased operating uncertainties. (Figure from Arghandeh et al., 2015.)	12
2·3	A simple circuit with DC-voltage sources and resistive loads.	13
2·4	From Gomez-Esposito <i>et al.</i>	18
2·5	The Wheatstone network.	22
2·6	A linear electric network.	24
2·7	Kron reduction of an area consisting of nodes $\{5, 6, 7, 8, 9\}$ and black edges. The embedded wheatstone bridge for the blue edge pair is shown in green in the right network.	29
2·8	Two possible topology relationships between two links belonging to two different biconnected components.	30
2·9	The generalized Norton equivalent circuit for a three-port network.	31
2·10	The generalized Norton equivalent circuit for two links (i, j) that share two nodes.	32
2·11	The equivalent relationship between a current-controlled circuit and a DC power flow problem.	34
2·12	An instance of topology control problem.	37
3·1	An example of parallel attachment and serial attachment.	43

3·2	(a) A circuit graph G where each black link denotes a resistor and each red link denotes a current source. (b) G 's associated resistance graph \tilde{G} where the dotted links form a spanning tree, Type 1 resistors are marked as magenta links, Type 2 resistors are marked as blue links, and Type 3 resistors are marked as orange links.	46
3·3	A simple circuit with DC-voltage sources and resistive loads.	50
3·4	(a) A 5-bus network with line overload at <i>Line</i> L_{25} . (b) The equivalent mixed-source circuit of (a) with the voltage source (blue) denoting the effect of load regulating equipment at <i>Bus</i> 2 and <i>Bus</i> 5.	56
3·5	(a) A mixed-source network with two current sources and one voltage source. (b) A mixed-source network with one current source and one voltage sources.	57
3·6	(a) A voltage-controlled circuit with nodes $\{1, 2, 3\}$. (b) A current-controlled circuit with nodes $\{1, 2\}$. (c) A mixed-source circuit with nodes $\{1, 2, 3\}$	58
3·7	The equivalent resistance network for an arbitrary 4-terminal resistance network.	59
3·8	The equivalent circuit for a mixed-source network.	68
4·1	The example of non-commutativity problem.	80
4·2	The example of non-monotonicity.	81
4·3	The first example of non-consistency problem.	83
4·4	The second example of non-consistency problem.	85
4·5	Visualization of the paradoxical phenomenon: no extra return for increased computational complexity of heuristics in topology control.	85
4·6	Flow chart describing general algorithm structure of the Random Heuristic.	87

4.7	Flow chart describing general algorithm structure of the Standard Greedy Heuristic.	89
4.8	One example of the decomposition based on a vertex cut set formed by the three red nodes in the middle.	94
4.9	The 4-terminal equivalent circuit of the original network.	100
4.10	The network simplification process.	102
4.11	Flow chart describing general algorithm structure of grid decomposition based on vertex cut set.	109

List of Abbreviations

ACOPF	Alternating Current Optimal Power Flow
CHP	Combined Heat and Power
DCOPF	Direct Current Optimal Power Flow
DG	Distributed Generation
FTR	Financial Transmission Right
HVAC	Heating, Ventilation and Air Conditioning
ISO	Independent System operator Operator
KCL	Kirchhoff's Current Law
KVL	Kirchhoff's Voltage Law
LCL	Loss Cost of the Link
LMP	Locational Marginal Prices
LODF	Line Outage Distribution Factors
LP	Linear Programming
MAP	Maximum Attainable Savings
MIP	Mixed Integer Programming
OPF	Optimal Power Flow
PEV	Plug-in Electric Vehicles
PMU	Phasor Measurement Unit
PTDF	Power Transfer Distribution Factors
SF	Shift Factor

Chapter 1

Introduction

1.1 Motivation

As highly variable renewable energy sources provide an increasing fraction of the power consumed in the grid, it is becoming significantly more difficult to assess the stability margins and the security of grid operation (Basak et al., 2012). The problem is of special concern in grids where intercommunicating Phasor Management Units (PMUs) and other network measurement devices are not uniformly deployed (Chowdhury et al., 2009). There is also the prospect of broader active consumer participation in the form of both demand response and incorporation of consumer-owned energy storage and renewable energy units (Medina et al., 2010). In addition to the historical uncertainties associated with weather and network and equipment reliability, future grid operations are going to need to account for time-varying preferences and levels of participation by the energy-consuming public. Because of these factors, the power grid and the distribution subnetworks to which consumers are connected are becoming highly dynamic stochastic systems.

These considerations suggest there will be qualitative differences in the way the grid is operated in the future. In large electric grids, transmission is traditionally characterized as a static and redundant network in order to ensure mandatory reliability standards, although it is well known that these network redundancies can cause dispatch inefficiency and, furthermore, a network branch that is required to be built in order to meet reliability standards during specific operational periods may

not be required to be in service during other periods. Consequently, whereas electric utilities have historically solved the standard optimal power flow (OPF) problem for transmission networks by minimizing generation costs over a single period (usually five minutes to one hour) subject to predicted system loads, reserve requirements, and fixed system topology, it is acknowledged that system operators can, and do, change the topology of systems, for day ahead or real time planning, to relieve overloads or improve voltage profiles (Shao and Vittal, 2005) by taking some lines out of service.

Based on the DC OPF problem, transmission grid topology control is typically formulated as a mixed integer programming problem (MIP) with some binary variables denoting the choices of transmission line switches (Ruiz et al., 2012b). There are a few difficulties that must be overcome before transmission topology control can be effectively implemented, including understanding and avoidance of voltage problems, transient instability, reactive power problems (Hedman et al., 2009) and, most importantly, the ability to find a good solution within a time that is short enough to be of practical use. Although as one of the most intensively studied problems in optimization, there are no known polynomial-time algorithms for the MIP (Papadimitriou and Steiglitz, 1998). Most system operators do employ topology control today, but mainly on an ad-hoc basis using operators previous experience rather than in an automated or systematic way (Hedman et al., 2011b), making such control unscalable and some times impossible. New policies such as promulgated in the National Energy Policy Act and the Energy Independence and Security Act together with new technologies including PMUs, synchro-phasors, and solid-state transformers also call for the development of smarter grid topology optimization algorithms that can be solved much more quickly.

Recently, dynamic optimization of transmission topology has become popular. A set of fast line switching heuristics have been proposed, and the running time records

have been consistently set and then shattered (Fisher et al., 2008; Ruiz et al., 2011; Fuller et al., 2012; Ruiz et al., 2012a; Ruiz et al., 2017). In all of these studies, simulations show that significant savings are indeed possible from transmission switching. While there is a clear need for computationally efficient approaches to implement fast topology control, an even greater need is to provide a theoretical foundation in selecting and editing topology control heuristics to maximize savings. Meanwhile, both challenges and opportunities are associated with the growing penetration of small-scale renewables (mainly photo-voltaics and wind) together with demand side assets such as networked control of heating, ventilation and air conditioning (HVAC) systems, variable-speed fans, plug-in electric vehicles (PEVs), distributed energy storage and generation, combined heat and power (CHP) micro generators, volt/var control devices, grid-friendly appliances, and smart transformers. Grid-centric information systems must now be developed to manage the operation of such varied assets while allowing topology control to shift or alleviate congestions.

1.2 Prior Work

Siting and maintaining massive power infrastructure is not cheap (Vajjhala and Fischbeck, 2007) and therefore makes the optimal use of existing network a priority. Because of the fast time constants in changing the system state and the very low costs, corrective switching operations, including transmission line switching, bus-bar switching, and shunt element switching, etc, are often the first post-contingency corrective action to be considered and implemented (Glavitsch, 1993; Sahraei-Ardakani et al., 2016).

Through long-term accumulation of experience, system operators usually know which switching operation is most effective for a familiar overload or voltage problem, and many of these are incorporated in the written operational rules (Capitanescu

et al., 2011). On the other hand, however, considering the forbidding complexities within the dynamic OPF problem and the limited coverage of the ad-hoc procedures, finding the sequence of switching actions that achieves the best trade-off between optimality and connectivity in an automatic and systematic way is very far from being trivial.

The use of switching actions has been explored as a control method for a variety of problems in the context of OPF since the early 1980s (Koglin and Muller, 1980): line overload alleviation (Bacher and Glavitsch, 1986; Mazi et al., 1986; Bertram et al., 1990; Wrubel et al., 1995; Lobato et al., 2003; Granelli et al., 2006), voltage violation mitigation (Bakirtzis and Meliopoulos, 1987; Hsu et al., 1992; Rolim and Machado, 1999; Feng et al., 2000), system reliability enhancement (Rossier and Germond, 1983; Schnyder and Glavitsch, 1988; Schnyder and Glavitsch, 1990), line loss reduction (Bacher and Glavitsch, 1988; Fliscounakis et al., 2007; Fliscounakis et al., 2009), or a combination of these objectives (Mazi et al., 1986; Bijwe et al., 1993; Arya et al., 2000; Shao and Vittal, 2005; Hedman et al., 2009).

Due to the combinatorial nature of the problem and the nonlinearities inherent to networks, the approaches proposed in the literature focus on the reduction of the search space of possible switching actions (Hedman et al., 2011b). Koglin and Muller, 1980 consider only the lines electrically close to the contingencies as candidates to alleviate line overloads. Rossier and Germond, 1983 propose a Maximal Flow Minimal Cost algorithm for system security enhancement. Mazi et al., 1986 relate the flows in the switchable elements to the other lines based on the distribution factors generated by a non-iterative DC approximate model which are then used as criteria for automatic selection and ranking all possible switchings. Bacher and Glavitsch, 1988 simulate the switching by using compensated currents injection under a linear programming problem formulation. Each single optimal switching operation

is then obtained by the LP-like operation followed by a load-flow update. Lobato et al., 2003 model the switching actions as an iterative process that first identifies the best switching candidates for each overloaded branch and then formulates a MIP to select one line to be opened in each step. Shao and Vittal, 2005 rank the candidate switching actions according to a performance index and simulate of the top candidates in a branch and bound fashion. Granelli et al., 2006 design a genetic algorithm-based procedure for the topological optimization of the network against overloads and congestions.

The focus of past research has been mainly on line overload, voltage violations, etc. Though acknowledging certain benefits of harnessing the control of transmission, the industry does not use currently the flexibility of the transmission grid to co-optimize the generation along with the network topology. Such co-optimization has been recently attracting a great deal of attention and popularity in research communities. Fisher et al., 2008 and Hedman et al., 2008 show that on the standard 118-bus IEEE test case a savings of 25% in system dispatch cost can be achieved by using an iterative partitioning and parallel solution approach to solve the the MIP formulation of the DCOPF problem to near optimality. Although their approach is computationally expensive and thus is almost certain to be intractable, they report that the majority of cost savings occur as a result of removing relatively few lines. Fuller et al., 2012 reduce the computational effort without significantly increasing dispatch cost by proposing two heuristics with one solving a sequence of LPs and the other solving a sequence of simplified MIPs that have far fewer binary variables than the original MIP. Simulation results on a 662-bus system suggest both heuristics may be practical for real-size systems with respect to the computing time issue. Ruiz et al., 2011 and Ruiz et al., 2012 find topology improvements by iteratively solving the MIPs by means of a heuristic algorithm that uses engineering judgment to translate

the global marginal cost of congestion to a small set of lines associated with the lion's share of cost savings. Such an approach further reduces the computational complexity of the MIPs to the degree for practical use for day ahead planning, and is expected to be even possible for correcting problems that arise in real time. The works reported in Hedman et al., 2009, Hedman et al., 2010 and Ruiz et al., 2012 also demonstrate that topology control can be beneficial even while preserving an $N-1$ *reliable* network, i.e. the system is planned such that, with all transmission facilities in service, the system is in a secure state, and for any one credible contingency event, the system moves to a satisfactory state.

1.3 Contribution and Organization of the Thesis

This thesis is organized into five chapters.

Chapter 2 first reviews the Braess paradox in transportation networks, and an analogous phenomenon in DC linear electric circuits is then studied. Here it is shown that changing the circuit topology by adding a small link can lead to relatively large losses in the circuit as a whole. In particular, we define the concept of *loss cost of a link (LCL)* which is the ratio of the power losses of a circuit in steady-state after/before adding or removing a link (two-port circuit element). How the effects of adding or removing a link from a linear network propagate to all parts of the network is then explored. It is shown that changing a link will generally change the losses unless the network contains embedded balanced Wheatstone bridges making contact with the classical paper Cohen and Horowitz, 1991. The NP-hardness of the switching problem is proved at the end by using the *subset sum problem* for the reduction.

Chapter 3 starts with the review of needed background on the topology of DC electric circuits, and then extends the analysis of the loss cost of the link from current-controlled circuits to voltage-controlled circuits and finally mixed-source circuits (see

Def. 5) of arbitrary size. It is shown that the sign of the overall change in I^2R loss of a current-controlled circuit or voltage-controlled circuit due to one disconnected line is always certain, and the effect of removing an edge from a mixed-source circuit can be perfectly decomposed into two sub-effects in its voltage-controlled sub-circuit and current-controlled sub-circuit (see Def. 10), respectively. Meanwhile, it gives a simple method to calculate the change of total I^2R loss based on the reduced equivalent circuit. It is also shown that the total loss of a mixed-source circuit is exactly the sum of total loss of its voltage-controlled sub-circuit and current-controlled sub-circuit. Four different approaches to calculate the total I^2R loss of an arbitrary mixed-source circuit are explored at the end. All of them are shown to be mathematically equivalent, pointing out a way to convert a certain type of constrained linear programming formulation to an unconstrained non-linear programming problem.

Chapter 4 focuses on providing theoretical support for developing topology control heuristics. Power grid topology control problem is typically formulated as a mixed integer programming problem (MIP). Global optimization of such problems can be computationally intractable, and therefore, works in the power systems literature mainly focus on proposing heuristic approaches. Indeed, some MIPs may admit efficient heuristics in practice as long as their inputs meet certain criteria (Fincke and Pohst, 1985; Kellerer et al., 2004). Due to the presence of binary variables, however, no pseudo-polynomial time algorithm has been found for optimal line switching. Via some low order networks (3-bus microgrids), we show that, among a reasonably large class of “greedy” algorithms, none can offer consistently superior performance with respect to generation cost reduction across all grid topologies, indicating a strong form of NP-hardness for topology control. Simulations on IEEE 118-bus systems, nevertheless, show that on average an additional savings of 15% in system congestion cost can be achieved through increasing computational effort to find the locally

optimal switches. It is argued that, among all iterative methods, the locally optimal switches at each stage have a better chance of not only approximating a global optimal solution but also enforcing grid connectivity. A fast grid decomposition partition algorithm is then proposed in order to overcome the computational complexity of the greedy heuristic while at the same time preserving the overall switching quality. Simulation results further confirm that it is indeed possible to design algorithms that isolate congestion effects to a relatively small part of the network.

Chapter 5 summarizes the document and proposes future research directions.

Chapter 2

Kirchhoff-Braess Phenomena in DC Electric Networks

It has long been recognized that contingencies like the loss of a major power line can pose significant threats to the secure operation of the power grid. The focus of this Chapter is on the way that seemingly small changes can have large effects. Taking inspiration from concepts of congestion in traffic networks, we first study what we call *Kirchhoff-Braess phenomena* — a situation in which a network branch that is required to be built in order to meet reliability standards during specific operational periods may cause or worsen congestion during other periods. Examples of simple circuits and networks that display the kinds of sensitivity to small changes in operating parameters are then presented. We also define a power network analogue of *the price of anarchy* that we call the *Loss Cost of the Link* of an added asset. This is simply the ratio of losses after and before the asset (e.g. a line) was added. Based on some fundamental analysis of the simplest non series-parallel circuit, the Wheatstone bridge, the magnitudes of the impacts on the circuit due to a disconnected line are proved to be closely related to the parameters associated with the embedded Wheatstone bridges derived from the the network, and it is zero only if the corresponding embedded Wheatstone bridge is precisely balanced. The comprehensive analysis of the challenging problem is ended with the proof showing the NP-hardness of the switching problem.

2.1 Problem Formulation

We begin by recalling the well-known Braess paradox that is generally associated with congestion in transportation networks. The setup, in simple form, is shown in Fig. 2.1. There is a network (of roads) with an origin O and destination D . A certain number of travelers will make the journey, and in the network in Fig. 2.1(a) they have a choice of the route with segments \mathcal{AB} or segments \mathcal{CD} . Congestion may enter either route in terms of travel times that depend on the number of users traveling on each segment. If f denotes the number of voyagers on the segment, the travel times on segments \mathcal{A} and \mathcal{D} are the same and equal to $f + \beta$ for some constant β . The travel times on segments \mathcal{B} and \mathcal{C} are similarly equal to αf for some positive α . There are many different values of the parameters used in the literature, but the basic idea is that because the left-hand and right-hand routes in Fig. 2.1 have the same congestion cost, $(\alpha + 1)f + \beta$, introducing the cross link will break the cost symmetry and could cause the cost of travel to increase. Taking the particular values of Steinberg and Zangwill, 1983, $\alpha = 10$, $\beta = 50$, $\gamma(\cdot) \equiv 0$, and letting the total number of travelers be $f = 6$, we find that without the cross link, the best choice for minimizing travel time is for three of the travelers to choose the left-hand route and three to choose the right hand route. This is a Nash equilibrium. The travel time for each traveler is $(\alpha + 1)f + \beta = 11 \times 3 + 50 = 83$. When the no-cost cross link is present, however, travelers will observe a possibly shorter route given by following the segments \mathcal{C} -cross-link- \mathcal{B} . Indeed, if only three of the six travelers took this route, the travel cost could be as low as $2\alpha f = 60$. Unfortunately, all six travelers may choose the route, in which case, the cost becomes 120. Taking the cost to be travel-time, Braess paradox is that adding a delay-free travel link can actually increase congestion and the users' travel time.

Braess' paradox in this setting involves selfish social choices. There is a similar

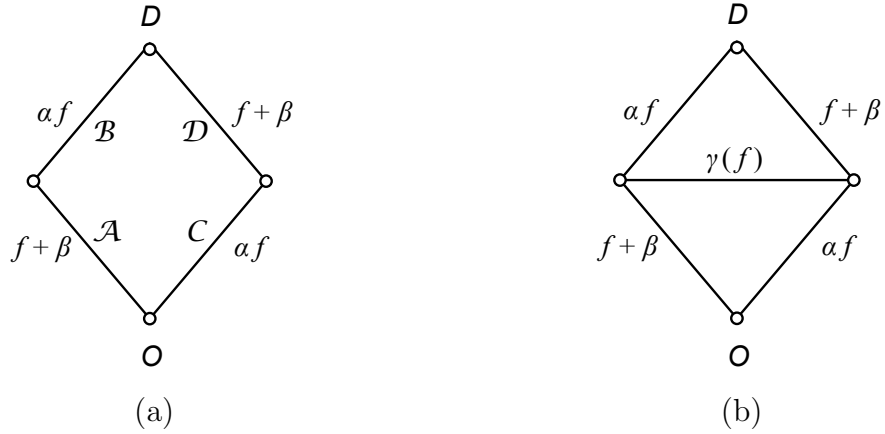


Figure 2-1: The classic Braess paradox of congested network flows.

apparent paradox in electric circuits, as noted Cohen and Horowitz, 1991, that is a consequence of the laws of electrophysics. In Fig. 2-3, the question immediately arises as to how the horizontal connection changes the characteristics of the circuit on the top and bottom links. Elementary invocation of Kirchhoff's current and voltage laws indicates that in the absence of the horizontal link, the currents i_1 and i_2 will be equal, but if the link is added with a moderate value of the resistance R_3 , one or both of i_1 and i_2 may be increased. This change is not surprising and is consistent with the observation in Cohen and Horowitz, 1991 that introducing the path changes the voltage drop across the circuit. It is also consistent with the observations in Blumsack et al., 2007 that adding this link may worsen congestion in similar models of power grid interconnections. The interesting question posed in Blumsack et al., 2007 is whether (and when) there is a useful tradeoff in grid design that balances the increased reliability of larger number of power lines against the congestion that may occur due to adding these lines to the network.

Such congestions due to network redundancy are quite common in the transmission networks especially when the grids are highly meshed. While distribution networks have historically had radial topologies, with distribution lines leading from

a single trunk or power source to various commercial and residential loads, this standard topology is likely to change with the ever increasing penetration of distributed generation in the form of wind, solar, plug-in electric vehicles, and many other forms of alternative energy. Microgrids as depicted in Fig. 2·2 will become prevalent, and these will increasingly resemble miniaturized transmission networks in which sources and loads will be connected through a multiplicity of lines that can be opened and closed as needed to maintain the needed balance between capacity and demand. It is against this backdrop that we examine the question of how the densely meshed network together with new electricity market models aimed at managing demand response will challenge the operating security of grids.

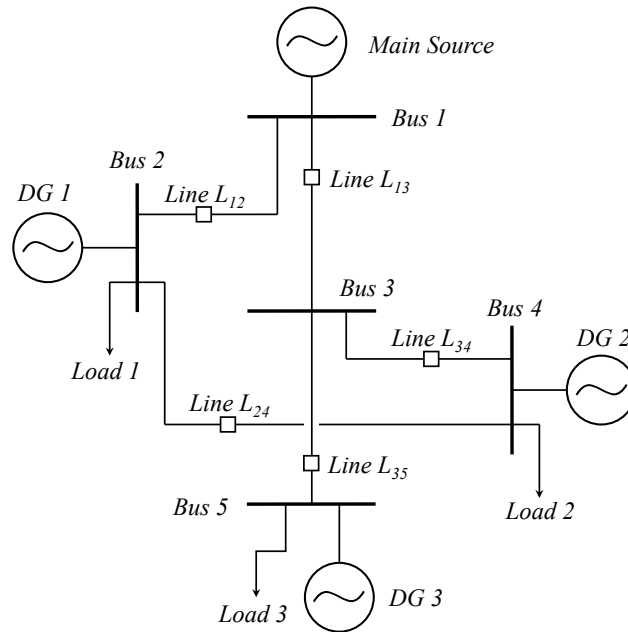


Figure 2·2: Distribution grids of the future will feature increased amounts of local generation involving power sources with widely varying capacities and increased operating uncertainties. (Figure from Arghandeh et al., 2015.)

2.2 Congestion Sensitivity to Small Changes in Circuit

Recent work has demonstrated how various communication protocols can be effectively employed in networks of smart grids to improve energy efficiency, decrease demand volatility, and ensure customer satisfaction (Zhang et al., 2014; Zhang and Baillieul, 2016). Although this work has examined packet switched energy delivery in terms of temporal uncertainty in the operation of microgrids, the effects of spatial and network topology variability are not well understood. While the precise magnitude of costs associated with mitigating the uncertainties of renewable generation sources is not known, some estimates suggest that higher reserve margins will be required. For instance, the historical averages of reserve requirements in the power grid point to 7% to 8% as generally sufficient to handle contingencies. There are now predictions that if renewable penetration gets to the 33% level (still a long way off) these requirements may go as high as 15% (Vartabedian, 2012).

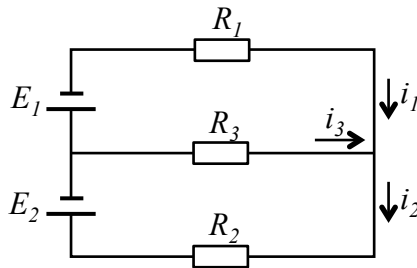


Figure 2-3: A simple circuit with DC-voltage sources and resistive loads.

The implications of renewables for transmission networks remains a work in progress. With the increasing likelihood that distribution networks will incorporate small-scale distributed generation as depicted in Fig. 2-2, we first turn to the question of how these intermittent sources will affect network congestion on a small scale. Our working definition of congestion will be in terms of Fig. 2-3, where we say that there is

congestion if there is a significant difference between currents i_1 and i_2 and more importantly, between the energy losses due to heat $i_1^2 R_1$ and $i_2^2 R_2$. We note that if there is no horizontal link (i.e. if $i_3 = 0$ or equivalently, if $R_3 \sim \infty$), then $i_1 = i_2$, and if $R_1 = R_2$, the heat losses at each resistor are equal as well. These conclusions remain true irrespective of the magnitudes of the voltage sources. If $R_1 = R_2$ and the voltage sources happen to be equal in magnitude, then $i_3 = 0$ no matter what value is assigned to R_3 . If there is any imbalance in the voltages E_1 and E_2 , or if one of them is zero (think of a wind turbine or solar array being out of service due to weather conditions), then a small value of R_3 on the cross link of Fig. 2-3 can produce a very large difference in the currents i_1 and i_2 . We summarize this as follows. Suppose $R_1 = R_2 = R$ and that $E_1 = 0$. Then if the cross link is not connected in Fig. 2-3 we have that $i_1 = i_2 = E_2/2R$ while if the cross *is* connected and R_3 is positive but small, we have $0 \sim i_1 \ll i_2 \sim E_2/R$. Moreover, the total heat loss across the entire circuit is approximately twice the loss if the cross link is disconnected.

Definition 1 *The Loss Cost of the Link (LCL) is defined as the ratio between the total network losses before and after the addition of a new link or other capacity enhancement. Denoting the system losses before and after the capacity enhancement as $Loss'$ and $Loss$, respectively. The LCL is defined as*

$$LCL = \frac{Loss}{Loss'}. \quad (2.1)$$

The LCL concept is our version of the *price of anarchy* that is discussed in routing congestion problems in transportation networks (Steinberg and Zangwill, 1983). The previous example shows that the LCL for the balanced load network with $R_1 = R_2$ in Fig. 2-3 is close to 2. A more general scenario is to consider that two voltage sources are connected in the opposite direction at the same time, namely both E_1 and E_2 are non-zero. In typical distribution networks, the level of voltage is the same, say

110V at the user level. Therefore a much more complex electric network with the same level of voltage sources can be equivalently transformed into the network of two voltage sources connected in the opposite direction with a series connected to equivalent resistors. In the following proposition, we show that the LCL will increase as the imbalance increases between the two resistors of the equivalent circuit.

Proposition 1 *Suppose that $E_1 = E_2 = E$, the LCL of Def. 1 will increase monotonically as $|R_1 - R_2|$ increases for a given R_1 or R_2 .*

Proof: According to Kirchhoff's circuit Law, the current i_j flows through the resistors are

$$\begin{aligned} i_1 &= \frac{E(R_2 + 2R_3)}{R_1R_2 + R_2R_3 + R_3R_1}, \\ i_2 &= \frac{E(R_1 + 2R_3)}{R_1R_2 + R_2R_3 + R_3R_1}, \\ i_3 &= \frac{E(R_1 - R_2)}{R_1R_2 + R_2R_3 + R_3R_1}. \end{aligned}$$

The total system loss is

$$Loss = i_1^2 R_1 + i_2^2 R_2 + i_3^2 R_3. \quad (2.2)$$

Since the total system loss before the connection of R_3 is

$$Loss' = \frac{(2E)^2}{R_1 + R_2}, \quad (2.3)$$

we will have the LCL as follows

$$\frac{Loss}{Loss'} = \frac{(R_1 - R_2)^2}{4(R_1R_2 + R_1R_3 + R_2R_3)} + 1 \geq 1, \quad (2.4)$$

where equality occurs if and only if $R_1 = R_2$ for balanced resistor equivalent systems. For an unbalanced resistor network (i.e. $R_1 \neq R_2$), we rewrite the expression for LCL in (2.4) by introducing the positive variable $h = |R_1 - R_2|$. A straightforward argument using elementary calculus and counting cases shows that for any $R_1, R_2, R_3 > 0$,

$R_1 \neq R_2$, LCL is an increasing function of h . \square

In decision theory, it is frequently desirable to base decisions on criteria that are known (or can be proven) to be monotonic in the decision variables. The previous discussion shows that if there is a lack of balance in the voltage source distribution that large current imbalances (congestion) can occur. Here we note that if there are imbalances in the resistances in our model network, then there will be a non-monotonic dependence of the losses $i_1^2 R_1$ and $i_2^2 R_2$ on the magnitude of the resistance R_3 .

Proposition 2 *Referring to the circuit of Fig. 2-3, suppose $R_1 < R_2$. If $E_1 = E_2$, then there is a non-monotonic dependence of the losses $i_1^2 R_1$ and $i_2^2 R_2$ on the cross-link resistance R_3 . Specifically, there is a critical value R_3^{cr} such that for $R_3 < R_3^{cr}$, $i_1^2 R_1 < i_2^2 R_2$, while for $R_3 > R_3^{cr}$, $i_1^2 R_1 > i_2^2 R_2$.*

Proof: We compare

$$i_1^2 R_1 = (E_2 R_3 + E_1 (R_2 + R_3))^2 R_1 / D_e \quad \text{with}$$

$$i_2^2 R_2 = (E_1 R_3 + E_2 (R_1 + R_3))^2 R_2 / D_e$$

where $D_e = (R_1 R_2 + R_1 R_3 + R_2 R_3)^2$. The loss $i_1^2 R_1$ will be larger than $i_2^2 R_2$ precisely when the numerators of these expressions have the same magnitude relationships. Recalling $E_1 = E_2 =$ (say) E , we have

$$i_1^2 R_1 \sim R_1 E^2 (R_2^2 + 4R_2 R_3 + 4R_3^2) \quad (2.5)$$

and

$$i_2^2 R_2 \sim R_2 E^2 (R_1^2 + 4R_1 R_3 + 4R_3^2) \quad (2.6)$$

Obviously, for small $R_3 > 0$, the expression (2.5) is greater than the expression (2.6), but as R_3 becomes larger, the terms that are quadratic in R_3 dominate—making the expression (2.6) the larger. \square

2.3 Power Flow Sensitivity to Small Changes in Network Parameters

The kinds of sensitivity illustrated in the resistive load circuits in the preceding section may be found as well in optimal power flow. We revisit Example 6.16, pp. 252-254 in (Gómez-Expósito et al., 2016).

Example 1 Consider the three-node network of Fig. 2.4. We examine a DC power flow model of the three bus network in which bus 1 and bus 2 are generators, while bus 3 is a load. The production costs of operating the generators are $C_j(P_j)$ for $j = 1, 2$, where P_j is the nodal power injection at the j -th bus. These costs of generation are convex functions, reflecting the fact that as the power increases, the incremental cost rises superlinearly due to wear and tear on the machinery, decreased efficiency margins. The “elastic price” load at bus 3 is $P_D = P_C + P_E$, where P_C is the inelastic component of the load and P_E is the “price elastic” component of the load. The line inductive reactances are x_{12}, x_{13}, x_{23} . The power flow P_{ij} on line ij is given by

$$\frac{\theta_i - \theta_j}{x_{ij}}, \quad (2.7)$$

where θ_j is the power phase angle at the j -bus. The nodal power injections are related to the power phase angles by the susceptance matrix:

$$\begin{pmatrix} P_1 \\ P_2 \\ P_3 \end{pmatrix} = B \begin{pmatrix} \theta_1 \\ \theta_2 \\ \theta_3 \end{pmatrix},$$

where

$$B = \begin{pmatrix} -b_{12} - b_{13} & b_{12} & b_{13} \\ b_{12} & -b_{12} - b_{23} & b_{23} \\ b_{13} & b_{23} & -b_{13} - b_{23} \end{pmatrix}.$$

and where the line susceptances b_{ij} are the negative reciprocals of the line reactances, i.e. $-\frac{1}{x_{ij}}$. The nodal power injections always sum to zero, as do the columns and rows of B , and since the power flow equations are invariant under a common phase shift of the θ_j 's it is convenient to choose a reference bus (say bus 1) at which we set the phase angle to be 0.

The OPF problem is to determine the nodal power injections P_1 and P_2 at the generator buses and the line flows P_{ij} that optimize an objective function that accounts

for generation costs $C_1(P_1)$ and $C_2(P_2)$ along with a consumer welfare cost that in the simplest formulation is evaluated only in terms of the price elastic load at bus 3, $C_W(P_E)$. The objective function to be minimized is written as $C_1(P_1) + C_2(P_2) - C_W(P_E)$. Minimization is subject to constraints that the power flow solution does not exceed the rated capacities of the lines or buses. Thus, feasible solutions must satisfy

$$0 \leq P_j \leq P_j^{max} \quad \text{and} \quad 0 \leq P_{ij} \leq P_{ij}^{max}. \quad (2.8)$$

In a power network, congestion is said to occur if the scheduled or desired power flow exceeds the rated capacity of either one or more of the lines or one or more of the generator buses.

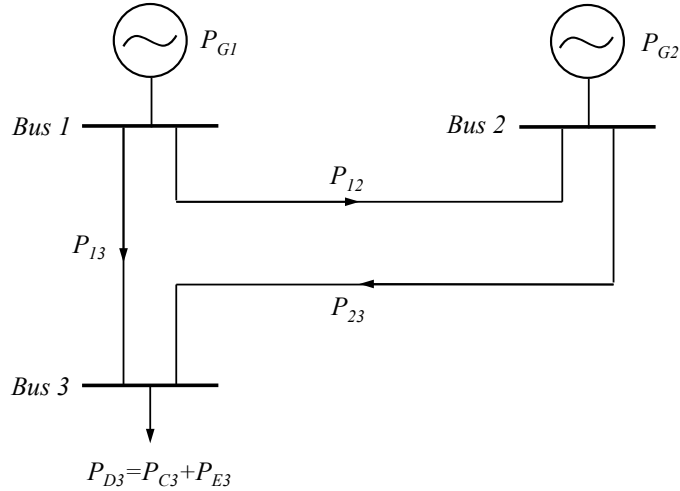


Figure 2·4: From Gomez-Esposito *et al.*.

Proposition 3 For the three-bus network depicted in Fig. 2·4, if the power flow solution (the configuration of phases) that minimizes the objective function

$$C_1(P_1) + C_2(P_2) - C_W(P_E) \quad (2.9)$$

does not result in congestion—i.e. if none of the constraints (2.8) holds with equality—then the solution is independent of the line susceptances.

Proof: The power injections are related to the power phase angles by

$$\begin{pmatrix} P_1 \\ P_2 \end{pmatrix} = B_r \begin{pmatrix} \theta_2 \\ \theta_3 \end{pmatrix}, \quad (2.10)$$

where

$$B_r = \begin{pmatrix} b_{12} & b_{13} \\ -b_{12} - b_{23} & b_{23} \end{pmatrix}$$

is the reduced susceptance matrix, and where we have assumed without loss of generality that the power phase angle at bus 1 is zero. If no two of the susceptances b_{ij} are zero, then B_r is nonsingular. Using the invertible relationship (2.10), we may rewrite the objective function as

$$f(\theta_2, \theta_3) = \hat{C}_1(\theta_2, \theta_3) + \hat{C}_2(\theta_2, \theta_3) - \hat{C}_W(\theta_2, \theta_3).$$

Solving the critical point equations $\partial f / \partial \theta_j = 0$ for $j = 2, 3$ leads to a minimizing solution, and this determines the optimal (P_1, P_2) via (2.10). This solution must be the same as what would have been obtained by minimizing (2.9) directly. \square

Remark 1 *It holds much more generally that for a connected power grid, the optimal power injections from generators is independent of the line conductances provided there is no congestion. The proof is a direct extension of the above and is provided in Appendix A.*

While optimal power flow solutions must always satisfy the network capacity constraints, the value of the proposition is in justifying a simple approach to finding potential sources of network congestion. We explore this further in terms of the example at hand. Adopting the cost functions of Gomez-Exposito et al., 2016, $C_j(P_j) = \beta_j P_j^2$ and $C_W(P_E) = \alpha P_E$, and recalling that $P_E = P_1 + P_2 - P_C$, the optimal power injections are easily seen to satisfy

$$P_j = \frac{\alpha}{2\beta_j}, \quad j = 1, 2, \quad \text{and} \quad P_E = \frac{1}{2} \left(\frac{\alpha}{\beta_1} + \frac{\alpha}{\beta_2} - 2P_C \right). \quad (2.11)$$

Clearly, the cost coefficients α, β_1, β_2 must be such that the power injections are within the ranges (2.8)—specifically the marginal value of consumer preference for load price elasticity must be in balance with the marginal costs of generation. To evaluate the line loading produced by the power injections (2.11), we solve (2.10) and use (2.7). This yields

$$\begin{aligned} P_{12} &= \frac{\alpha}{2\beta_1} \frac{b_{12}b_{23}}{D} - \frac{\alpha}{2\beta_2} \frac{b_{12}b_{13}}{D} \\ P_{13} &= \frac{\alpha}{2\beta_1} \frac{(b_{12}+b_{23})b_{13}}{D} + \frac{\alpha}{2\beta_2} \frac{b_{12}b_{13}}{D} \\ P_{23} &= \frac{\alpha}{2\beta_1} \frac{b_{12}b_{23}}{D} + \frac{\alpha}{2\beta_2} \frac{(b_{12}+b_{13})b_{23}}{D}, \end{aligned} \tag{2.12}$$

where

$$D = b_{12}b_{13} + b_{23}b_{13} + b_{12}b_{23}.$$

The power flows depend on the susceptances in essentially the same way the currents in Gomez-Exposito et al., 2016 depend on the circuit resistances.

It is expected that power grids will exhibit the same kinds of sensitivity to changes in network topology and operating parameters that were noted in Ch. 2.2 and Ch. 2.3. Indeed this turns out to be the case. For the generation cost values considered in Example 6.16 in Gomez-Exposito et al., 2016 ($\beta_1 = 1, \beta_2 = 1.675$), the explicit form of the uncongested optimum power injection at generator nodes 1 and 2 favors power produced by the cheaper generator (generator 1), although it is never the case that the DC load flow results in zero power being injected at bus 2. The line loading between the less costly generator and the load (P_{13}) turns out to be a monotonically increasing function of the susceptance b_{13} . It is interesting to note that if b_{13} is small enough in relation to b_{23} , the line loading will have $P_{23} > P_{13}$.

Write the phase and line-loading relationship in matrix form: $P_{line} = H \cdot (\theta_2, \theta_3)^T$,

where $P_{line} = (P_{12}, P_{13}, P_{23})^T$ and H is the matrix representation specified by (2.7):

$$H = \begin{pmatrix} b_{12} & 0 \\ 0 & b_{13} \\ -b_{23} & b_{23} \end{pmatrix}.$$

We can then express the line loadings directly in terms of the power injections by writing

$$\begin{pmatrix} P_{12} \\ P_{13} \\ P_{23} \end{pmatrix} = H B_r^{-1} \begin{pmatrix} P_1 \\ P_2 \end{pmatrix}.$$

For small values of $|b_{13}|$, this relationship is

$$\begin{pmatrix} P_{12} \\ P_{13} \\ P_{23} \end{pmatrix} = \begin{pmatrix} 1 + \epsilon & \epsilon \\ \epsilon & \epsilon \\ 1 + \epsilon & 1 + \epsilon \end{pmatrix} \begin{pmatrix} P_1 \\ P_2 \end{pmatrix}.$$

where $\epsilon = O(b_{13})$. With the power injected by generator G_1 being shifted from line (1,3) to lines (1,2) and (2,3), it is reasonable to expect that congestion on these lines will be sensitive to changes in P_1 and generation cost parameter β_1 . Indeed a straightforward calculation shows that there is extreme sensitivity to the cost parameter with

$$P_{23} = \frac{C}{\beta_1} + f(|b_{13}|),$$

where C is a positive constant, and f is a smooth function of $|b_{13}|$.

The foregoing has not taken operating limits (2.8) into account. Of course, once an uncongested optimum power flow lies outside the operating range of any component, the operating limit of that component becomes a binding constraint in terms of which the optimal power flow problem must be resolved. (See Gomez-Exposito et al., 2016.) Rather than pursuing constrained optimal power flow at this point, we extend the discussion in Ch. 2.2 and explore how common Kirchhoff-Braess phenomena is in electric circuits.

2.4 Embedded Wheatstone bridge and Biconnected Component

The above sections have studied the Kirchhoff-Braess phenomena in relatively small circuits and grids. Rather than pursuing a set of more detailed conclusions for the analysis of system losses, we now briefly explore the impact sphere of a line in the network, i.e. the losses or power flows of which lines will be changed after switching on/off a given line.

In consideration of the technical implications offer by Duffin, 1965, Calvert and-Keady, 1993, Korilis et al., 1999 and Bean et al., 1997 that Braesss Paradox may occur in any network that is not purely series-parallel, the discussion starts with the analysis of the well-known Wheatstone bridge, the simplest non-series-parallel circuit topology. We first define a set of fundamental concepts related to circuit topology.

Definition 2 *An edge in a circuit graph represents a single element such as a voltage source, a current source or a resistor, a node denotes the position of connection where two or more circuit elements (edges) meet and is exactly where the newly introduced external circuit can be connected, and a cycle is any closed path. Note that vertex/node/bus and line/link/edge are used interchangeably in this thesis.*

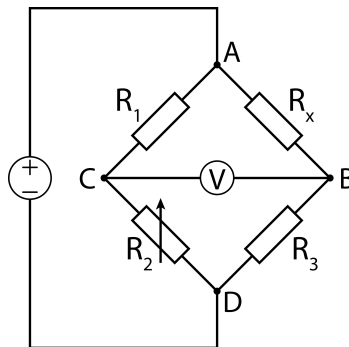


Figure 2.5: The Wheatstone network.

The Wheatstone network describes a graph consisting of four nodes, with four corresponding edges on the boundary creating a diamond shape and a fifth edge

connects two of the nodes across the interior of the network as shown in Fig. 2.5. The network is named for Charles Wheatstone since he was the first to publish the topology in 1843.

The original motivation for the Wheatstone network was the precise measurement of resistances, as shown in Figure 2.5. In the network, resistances R_1 , R_2 , and R_3 are of fixed and known value, and R_x is adjustable. The problem is to measure R_x . The voltage V across the bridge is equal to:

$$V = \left(\frac{R_2}{R_1 + R_2} - \frac{R_3}{R_3 + R_x} \right) V_{in} \quad (2.13)$$

where V_{in} is the voltage source on the left side of the circuit. The voltage drop across the bridge will be zero when $R_2/R_1 = R_3/R_x$. If this condition is satisfied, then the Wheatstone network is said to be *balanced*. Otherwise, there will be a voltage drop across the bridge and the network is said to be *imbalanced*.

Clearly, the change of the voltage source connecting node A and D has no impact on the bridge connecting node B and C if the Wheatstone network in Fig. 2.5 is balanced. The circuit in Fig. 2.6 keeps the core structure of the Wheatstone network and expands the network by adding a few more resistors and using a set of current sources to power the circuit. Similarly, we can show that the change of the edges connecting node 3 and 4 has no impact on the bridges connecting node 1 and 2 in Fig. 2.6 as long as the Wheatstone bridge is balanced.

Lemma 1 *For a linear electric network with structure shown in Fig. 2.6, any change in the dotted green box will have no influence on the dotted red box in terms of the power losses and vice versa if the embedded Wheatstone bridge formed by R_a through R_d is balanced, i.e. if $R_a R_d = R_b R_c$.*

Proof. It is easy to prove that any red box circuit or green box circuit that is comprised purely of resistances, voltage sources and/or current sources can be reduced to Norton's equivalent circuits (R_i in parallel connection with I_i , and R_j in parallel

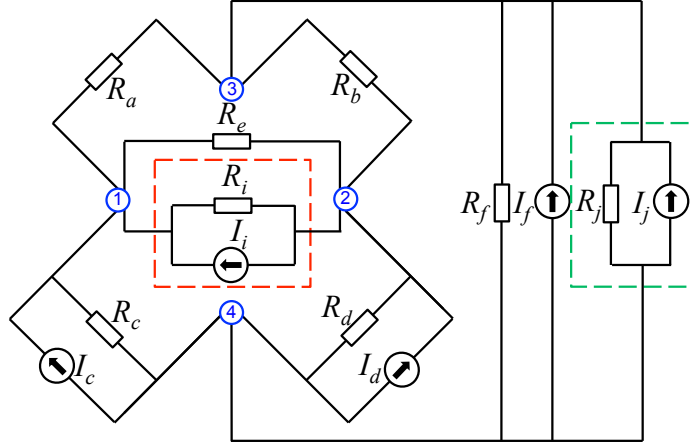


Figure 2-6: A linear electric network.

connection with I_j in Fig. 2-6, respectively). Then the circuit is fully determined by the following equations:

$$\left\{ \begin{array}{l} i_a R_a - i_b R_b - i_e R_e = 0 \\ i_c R_c - i_d R_d - i_e R_e = 0 \\ i_b R_b - i_d R_d + i_f R_f = 0 \\ i_e R_e = i_i R_i \\ i_f R_f = i_j R_j \\ i_a + i_c + I_c + i_e + i_i + I_i = 0 \\ i_b + i_d + I_d - i_e - i_i - I_i = 0 \\ i_a + i_b - i_f - I_f - i_j - I_j = 0 \\ i_c + I_c + i_d + I_d + i_f + I_f + i_j + I_j = 0 \end{array} \right. \quad (2.14)$$

where $i_a, i_b, i_c, i_d, i_e, i_f, i_i, i_j$ denote the currents flowing on $R_a, R_b, R_c, R_d, R_e, R_f, R_i, R_j$, respectively. The convention defining the positive direction of currents is from nodes with higher indices to nodes with lower indices.

We first prove that any change in the green box will have no influence on the red box. Supposing that some changes happened in the green box, and therefore its Norton's equivalent circuit was changed from $\{R_j, I_j\}$ to $\{R'_j, I'_j\}$. We define the voltage differences between node 1 and node 2 before and after the change as $V_{1,2}$ and

$V'_{1,2}$, respectively. Then by resolving the Equ. 2.14, we have

$$\begin{aligned}\Delta_{V_{1,2}} &= V_{1,2} - V'_{1,2} \\ &= \frac{R_e R_i}{R_e + R_i} [|A|^{-1} |A'|^{-1} \left(\frac{R_f R_j}{R_f + R_j} - \frac{R_f R'_j}{R_f + R'_j} \right) V_{3,4} \\ &\quad - |A'|^{-1} (I_j - I'_j) \frac{R_f R'_j}{R_f + R'_j}] (R_a R_d - R_b R_c)\end{aligned}\quad (2.15)$$

where $V_{3,4}$ is the voltage difference between node 3 and node 4 before the change, and

$$A = \begin{bmatrix} \sum_{i=a}^d R_i & R_c + R_d & R_b + R_d \\ R_c + R_d & R_c + R_d + \frac{R_e R_i}{R_e + R_i} & R_d \\ R_b + R_d & R_d & R_b + R_d + \frac{R_f R_j}{R_f + R_j} \end{bmatrix}\quad (2.16)$$

and A' is a 3×3 matrix that almost duplicates A except that

$$A'(3,3) = R_b + R_d + \frac{R_f R'_j}{R_f + R'_j}.\quad (2.17)$$

where $A'(3,3)$ is the last entry of A' . It is easy to show that $\Delta_{V_{1,2}}$ is zero if $R_a R_d = R_b R_c$.

With the same idea, we can prove that any change in the red box will have no influence on the green box if $R_a R_d = R_b R_c$. \square

In spite of the simple formation, an apparent Wheatstone bridge may not exist for each pair of edges in a graph. For those pairs of edges that are connected by multiple edges and nodes, however, the *embedded Wheatstone bridge* between them can always be created by applying node reduction to the graph to get the simple canonical form of the Wheatstone bridge as shown in Fig. 2-6.

Proposition 4 (Generalized Norton Theorem) *Any n -terminal linear circuit network is electrically equivalent to a set of circuits which consist of $n(n-1)/2$ resistances and $(n-1)$ current sources. The resistances' graph is a complete graph, and the current sources are connected to each other so that they make a tree.*

Proof. It is well known that any two-terminal network has simple equivalent circuit

given by the Thevenin's theorem and Norton's theorem. The equivalent circuits given by both theorems consist of two elements, a resistor and a voltage/current source. Because neither elements can be further reduced to simulate the network completely, both theorems are regarded as to give the simplest equivalent circuits to any two-terminal network. Since the Thevenin's theorem gives an equivalent circuit with three nodes while the Norton's theorem gives one with two nodes, however, Norton's circuit is regarded as simpler than Thevenin's one as to the number of nodes. Thus the Norton-like equivalent circuit is preferred in this thesis and we first prove the existence of the purely current-driven equivalent circuit for any n -terminal circuit in this proposition. The purely voltage-driven (Thevenin-like) equivalent circuit for any n -terminal circuit is given in Proposition 5.

In order to get the simplest equivalent circuit for any n -terminal network, we should reduce the nodes and branches as many as possible. Each step of the reduction can be performed with either one of the following procedures.

- Merging series connection, which decreases one node and one branch.
- Merging parallel connection, which decreases one branch.
- Applying generalized $Y-\Delta$ (star-mesh) transformation, which decreases node at the expense of increasing some branches whenever the original branches are more than 3.
- Applying generalized $\Delta-Y$ (mesh-star) transformation, which decreases branches at the expense of increasing some nodes whenever the original branches are more than 3.

Let us treat each resistor as a single Norton circuit with zero current source and treat each current source as a single Norton circuit with infinite resistor, and apply the above procedures as far as there remains node or Norton circuit parallel to another

branch within the network. Then we will finally get a complete graph with exactly one Norton circuit connecting each pair of terminals and no inner nodes.

Even after we have obtained the complete graph, there remains another possibility of reduction. Some current sources may be eliminated. If any current sources make loop, at least one can be eliminated. After completely trimming the loops, we will reach the final circuit that has no loop of the current sources. In the graph theory, the set of branches with no loop is said to make a tree. \square

The Thevenin-like theorem for any n -terminal circuit is given as follows whose proof is a direct extension of Proposition 4 and thus is omitted here.

Proposition 5 (Generalized Thevenin Theorem) *Any n -terminal linear circuit network is electrically equivalent to a set of circuits which consist of $n(n-1)/2$ resistances and $(n-1)$ voltage sources. The resistances' graph after replacing all voltage sources with short circuits is a complete graph, and those branches with one voltage source in serial connection with one resistor are connected to each other so that they make a tree.*

By Proposition 4, it is easy to see that the six resistors $\{R_a, R_b, R_c, R_d, R_e, R_f\}$ and three current sources $\{I_c, I_d, I_f\}$ in Fig. 2-6 form the 4-terminal current-driven equivalent circuit. Moreover, Lemma 1 reveals a useful result: whether the embedded Wheatstone bridge is balanced or not has nothing to do with the value of the current sources, suggesting the possibility for further simplification. Thus we introduce the following definition of *resistance network*.

Definition 3 *Given an arbitrary DC circuit network consisting of current sources, voltage sources and resistors, its resistance network is formed by:*

- (1) *replacing the original position of every current source with its internal resistance: an open circuit;*
- (2) *replacing the original position of every voltage source with its internal admittance: an short circuit;*
- (3) *keeping every resistor unchanged.*

Clearly the number of links on the resistance network is exactly the number of resistors on the original DC circuit. A simple derivation of Proposition 4 tells us that any n -terminal resistance network is electrically equivalent to a K_n complete graph which consists of $n(n-1)/2$ resistances. Such reduction exactly echoes the result of the well known *Kron Reduction* (Dobson, 2012).

Consider a connected resistance network with N nodes. By Kirchhoff's and Ohm's laws, the equations $I = GV$ are obtained, where $I \in \mathbb{R}^{N \times 1}$ are the currents injected at the nodes, $V \in \mathbb{R}^{N \times 1}$ are the nodal voltages, and $G \in \mathbb{R}^{N \times N}$ is the conductance matrix. Suppose we would like to obtain a lower dimensional equivalent network including only the terminal nodes $\alpha \subseteq \{1, \dots, N\}$, $|\alpha| \geq 2$. Let $\beta = \{1, \dots, N\} \setminus \alpha$ denotes the set of interior nodes to be eliminated, then we have

$$\begin{bmatrix} I_\alpha \\ I_\beta \end{bmatrix} = \begin{bmatrix} G_{\alpha\alpha} & G_{\alpha\beta} \\ G_{\beta\alpha} & G_{\beta\beta} \end{bmatrix} \begin{bmatrix} V_\alpha \\ V_\beta \end{bmatrix}. \quad (2.18)$$

Gaussian elimination of the interior voltages V_β in Equ. 2.18 gives an electrically equivalent reduced network with $|\alpha|$ nodes obeying the reduced equations:

$$I_\alpha = G_{re}V_\alpha + G_{ac}I_\beta \quad (2.19)$$

where the reduced conductance matrix $G_{re} \in \mathbb{R}^{|\alpha| \times |\alpha|}$ and the accompanying matrix $G_{ac} \in \mathbb{R}^{|\alpha| \times |\beta|}$ are given by

$$G_{re} = G_{\alpha\alpha} - G_{\alpha\beta}G_{\beta\beta}^{-1}G_{\beta\alpha}, \quad (2.20)$$

$$G_{ac} = G_{\alpha\beta}G_{\beta\beta}^{-1}. \quad (2.21)$$

Since the current injections at the interior nodes are always zero, we finally have

$$I_\alpha = G_{re}V_\alpha. \quad (2.22)$$

The Kron reduction procedure can be best illustrated with a simple example. In Fig. 2-7, there is a graph of 9 nodes with each edge denoting a resistor, and we ask whether there is an embedded Wheatstone bridge between the two blue edges with endpoints pairs $\{1, 2\}$ and $\{3, 4\}$. After applying Kron reduction to eliminate the nodes $\{5, 6, 7, 8, 9\}$, we reduce the graph to a K_4 complete graph. The green edges on the reduced equivalent graph constitute the embedded Wheatstone bridge between the pair of blue edges.

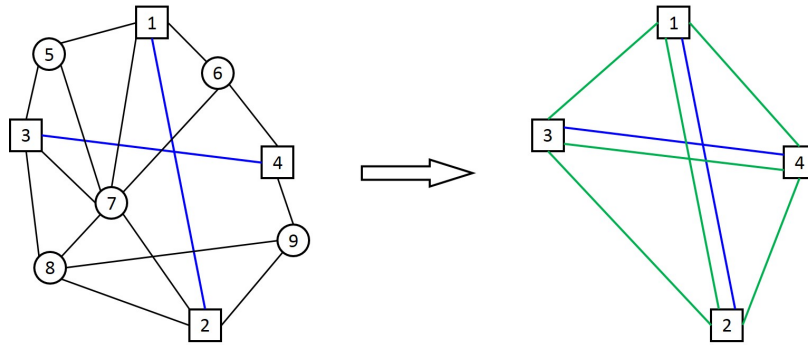


Figure 2-7: Kron reduction of an area consisting of nodes $\{5, 6, 7, 8, 9\}$ and black edges. The embedded wheatstone bridge for the blue edge pair is shown in green in the right network.

Next, we explore when the embedded Wheatstone bridge in the 4-terminal equivalent circuit is likely to be balanced. It is shown in the following discussion that two topology concepts, *cut vertex* and *biconnected component* whose definition is given below, play key roles in determining how balanced the embedded Wheatstone bridge is.

Definition 4 (Behzad and Chartrand, 1972) *A cut vertex (also called as articulation point) in a connected graph is any node that when removed with its incident edges disconnects the graph; a graph with no cut vertices is called a biconnected graph; and a maximal biconnected subgraph is called a biconnected component.*

Proposition 6 *For a DC circuit network consisting of current sources, voltage sources and resistors, the influence of switching off an arbitrary link on the I^2R losses of the*

rest of the resistance links will be confined within the biconnected component containing that link in the resistance network, *i.e.* the influence will never propagate through a cut vertex to another biconnected component in the resistance network.

Proof. We assume without loss of generality that we are going to switch off a link that corresponds to the i -th link of the m -th biconnected component in the resistance network derived from the DC circuit. It is easy to prove that its topology relationship with any link of another biconnected component, say the j -th link of the n -th biconnected component, must fall into one of the two following categories: (1) sharing the cut vertex (Fig. 2-8(a)), or (2) having no nodes in common (Fig. 2-8(b)).

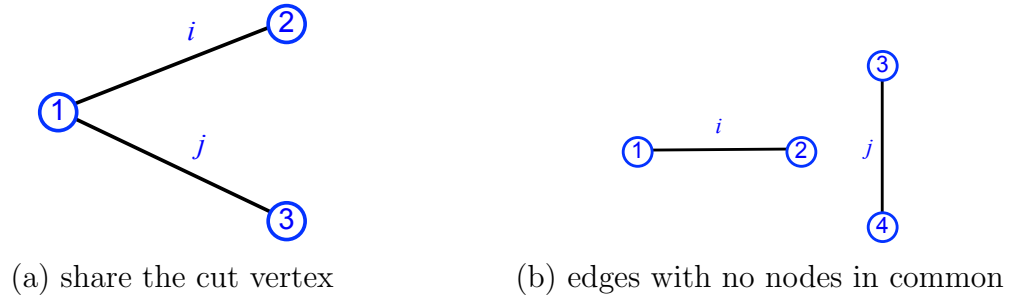


Figure 2-8: Two possible topology relationships between two links belonging to two different biconnected components.

For both categories, we can reduce the rest of the network to a set of equivalent currents based on the generalized Norton's Theorem.

(a) If link i and link j share the cut vertex (Fig. 2-9), then by Norton's Theorem, we must have

$$R_{1,2} + R_{1,3} = R_{2,3} \quad (2.23)$$

where $R_{1,2}$, $R_{1,3}$ and $R_{2,3}$ are Norton's equivalent resistances at terminals 1-2, 1-3 and 2-3, respectively, *i.e.*

$$\frac{R_a(R_b + R_c)}{R_a + R_b + R_c} + \frac{R_b(R_a + R_c)}{R_a + R_b + R_c} = \frac{R_c(R_a + R_b)}{R_a + R_b + R_c} \quad (2.24)$$

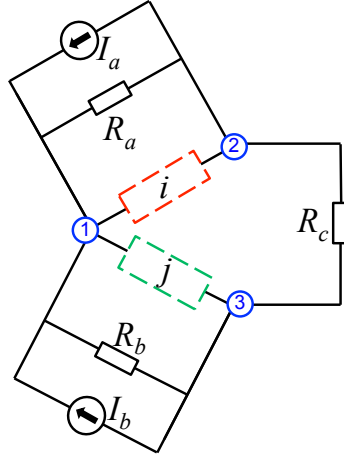


Figure 2-9: The generalized Norton equivalent circuit for a three-port network.

Thus we have $R_a = 0$ or $R_b = 0$, which means the change of link i will have no influence on link j and vice versa.

(b) If link i and link j have no nodes in common (Fig. 2-6), then by Norton's Theorem, we must have

$$R_{1,3} - R_{2,3} = R_{1,4} - R_{2,4} \quad (2.25)$$

where $R_{1,3}$, $R_{1,4}$, $R_{2,3}$ and $R_{2,4}$ are Norton's equivalent resistance at terminals 1-3, 1-4, 2-3 and 2-4, respectively. By computing the value of $R_{1,3}$, $R_{1,4}$, $R_{2,3}$ and $R_{2,4}$ with the use of R_a through R_f , we must have $R_a R_d = R_b R_c$ in order to satisfy Equ. 2.25. Then by Lemma 1, we know that the change of link i will have no influence on link j and vice versa. \square

Proposition 7 *For a DC circuit network consisting of current sources, voltage sources and resistors, all currents flowing in a biconnected component of its resistance network will be changed after switching off an arbitrary link in that biconnected component if and only if every link in that biconnected component has nonzero current and there are no embedded balanced Wheatstone bridges in that biconnected component.*

Proof. We assume without loss of generality that there are N links in the biconnected component, and we are going to switch off the i -th link and mark its current

as I_i ($I_i > 0$). It is easy to prove that its topology relationship with any other link, say the j -th link ($j \neq i$), in the same biconnected component must fall into one of the three following categories: sharing no nodes; sharing one node; or sharing two nodes. For each above category, we can reduce the rest of the network to a set of equivalent circuits based on the Generalized Norton's Theorem.

(a) If link i and link j share two nodes (Fig. 2-10, $R_j, R_a > 0$), the current flowing

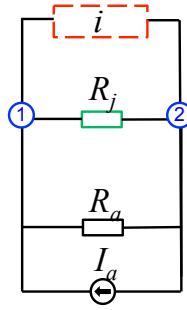


Figure 2-10: The generalized Norton equivalent circuit for two links (i, j) that share two nodes.

on link j before switching off link i is

$$I_j = \left(\frac{R_a}{R_j + R_a} \right) (I_a + I_i) \quad (2.26)$$

and the current flowing on link j after switching off link i is

$$I'_j = \left(\frac{R_a}{R_j + R_a} \right) I_a \quad (2.27)$$

then

$$\Delta_{I_j} = I_j - I'_j = \left(\frac{R_a}{R_j + R_a} \right) I_i \neq 0 \quad (2.28)$$

(b) If link i and link j share one node (Fig. 2-9, $R_j, R_a, R_b, R_c > 0$), then the difference

between the currents flowing on link j before and after switching off link i is

$$\begin{aligned}\Delta_{I_j} &= I_j - I'_j \\ &= \frac{R_a R_b}{R_a R_b + R_a R_j + R_b R_c + R_b R_j + R_c R_j} (-I_i) \neq 0\end{aligned}\quad (2.29)$$

(c) If link i and link j have no nodes in common (Fig. 2.6, $R_j, R_a, R_b, R_c, R_d > 0$), then the difference between the currents flowing on link j before and after switching off link i is

$$\begin{aligned}\Delta_{I_j} &= I_j - I'_j \\ &= \frac{R_f}{R_f + R_j} |A|^{-1} I_i R_e (R_a R_d - R_b R_c)\end{aligned}\quad (2.30)$$

where A is given by Equ. 2.16. Thus Δ_{I_j} is zero if and only if $R_b R_c = R_a R_d$. This ends the proof of Proposition 3. \square

Before we end this section, we show that there is an equivalent relationship between the analysis of the current-controlled circuit and the DC power flow model by using the following nomenclature.

DC power flow model:

P_i = Power injection at the i -th bus.

$B_{i,j}$ = Susceptance of the link connecting buses i and j .

$X_{i,j}$ = Reactance of the link connecting buses i and j .

θ_i = Phase angle at the i -th bus.

$P_{i,j}$ = Power flowing through the line connecting bus i and bus j .

Current-controlled circuit:

I_i = Current source connected to node i .

$G_{i,j}$ = Conductance of the link connecting nodes i and j .

$R_{i,j}$ = Resistance of the link connecting nodes i and j .

V_i = Voltage at the i -th node

$I_{i,j}$ = Current flowing through the resistor connecting node i and node j .

We can then create an equivalent current-controlled circuit for any DC power flow problem by following the rules below:

$$P_i = I_i$$

$$B_{i,j} = -1/X_{i,j}$$

$$G_{i,j} = 1/R_{i,j}$$

$$\theta_i = -V_i$$

$$P_{i,j} = I_{i,j}$$

$$P_{i,j} = B_{i,j}(\theta_j - \theta_i)$$

$$P_{i,j} = G_{i,j}(V_i - V_j)$$

Fig 2-11 shows an example of such equivalent relationship.

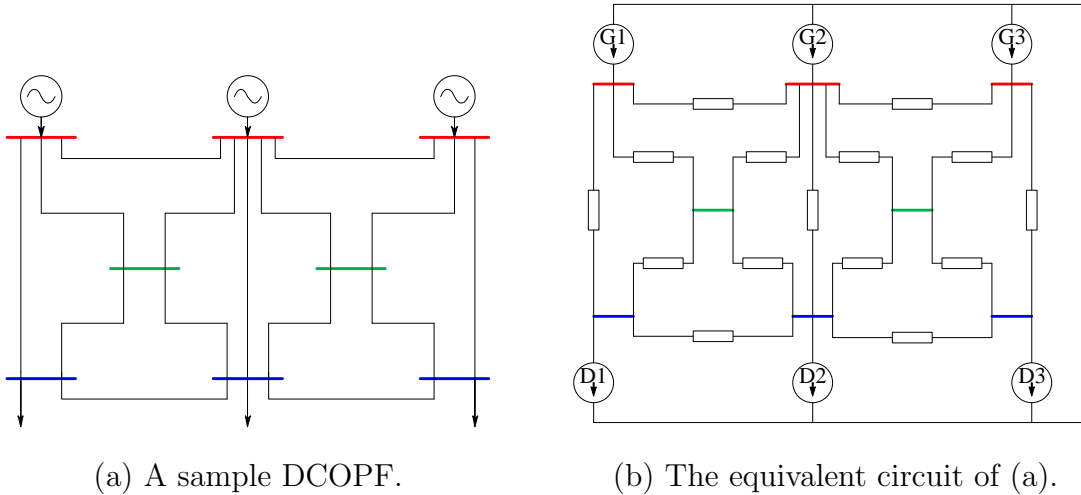


Figure 2-11: The equivalent relationship between a current-controlled circuit and a DC power flow problem.

In short, the DC model of power flow is equivalent to a current driven network, where power injections are equivalent to current sources; power flowing through lines is equivalent to current through edges, etc. See Table 2.1.

Table 2.1: The equivalence between current driven circuits and DC power flow models of transmission grids.

network	potential	injection	admittance	equation
circuit	voltage V	current I	conductance G	$I = GV$
grid	phase θ	power P	susceptance B	$P = B\theta$

2.5 The NP-hardness of Topology Control

An embedded balanced Wheatstone bridge existing in a biconnected circuit is clearly a singular case and thus is trivial for the analysis of any real network. By the equivalence between the current driven circuits and DC power flow models of transmission grids (Table 2.1), it is almost always the case that disconnecting a transmission line will change every line flow within the biconnected component that contained the disconnected line. The N-1 reliability standard of today’s transmission network, requiring the system to move to a satisfactory state for any one credible line outage event, significantly increases the likelihood of the whole network or a large portion of the network being biconnected. What comes with the seemingly ubiquitous opportunities of relieving line congestions provided by a large biconnected component is the forbidding combinatorial explosion.

By generalizing the problem formulation mentioned in Example 1, we can get the standard linearized lossless DC OPF for a connected transmission network with N buses and L lines:

$$\mathcal{C} = \min \quad c'p \tag{2.31}$$

subject to

$$1'p = 1'l \tag{2.32}$$

$$\underline{f} \leq \Psi(p - l) \leq \bar{f} \tag{2.33}$$

$$\underline{p} \leq p \leq \bar{p} \tag{2.34}$$

where $c \in \mathbb{R}^{N \times 1}$ are the nodal generation costs which are assumed to be piecewise linear, $p \in \mathbb{R}^{N \times 1}$ and $l \in \mathbb{R}^{N \times 1}$ are the nodal power injections and withdrawals, respectively, $\Psi \in \mathbb{R}^{L \times N}$ is the famous *transmission sensitivity matrix*, also known as the *injection shift factor matrix*, $\underline{f} \in \mathbb{R}^{L \times 1}$ and $\bar{f} \in \mathbb{R}^{L \times 1}$ are the flow limits on transmission lines with lower limits usually representing the limit in the opposite flow direction, $\underline{p} \in \mathbb{R}^{N \times 1}$ and $\bar{p} \in \mathbb{R}^{N \times 1}$ are the lower and upper generation capacities. Constraints (2.32), (2.33), and (2.34) enforce the total load-generation balance, the line flow limits, and the generation limits, respectively.

In order to fully capture all possible changes due to topology control that are discussed at the beginning of this section, the standard DC OPF has traditionally been modified as a mixed integer programming problem (Hedman et al., 2011b) with some additional binary variables indicating the status of lines. Such formulations are known to be computationally intractable, and accordingly, it is natural for us to ask if the feasibility problem of topology control is NP-hard. We end the comprehensive discussion in the chapter about the challenges associated with topology control by answering this question.

Proposition 8 *Given the capacity of each line and the net power injection/withdrawal of each bus in an arbitrary DC model of a power network, the topology control problem is NP-complete.*

Proof: First we know that the feasibility problem of topology control is NP because we can verify in polynomial time whether an instance is a feasible solution. The verification involves two steps. The first is to calculate the new line flows by solving the updated OPF problem. Next, we check whether line congestions still exist. Clearly, both steps can be done in polynomial time.

The second part of the proof involves a reduction from an arbitrary instance of an NP complete problem to an instance of the topology control problem.

Here, we use the well known *subset sum problem* for the reduction. The subset

sub problem is this: given a set of numbers, is there a non-empty subset whose sum is zero? For instance, given the set $\{-1, -2, -3, 4, 8\}$, the answer is yes because the subset $\{-1, -3, 4\}$ sums to zero. The problem is known to be NP-complete (Murty and Kabadi, 1987). We take an instance of the subset sum problem and reduce it to a topology control instance that has a feasible solution if and only if the subset sum problem has a non-empty subset whose sum is zero.

Let $X = \{x_1, \dots, x_m, y_1, \dots, y_n\}$ ($x_i > 0, i = 1, \dots, m$ and $y_j < 0, j = 1, \dots, n$) be an instance of the subset sum problem. We then can reduce it to the topology control problem shown in Fig. 2.12.

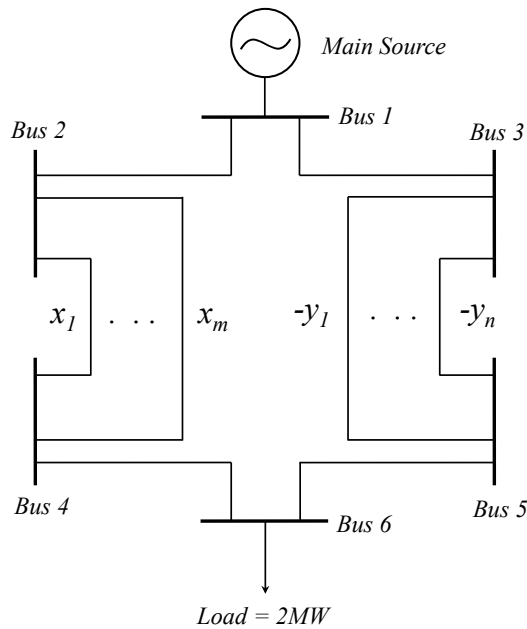


Figure 2.12: An instance of topology control problem.

In Fig. 2.12, we assume that the susceptances of vertical lines are $\{x_1, \dots, x_m\}$ ($x_i > 0, i = 1, \dots, m$) and $\{-y_1, \dots, -y_n\}$ ($y_j < 0, j = 1, \dots, n$), respectively. All other lines are assumed to be of same susceptance. In addition, the line capacities of the lowest two lines $\{L_1, L_2\}$ are both 1 MW, and we assume the line capacities of other lines are all large enough. To satisfy the 2 MW demand of the lower bus, we must

balance the susceptance of the left group of lines $\{x_1, \dots, x_m\}$ with that of the right group of lines $\{-y_1, \dots, -y_n\}$. Then we see that the topology control instance has a feasible solution if and only if the subset sum problem $\{x_1, \dots, x_m, y_1, \dots, y_n\}$ has a non-empty subset whose sum is zero. \square

Chapter 3

Paradigm of Topology Control

We have shown that changing the network topology may greatly vary certain line flows in a grid. Moreover, the impacts can be expected to propagate to every corner of the grid under current reliability standards. In this chapter, we study some useful properties of the *loss cost of the link* (LCL) for networks of arbitrary size with the hope of offering some theoretical support for developing heuristic approaches to the NP-hard problem of optimal line switching.

The way in which electric power depends on the topology of circuits with voltage sources, current sources, and mixed current sources is systematically examined in this chapter, and its possible relationship to topology control in electric grid operations is discussed. It is shown that the status of any DC circuit only depends on a minimal set of key variables called *fundamental node voltages* and *fundamental edge currents*. We then prove that the I^2R losses of voltage controlled circuit are always decreased after disconnecting a line, and the opposite occurs for the current controlled circuit. In addition, every mixed-source circuit can be decomposed into a voltage controlled subcircuit and a current controlled subcircuit. In terms of such a decomposition, the I^2R losses of a mixed source circuit are always the sum of losses of the voltage controlled subcircuit and the current controlled subcircuit. The chapter concludes by showing that the total power flowing in a mixed source circuit can be found as critical points of the power expressed in terms of the key voltage and current variables mentioned above.

3.1 The Case of Current-Controlled Networks

We first give a set of definitions used in this chapter before the start of detailed discussion.

Definition 5 *A voltage-controlled circuit is comprised purely by resistors and voltage sources; a current-controlled circuit is comprised purely by resistors and current sources; and a circuit that has both current sources and voltage sources is called a mixed-source circuit.*

As there exists a mathematic equivalence between the current-controlled circuits and DC power flow models of transmission grids, we first consider the effect of attaching an arbitrary two-port current controlled circuit (e.g. a single resistor or single current source in the simplest cases) to any two nodes of an existing current controlled circuit of arbitrary topology.

Kirchhoff's current law tells us the algebraic sum of currents in a circuit meeting at a node is zero, showing the linear dependency among the currents in a circuit. To simplify the calculation, it is desirable to find a minimal set of key currents that is able to determine the state of the circuit. In graph theory, a *cycle basis* is defined as a minimal set of simple cycles that forms a basis of the cycle space of the graph, and the flow through given edge is simply the algebraic sum of cycle flows through that edge. Therefore, using the currents flowing on the cycle basis as the set of key variables in circuit modeling is able to fully capture all possible state changes of a circuit.

One standard way to create a cycle basis is based on a given spanning tree. Such cycle basis is also called the *fundamental cycle basis*.

Definition 6 (Liebchen and Rizzi, 2007) *If there exists some spanning tree or spanning forest T for a given graph G , and e denotes an edge that is not in T , then the simple cycle consisting of e together with the path in T connecting the endpoints of e*

is called the fundamental cycle defined by e . Each fundamental cycle is linearly independent of all other fundamental cycles associated with T , and together they construct a basis for the cycle space. A cycle basis formed in this way is called a fundamental cycle basis.

Clearly, the fundamental cycle basis is highly dependent on the choice of the spanning tree but its dimension is always uniquely determined.

We first show one useful property of the fundamental cycle basis which is related to determine whether the embedded Wheatstone bridge between a pair of edges is balanced or not.

Proposition 9 *For a given biconnected resistance network derived from a current-controlled circuit, a fundamental cycle basis can be created from one of its spanning trees. We define a matrix \mathbb{A} such that the ij -th entry denotes the sum of all resistances shared by the i -th and j -th fundamental cycles. Then there exists an embedded balanced Wheatstone bridge between the edges defining the i -th and j -th fundamental cycles if and only if $(\mathbb{A}^{-1})_{ij} = 0$.*

Proof. We assume without loss of generality that there are N fundamental cycles in the biconnected resistance network \tilde{G} . By Definition 3, we know that the original circuit graph can be reconstructed from \tilde{G} by putting all source edges back. With all power sources active, we denote the currents flowing on the edges defining the fundamental cycles of \tilde{G} by $I = \{i_1, \dots, i_N\}$. We then can write down the circuit equations $\mathbb{A}I = b$ based on Kirchhoff's Laws. The matrix \mathbb{A} must be symmetric and invertible in order to make the circuit feasible. In addition, $(\mathbb{A}^{-1})_{ii} = \frac{[A]_{i,i}}{\det(A)}$ ($i = 1, \dots, N$) must be nonzero since the minor $[A]_{ii}$ corresponds to the circuit matrix associated with the circuit obtained by removing the i -th fundamental cycle from the original circuit.

We now assume that the i -th entry of b is changed by Δb_i . The circuit equation becomes

$$\mathbb{A}I' = b + e_i \Delta b_i \tag{3.1}$$

where e_i is the i -th unit vector, and I' denote the currents on the edges defining the fundamental cycles after the change. We then have

$$\Delta I = \mathbb{A}^{-1} e_i \Delta b_i \quad (3.2)$$

where $\Delta I = I' - I$. The i -th entry of ΔI must be nonzero since $(\mathbb{A}^{-1})_{ii} \neq 0$ which means there must be a change of the current flowing on the edge defining the i -th fundamental cycle. The j -th entry of ΔI is zero if and only if $(\mathbb{A}^{-1})_{ji} = 0$. Since \mathbb{A} is symmetric, it is equivalent to having $(\mathbb{A}^{-1})_{ij} = 0$. \square

Though highly desirable, such balanced embedded Wheatstone bridges rarely exist in real network. In fact, the value of fundamental cycle basis lies more in calculating the change of total $I^2 R$ losses of a circuit due to changing the status of a line.

Let $G = (V, E)$ be a graph with vertex set V and edge set E . It is of interest to consider the following elementary transformations:

1. Suppose a new graph G' is created from G by keeping the vertex set fixed and adding a new edge to E . Then G' has either one more fundamental cycle than G or one fewer connected components.
2. Suppose a new graph G' is created from G by keeping the edge set fixed and adding a new vertex to E . Then either G' has one more connected component than G or the number of connected components remains the same, but the number of edges increases by one. (In the second case, the vertex addition creates an edge subdivision.)
3. Suppose a new graph G' is created from G by removing an edge from E while keeping the vertex set V fixed. Then either G' has one fewer fundamental cycle than G or the number of fundamental cycles is the same but the number of connected components increases by one.
4. Suppose a new graph G' is created from G by removing an edge e from E and identifying the two vertices of e . (This operation is called *edge contraction*.) Then

G' will have the same number of connected components as G and one fewer edges. We note that if one of the two vertices of e has degree 2, then we may think of edge contraction as simply merging the two edges that are incident on this vertex.

Definition 7 We call transformations 1 and 2 parallel attachment and serial attachment, respectively, and call transformations 3 and 4 parallel removal and serial removal, respectively.

Fig. 3-1 shows an example of parallel attachment and serial attachment of a resistor R_2 to a circuit comprised by a voltage source V and a resistor R_1 .

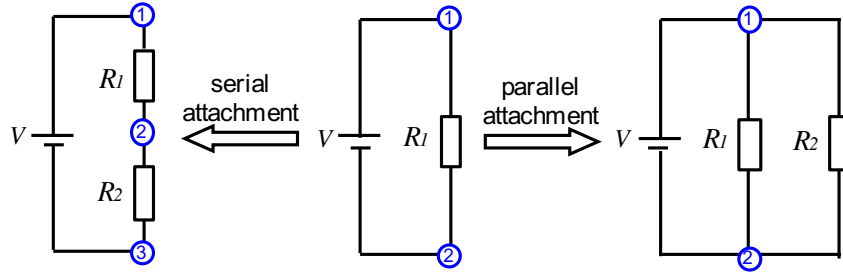


Figure 3-1: An example of parallel attachment and serial attachment.

In general, parallel operation is much more common than serial operation in transmission topology control, and therefore the following discussion focuses on parallel attachment/removal unless particularly specified.

Then the question we would like to explore is whether the attachment/removal of an arbitrary 2-port current controlled circuit (e.g. a single resistor or single current source in the simplest case) can increase the congestion of an existing current-controlled circuit. The answer is both yes and no. It will be shown that the LCL resulting from the attachment will be ≤ 1 if the new 2-port circuit serves as a *passive element*, and will be ≥ 1 otherwise. The definition of *passive element* and *active element* is given below.

Definition 8 An electric element in the circuit is called a passive element if its current and voltage are of opposite polarity (and therefore the element consumes power),

and an active element if its current and voltage are of same polarity (and therefore the element delivers power).

Proposition 10 The LCL of REMOVING a resistance link from a current-controlled circuit must be ≥ 1 no matter what topological structure the original circuit has.

Proof. We start the proof by creating a graph representation $G = (V, E)$ for the circuit. The graph G can be created by placing nodes where two or more circuit elements meet. If two nodes are connected by a resistor or a current source, then we join the corresponding nodes by an edge.

We then create a sub-graph $\tilde{G} = (V, \tilde{E})$. \tilde{G} has the same vertex set as G , but only contains the resistor edge set of G . In other word, the undirected adjacency matrix \tilde{E} can be formed by setting $\tilde{E}_{i,j} = 1$ if node i and node j in G are connected by a resistor edge and $\tilde{E}_{i,j} = 0$ otherwise.

A spanning tree (or forest) of \tilde{G} can be easily found by using depth-first search. Call it \mathcal{T} . Then a fundamental cycle basis of \tilde{G} can be formed based on \mathcal{T} . We assume without loss of generality that there are N fundamental cycles $\{c_1, c_2, \dots, c_N\}$, and the edges in \tilde{G} that define the fundamental cycles are $\{e_1, e_2, \dots, e_N\}$. We write $\tilde{G} = (V, \mathcal{T} \cup \{e_1, \dots, e_N\})$. The original circuit graph G can be reconstructed from \tilde{G} by adding all current source edges (while keeping the vertex set V fixed) . With all current source operating, we denote the current flowing on the edge e_i that defines the i -th fundamental cycle of \tilde{G} by I_{e_i} ($i = 1, \dots, N$).

We can then classify the resistor links into three categories based on their relationship to the topological structure of \tilde{G} . For a resistor link that doesn't belong to any fundamental cycle of \tilde{G} , its power loss will be unchanged when an edge is removed from any fundamental cycle as the current flowing through the resistor is fixed. We call such resistors Type 1 resistors, and we can use a scalar, say P_{T1} , to denote the total loss of such resistor links.

For a resistor link that is exclusively owned by one fundamental cycle of \tilde{G} , say the i -th fundamental cycle, we call it a Type 2 resistor of the i -th fundamental cycle. We can denote the number of i -th fundamental cycle's exclusive links by O_i ($i = 1, \dots, N$), and the resistor on the k -th exclusive link as $R_{i,i,k}$, then the total loss of such resistor links can be computed by

$$P_{T2} = \sum_{i=1}^N \sum_{k=1}^{O_i} (I_{e_i} + I_{P_{e_i,k}})^2 R_{i,i,k} \quad (3.3)$$

where $I_{P_{e_i,k}}$ denotes the algebraic sum of current injections from current source links and/or the Type 1 resistor links to the path connecting e_i and the k -th exclusive link.

For those resistor links that are shared by two or more fundamental cycles of \tilde{G} , we call them Type 3 resistors. We can denote the number of such resistor links by M , the resistor on the k -th ($k = 1, \dots, M$) link by R_k , the number of fundamental cycles that are associated with the k -th link by n_k , and the edges defining these associated fundamental cycles by $\{e_{k_1}, e_{k_2}, \dots, e_{k_{n_k}}\}$ ($1 < k_1, \dots, k_{n_k} < N$). Then the total loss of such resistor links can be computed by

$$P_{T3} = \sum_{k=1}^M \left(\sum_{i=1}^{n_k} I_{e_{k_i}} + I_{P_k} \right)^2 R_k \quad (3.4)$$

where I_{P_k} denotes the algebraic sum of current injections from current source links and/or the Type 1 resistor links to the paths connecting the edges defining the associated fundamental cycles and the k -th Type 3 link.

Fig. 3.2 shows a circuit graph G and its associated resistance graph \tilde{G} in which all resistors are classified into the three categories defined above.

Then a potential function whose physical meaning is the total loss of all resistors

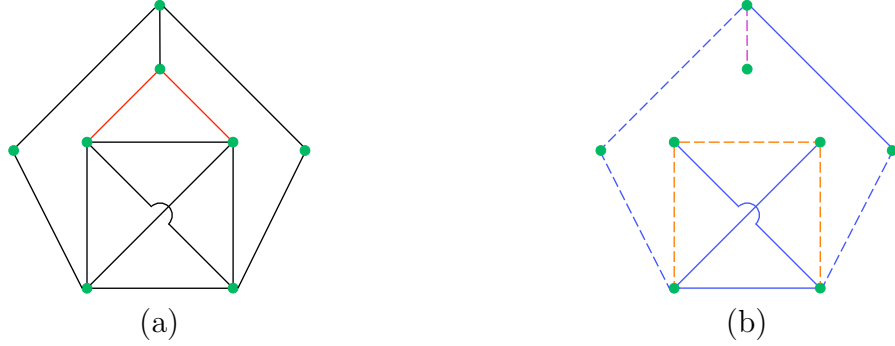


Figure 3.2: (a) A circuit graph G where each black link denotes a resistor and each red link denotes a current source. (b) G 's associated resistance graph \tilde{G} where the dotted links form a spanning tree, Type 1 resistors are marked as magenta links, Type 2 resistors are marked as blue links, and Type 3 resistors are marked as orange links.

in the original circuit can be given:

$$\begin{aligned}
 P &= P_{T1} + P_{T2} + P_{T3} \\
 &= P_{T1} + \sum_{i=1}^N \sum_{k=1}^{O_i} (I_{e_i} + I_{P_{e_i,k}})^2 R_{i,i,k} \\
 &\quad + \sum_{k=1}^M \left(\sum_{i=1}^{n_k} I_{e_{k_i}} + I_{P_k} \right)^2 R_k
 \end{aligned} \tag{3.5}$$

where $\{I_{e_i}\}$ ($i = 1, \dots, N$) is the variable set.

We first show that the potential function is a strictly convex function. Suppose

$$P_{i,i,k} = (I_{e_i} + I_{P_{e_i,k}})^2 R_{i,i,k}, \tag{3.6}$$

and

$$P_k = \left(\sum_{i=1}^{n_k} I_{e_{k_i}} + I_{P_k} \right)^2 R_k. \tag{3.7}$$

It is easy to prove the strict convexity of $P_{i,i,k}$ and P_k since their Hessian matrices

are positive definite. Since

$$P = P_{T1} + \sum_{i=1}^N \sum_{k=1}^{O_i} P_{i,i,k} + \sum_{k=1}^M P_k, \quad (3.8)$$

P is also a strictly convex function and must take its global minimum where all its partial derivatives are zero.

We show that all partial derivatives of the potential function are zero before the removal of a resistor link. Differentiating

$$\begin{aligned} \frac{\partial P}{\partial I_{e_i}} = & 2 \times \left[\sum_{k=1}^{O_i} (I_{e_i} + I_{P_{e_i,k}}) R_{i,i,k} \right. \\ & \left. + \sum_{l=1}^{S_i} \left(\sum_{m=1}^{n_{k_l}} I_{e_{k_l m}} + I_{P_{k_l}} \right) R_{k_l} \right] \end{aligned} \quad (3.9)$$

where S_i denotes the number of Type 3 links on the i -th fundamental cycle, and R_{k_l} ($1 \leq k_l \leq M$) denotes the resistor of the l -th Type 3 link in the i -th fundamental cycle.

This means the partial derivative of P in the direction I_{e_i} is exactly double the algebraic sum of all voltages on the fundamental cycle defined by e_i . Because the original circuit must satisfy Kirchhoff's Voltage Law which is equivalent to setting (3.9) to zero, the potential function must reach its global minimum loss level before removing a link. \square

Remark 2 *The parallel removal of a resistance link is electrically equivalent to the serial attachment of a resistance link, thus the LCL of the serial attachment of a resistance link to a current-controlled circuit must be ≥ 1 no matter what topological structure the original circuit has.*

Corollary 1 *The LCL of REMOVING a passive current source link from a current-controlled network must be > 1 no matter what topological structure the original circuit had, and the LCL of REMOVING an active current source link from a current-controlled network must be < 1 no matter what topological structure the original circuit had.*

Proof. The proof of the “passive current source” part is straightforward by using Proposition 10 and by treating a passive current source as certain kind of resistance. We then only need to prove the “active current source” part. It is easy to prove that removing an active current source link e is equivalent to attaching a passive current source with appropriate amount of output to the endpoints of e . Thus the “active current source” case is automatically proved by the “passive current source” case. \square

Remark 3 *Results similar to Proposition 10 and Corollary 1 hold for the removal of an n -port external circuit, although the proof becomes more involved.*

It is reasonable to assume that the line susceptances and line flow capacities of a transmission grid are usually fixed within a moderate period of time, and the line capacities are usually symmetric, i.e. $|\bar{f}| = |\underline{f}|$. Recalling the equivalence between the current-controlled circuits and DC power flow models of transmission grids, Proposition 10 states that the total real f^2/B (squared line flow over line susceptance) of the transmission network must be increased after switching off a transmission line. Defining \bar{f}^2/B as the squared line flow limit over line susceptance, we know the total \bar{f}^2/B capacity must strictly decrease after disconnecting a line. This means that the total f^2/B *stability margin*, the difference between the total \bar{f}^2/B capacities and actual real f^2/B , must decrease after each step switching out lines. This suggests a good rule of thumb of line switching in transmission networks: do not switch out lines in a congested network with relatively low \bar{f}^2/B stability margin on those uncongested lines.

3.2 The Case of Voltage-Controlled Networks

In Ch. 3.1, we showed that the congestion in a current-controlled circuit of arbitrary topology is made worse after the removal of a new resistor link. It is natural to ask if

something similar can be found in other types of circuits. We now turn our attention to the problem of voltage-controlled circuits.

We begin by recalling that a voltage controlled DC circuit is made up of resistors and voltage sources. We first consider the effect of attaching an arbitrary two-port voltage controlled circuit (e.g. a single resistor or single voltage source in the simplest cases) to any pair of nodes of an existing voltage controlled circuit of arbitrary topology. It will be shown that the LCL resulting from the attachment will be ≤ 1 in all cases, i.e. we won't make any distinction between passive elements and active elements in voltage controlled circuit.

As always, we try to find a minimal set of variables that is able to fully capture the changes due to line switching. Our selection here is inspired by the Kirchhoff's voltage law. The fact that the algebraic sum of the voltage drops around any cycle is zero indicates the linear dependency among the voltages in a cycle, and the node-cycle duality suggests a counterpart for the fundamental cycle basis introduced in last section. We call such a counterpart as the *fundamental node basis*, and its definition is given below.

Definition 9 (*Baillieul et al., 2015*) *For a voltage controlled circuit, a fundamental node basis is a maximal set of nodes among which there exist no paths comprised purely of voltage source edges. Their voltages are called fundamental nodal voltages.*

A fundamental node basis may be formed by using the following method. We first find the set of all nodes V where two or more circuit elements meet, and then create a sub-graph of the original circuit $G_v = (V, E_v)$ that is comprised of the whole set of nodes V and all voltage source links. The case that $G_v = (V, E_v)$ is a connected graph (whose fundamental node basis can be any single node) is trivial since the voltage drops between any pair of nodes are fixed and thus the newly introduced link will have no influence on the loss of the original circuit. If $G_v = (V, E_v)$ is disconnected, we then can find all its connected components (since any vertex is strongly connected

to itself by definition, one connected component may contain only one vertex). Then a fundamental cycle basis may be formed from the set of connected components of the graph G_v , by arbitrarily selecting one node from each connected component.

Since there exists at least one path comprised purely by voltage source links between every node pairs in a connected component of G_v , we can easily get the voltage difference between the fundamental node and other nodes in that connected component by computing the algebraic sum of voltage sources on their connecting paths. Thus once the fundamental node voltages are known, all node voltages of the circuit can be determined easily without solving the Kirchoff's equations.

Just like a current controlled circuit may have multiple fundamental cycle basis, the fundamental node basis may not be unique for a voltage-controlled circuit, but its dimension is always uniquely determined. For example, the fundamental node basis for the circuit in Fig. 3-3 can be nodes $\{1, 2\}$, $\{3, 2\}$ or $\{4, 2\}$.

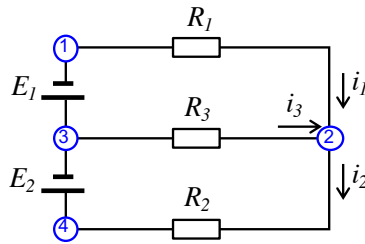


Figure 3-3: A simple circuit with DC-voltage sources and resistive loads.

Proposition 11 *The LCL resulting from ADDING a resistance link to a voltage-controlled circuit must be ≥ 1 no matter what topological structure the original circuit has.*

Proof: We start the proof by creating a graph representation $G = (V, E)$ for the voltage-controlled circuit. The graph G can be created by placing nodes where two or more circuit elements meet and making them as $V = \{1, \dots, N\}$, where N is the

total number of nodes. If two nodes are connected by a resistor or a current source, then we join the corresponding nodes by an edge.

We then create the voltage source sub-graph of the original circuit $G_v = (V, E_v)$ which is comprised of the whole set of nodes $V = \{1, \dots, N\}$ and all voltage source links. The case that the voltage source sub-graph $G_v = (V, E_v)$ is a connected graph has been proved to be trivial and thus is ignored here. Suppose $G_v = (V, E_v)$ is disconnected, we then can find all its connected components and assume that they are $G_1 = (V_1, E_1), \dots, G_M = (V_M, E_M)$ (M is the total number of the connected components in G_v). A fundamental node basis then can be formed by arbitrarily selecting one node from each connected component, and mark the basis as $V_F = \{v_1, \dots, v_M\}$. We denote the voltage at node v_i as e_{v_i} ($i = 1, \dots, M$), and choose v_M as the reference ground node, i.e. $e_{v_M} = 0$.

It is easy to prove that the pair of endpoints of any resistor link on the original circuit belong to either one connected component or two connected components defined above. For those resistor links whose pair of endpoints belong to one connected component, their power loss will be unchanged no matter what kind of new link is introduced as the voltage drops between the pairs of endpoints are fixed. Thus we can use a scalar, say P_1 , to denote the total loss of such resistor links.

Next we compute the loss of the resistor links whose pair of endpoints belong to two connected components. We denote the number of resistor links between the pair of connected components $\{G_i, G_j\}$ ($i, j = 1, \dots, M$, and $i \neq j$) by $L_{i,j}$, the current flowing away from the i -th connected component towards the j -th connected component on the k -th ($k = 1, \dots, L_{i,j}$) resistor link between $\{G_i, G_j\}$ as $I_{i,j,k}$ ($I_{i,j,k} = -I_{j,i,k}$), the resistor on the k -th link between $\{G_i, G_j\}$ as $R_{i,j,k}$ ($R_{i,j,k} = R_{j,i,k} > 0$), then the total

loss of of such resistor links can be computed by

$$P_2 = \sum_{i=1}^{M-1} \sum_{j=i+1}^M \sum_{k=1}^{L_{i,j}} I_{i,j,k}^2 R_{i,j,k} \quad (3.10)$$

where $I_{i,j,k}$ can be computed by

$$I_{i,j,k} = \frac{e_{v_i} + e_{P_{v_i,k}} - e_{v_j} - e_{P_{v_j,k}}}{R_{i,j,k}} \quad (3.11)$$

where $e_{P_{v_i,k}}$ denotes the algebraic sum of voltage sources on the path connecting the fundamental node v_i and one endpoint of the resistor $R_{i,j,k}$ in the connected component G_i ($e_{P_{v_i,k}} = 0$ if one endpoint of the resistor $R_{i,j,k}$ is directly connected to the fundamental node v_i), and $e_{P_{v_j,k}}$ is the path connecting the other endpoint of the resistor to the fundamental node v_j ($e_{P_{v_j,k}} = 0$ if the other endpoint of the resistor $R_{i,j,k}$ is directly connected to the fundamental node v_j).

Then a potential function whose physical meaning is the total loss of all resistors on the original circuit can be created based on the variables in the fundamental node set:

$$\begin{aligned} P &= P_1 + P_2 \\ &= P_1 + \sum_{i=1}^{M-1} \sum_{j=i+1}^M \sum_{k=1}^{L_{i,j}} \frac{(e_{v_i} + e_{P_{v_i,k}} - e_{v_j} - e_{P_{v_j,k}})^2}{R_{i,j,k}} \end{aligned} \quad (3.12)$$

where $\{e_{v_1}, \dots, e_{v_M}\}$ is the variable set.

We assume $e_{v_M} = 0$, and the value of other node voltages before and after adding a new link are $(\bar{e}_{v_1}, \dots, \bar{e}_{v_{M-1}})$ and $(e'_{v_1}, e'_{v_2}, \dots, e'_{v_{M-1}})$, respectively. Then we will show that the potential function reaches its minimum loss level before adding a new link, i.e. $P(\bar{e}_{v_1}, \dots, \bar{e}_{v_{M-1}})$ is always $\leq P(e'_{v_1}, e'_{v_2}, \dots, e'_{v_{M-1}})$.

We first show that the potential function is a strict convex function. Supposing

$$P_{i,j,k} = \frac{(e_{v_i} + e_{P_{v_i,k}} - e_{v_j} - e_{P_{v_j,k}})^2}{R_{i,j,k}} \quad (3.13)$$

It is easy to prove the convexity of $P_{i,j,k}$ since its Hessian matrix is positive semidefinite. Since we assume $e_{v_M} = 0$ and suppose

$$P_{i,M,k} = \frac{(e_{v_i} + e_{P_{v_i,k}} - e_{P_{v_M,k}})^2}{R_{i,M,k}} \quad (i = 1, \dots, M-1) \quad (3.14)$$

then $P_{i,M,k}$ is convex if $R_{i,M,k}$ is infinite and is strict convex otherwise. Since

$$P = \sum_{i=1}^{M-1} \sum_{j=i+1}^M \sum_{k=1}^{L_{i,j}} P_{i,j,k} \quad (3.15)$$

then P is also a strict convex function and must take its global minimum where all its partial derivatives are zero.

We then show that all partial derivatives of potential function are zero when $(e_{v_1}, e_{v_2}, \dots, e_{v_{M-1}}) = (\bar{e}_{v_1}, \dots, \bar{e}_{v_{M-1}})$. It is easy to show that P is differentiable and

$$\begin{aligned} \frac{\partial P}{\partial e_{v_i}} = & 2 \times \left(\sum_{j=1}^{i-1} \sum_{k=1}^{L_{i,j}} \frac{e_{v_i} + e_{P_{v_i,k}} - e_{v_j} - e_{P_{v_j,k}}}{R_{i,j,k}} + \right. \\ & \left. \sum_{j=i+1}^M \sum_{k=1}^{L_{i,j}} \frac{e_{v_i} + e_{P_{v_i,k}} - e_{v_j} - e_{P_{v_j,k}}}{R_{i,j,k}} \right) \end{aligned} \quad (3.16)$$

which means the partial derivative of P in the direction e_{v_i} is exactly double the algebraic sum of all currents flowing on the original resistors that meet at the i -th connected component. Because $(e_{v_1}, e_{v_2}, \dots, e_{v_{M-1}}) = (\bar{e}_{v_1}, \dots, \bar{e}_{v_{M-1}})$ must satisfy Kirchhoff's Current Law which is equivalent to set (3.16) to zero, the potential function must reach its global minimum loss level before adding a new link. If both endpoints of the newly introduced link are added to the same connected component defined above, then the total loss of the original circuit will remain the same as

$(\bar{e}_{v_1}, \dots, \bar{e}_{v_{M-1}}) = (e'_{v_1}, e'_{v_2}, \dots, e'_{v_{M-1}})$. However, if the two endpoints of the new link are added to two different connected components, say G_i and G_j , and denote the current flowing on the new link from G_i to G_j as $I_{i,j}^{new}$, then we will have

$$\begin{aligned} \frac{\partial P}{\partial e'_{v_i}} &= 2 \times \left(\sum_{j=1}^{i-1} \sum_{k=1}^{L_{i,j}} \frac{e'_{v_i} + e_{P_{v_i,k}} - e'_{v_j} - e_{P_{v_j,k}}}{R_{i,j,k}} + \right. \\ &\quad \left. \sum_{j=i+1}^M \sum_{k=1}^{L_{i,j}} \frac{e'_{v_i} + e_{P_{v_i,k}} - e'_{v_j} - e_{P_{v_j,k}}}{R_{i,j,k}} \right) \\ &= 2 \times I_{i,j}^{new} \end{aligned} \quad (3.17)$$

After adding the new link, the algebraic sum of all currents flowing on the original resistors that meet at the i -th connected component is determined by the current $I_{i,j}^{new}$ which is not necessarily zero as there may be current import and export to the newly added link from the original system. Therefore the original loss equilibrium is perturbed away from its minimum level, and thus the system loss of the original system would increase. \square

Remark 4 *The multi-node connected components of $G_v = (V, E_v)$ may have arbitrarily complex topologies including tree and loop components. If a fundamental node basis that differs from the one chosen to define the loss in (3.12) is chosen, the form of the loss function (3.12) will differ accordingly. The critical point determined by setting the partial derivatives in (3.16) equal to zero will minimize the new expression for loss. It follows from the Kirchhoff circuit laws, that the minimizing values in both representations are the same—as we would expect.*

Remark 5 *A more general version of Proposition 11 can be established. Indeed, the proof as given applies to the connection any two-port voltage controlled circuit to an existing voltage controlled circuit in steady state. Although the proof becomes more involved, a similar result holds for the addition of an n -port external circuit.*

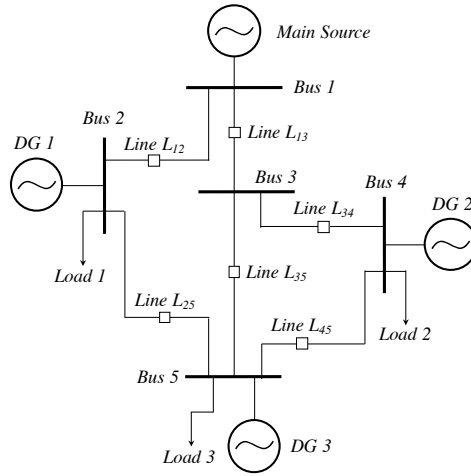
In short, the Kirchhoff-Braess phenomenon that adding a new link worsens the overall congestion can be universally observed in voltage controlled circuit.

3.3 The Case of Mixed-Source Networks

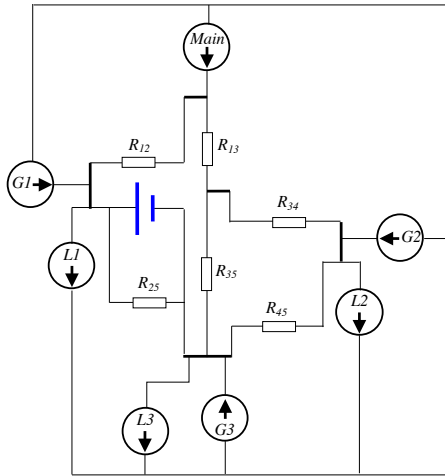
While there is a well established correspondence between current-controlled DC-circuits and linearized DC power flow models, the recent increase in load shifting and demand response programs suggest that the formulation of the standard OPF problem should be modified to take advantage of the flexibility (e.g., load shifting, reserve provisioning through demand response, and transmission topology reconfiguration) provided by the smart grid framework. Regulating generator outputs to exploit this flexibility can be thought of as physically equivalent to changing nodal injections with the aim of mitigating line overloads. Scheduling generator output will have the primary purpose of meeting load demand while at the same time allowing the use of smart grid flexibility to alleviate congestion by locking phases across overloaded lines. This approach is seen to be well modeled by an equivalent voltage controlled circuit. By using the Thevenin/Norton theorems or circuit duality relationships, the current-controlled circuit and voltage controlled circuit can always be converted from one to the other, and thus the mixed source model described in the following is better able to capture the features of power grids in which renewables, storage, and demand response play significant roles.

For example, consider the 5-bus network of Fig. 3.4 with a power flow in which there is an overload of *Line* L_{25} . Traditionally, such line overloads can be alleviated either through regulating the generators' output or through dynamic control of the underlying network topology. The increase of demand-side participation and the development in electrical energy storage in power markets, however, makes it also possible to alleviate the congestion through load regulation or load shifting in time or space or both. In the simplest case, suppose *Bus* 2 and *Bus* 5 are equipped with enough energy storage capacities that they are able to release energy during peak times while storing energy at off-peaks. The effect of such system flexibility can be

well abstracted as a “phase lock” to the overloaded *Line L₂₅* during peak times which is equivalent to adding a voltage source to the traditional current-controlled circuit model.



(a)



(b)

Figure 3·4: (a) A 5-bus network with line overload at *Line L₂₅*. (b) The equivalent mixed-source circuit of (a) with the voltage source (blue) denoting the effect of load regulating equipment at *Bus 2* and *Bus 5*.

In addition, due to the heterogeneity of the controllers (e.g. the current-control loop and voltage regulator), distribution networks and microgrids can hardly be mod-

eled as systems with a single class of primary energy sources which as well points out the need for additional research on the mixed source model.

Proposition 10 or Proposition 11 both state that the parallel attachment of an active element always increases the total losses of a current-controlled circuit or a voltage-controlled circuit. It is natural to ask if such results hold for an arbitrary mixed-source circuit. The answer is no. An interesting paradoxical behavior may happen in a mixed-source circuit: the removal of an active element may cause a redistribution of the current that results in higher total losses.

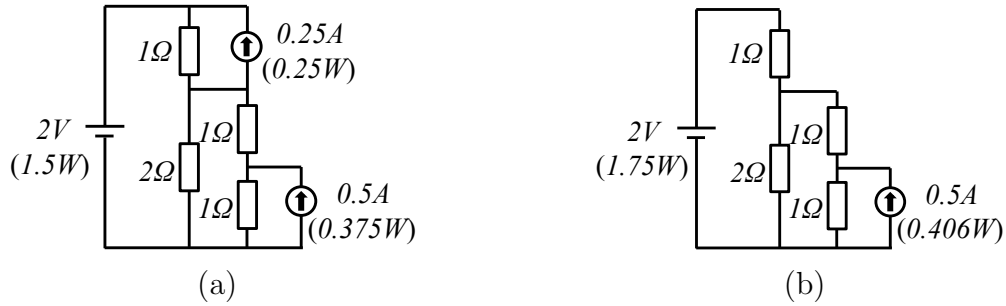


Figure 3-5: (a) A mixed-source network with two current sources and one voltage source. (b) A mixed-source network with one current source and one voltage sources.

Fig. 3-5 shows an example of such paradoxical behavior. The original heat power of Fig. 3-5(a) is only 2.125 W, and it increases to 2.156 W after the removal of an active current source (Fig. 3-5(b)).

In order to explore this paradox, we have the following:

Definition 10 For a given mixed-source circuit, C_M , its voltage-controlled sub-circuit, C_V , is created by replacing all current source edges with open circuits in C_M ; and its current-controlled sub-circuit, C_I , is created by replacing all voltage source edges with short circuits in C_M . It is easy to see that C_M , C_V , and C_I have the same set of resistance edges. To prevent confusion, we denote the i -th resistance edge by R_i^M in C_M , R_i^V in C_V , and R_i^I in C_I , respectively, and denote the current flowing on the i -th resistance edge by I_i^M in C_M , I_i^V in C_V , and I_i^I in C_I , respectively.

For example, the circuits in Fig. 3·6(a) and Fig. 3·6(b) are the voltage-controlled sub-circuit and current-controlled sub-circuit of the circuit in Fig. 3·6(c), respectively.

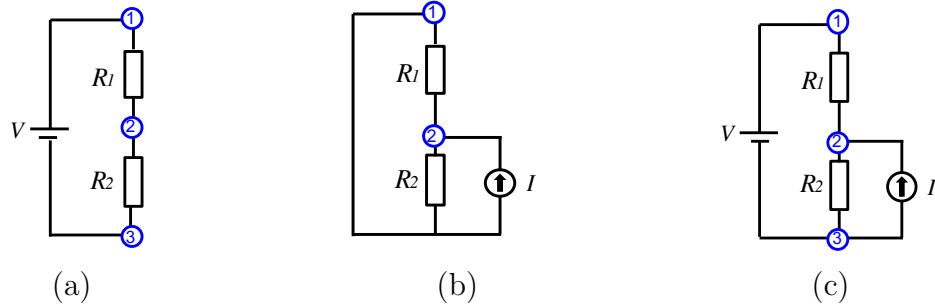


Figure 3·6: (a) A voltage-controlled circuit with nodes $\{1, 2, 3\}$. (b) A current-controlled circuit with nodes $\{1, 2\}$. (c) A mixed-source circuit with nodes $\{1, 2, 3\}$.

In electric systems, while the voltage drop across a resistor (or the current flowing through a resistor) is simply the sum of the effects that would have been caused by each source individually, no such additivity property exists for the loss of a resistor as I^2R is a non-linear function. In the following discussion, however, we will show that there does exist a certain level of additivity with respect to the total losses of a circuit associated with the decomposition described in Definition 10.

First, we are going to prove that the CHANGE of I^2R losses of a mixed source circuit are always the sum of corresponding CHANGE of losses in its voltage controlled sub-circuit and current controlled sub-circuit. Here a new term *source factor* is introduced in this section to simplify the proofs.

Definition 11 *A source factor in a circuit is defined to be the sensitivity of the current flowing through a voltage source (or of voltage difference between the endpoints of a current source) with respect to a change in the value of another voltage source or current source.*

By above definition, we have the following notations:

- the sensitivity of the current flowing through voltage source i with respect to a change in the value of voltage source j is denoted as $s_{j,i}^{\text{VV}}$;
- the sensitivity of the current flowing through voltage source i with respect to a change in the value of current source j is denoted as $s_{j,i}^{\text{IV}}$;
- the sensitivity of the voltage difference between the endpoints of current source i with respect to a change in the value of voltage source j is denoted as $s_{j,i}^{\text{VI}}$;
- the sensitivity of the voltage difference between the endpoints of current source i with respect to a change in the value of current source j is denoted as $s_{j,i}^{\text{III}}$.

By Proposition 4, we know any 4-terminal resistance graph can be reduced to an equivalent resistance network. The equivalent network consists of 6 resistors, and its graph is the complete one as shown in Fig. 3-7.

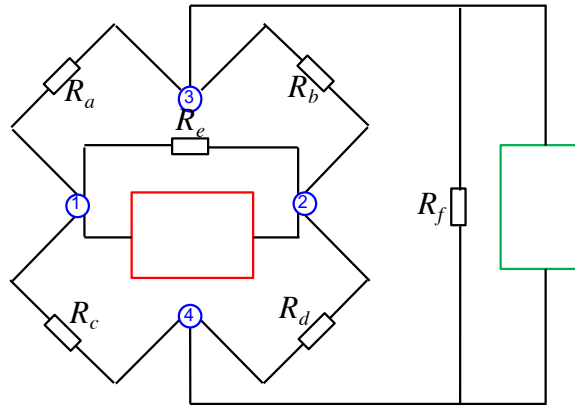


Figure 3-7: The equivalent resistance network for an arbitrary 4-terminal resistance network.

The red box (and green box) in Fig. 3-7 can then be filled with a voltage source or current source in order to study some useful properties of the source factor. Basically, we have following results (whose proof is some basic calculation based on Fig. 3-7

and thus is omitted here):

$$\begin{aligned}
s_{j,i}^{\text{VV}} &= s_{i,j}^{\text{VV}} \\
s_{j,i}^{\text{IV}} &= -s_{i,j}^{\text{VI}} \\
s_{j,i}^{\text{III}} &= s_{i,j}^{\text{III}}
\end{aligned} \tag{3.18}$$

Remark 6 *Unlike the well known sensitivity, power transfer distribution factor or PTDF, which is mathematically equivalent to the sensitivity of the current flowing through one resistance edge with respect to a change in the value of current source, the two circuit elements associated with a source factor described above are both source elements. Moreover, while s^{VV} and s^{III} are both symmetric, no such property exists for s^{IV} or s^{VI} .*

Proposition 12 *The change of total I^2R losses, ΔP , resulting from the parallel removal (parallel attachment) of a resistance link R_j^M from a mixed-source circuit is given by $\Delta P = \Delta P_V + \Delta P_I$, where ΔP_V denotes the change of losses resulting from removing (adding) the link R_j^V from its voltage-controlled sub-circuit, and ΔP_I denotes the change of losses resulting from removing (adding) the link R_j^I from its current-controlled sub-circuit.*

Proof: It is easy to prove that the parallel attachment and parallel removal have exactly the opposite effect on the total loss of a circuit. The proof for the parallel removal part of the proposition is thus logically equivalent to that for the parallel attachment part of the proposition. Hence we just need to prove the parallel removal part of the proposition.

We assume without loss of generality that there are k current sources $\{\mathbb{I}_1, \dots, \mathbb{I}_k\}$, and l voltage sources $\{\mathbb{V}_1, \dots, \mathbb{V}_l\}$, in the circuit. Suppose we are going to remove the j -th resistor edge R_j whose endpoint pair is $\{m, n\}$.

By the principle of energy conservation, the change of total I^2R loss must be equivalent to the change of total sources' energy output $\sum_{i=1}^k \mathbb{I}_i \Delta V_i + \sum_{i=1}^l \mathbb{V}_i \Delta I_i$ where ΔV_i denotes the change of voltage difference between the endpoints of the i -th current source, and ΔI_i denotes the change of current flowing through the i -th voltage

source. Here, in order to calculate ΔV_i and ΔI_i , we replace the j -th resistor edge by a passive current source with value I_{mn} , i.e. the current flowing on the resistor edge before its removal. Clearly, such a replacement increases the number of source edges by 1 and decreases the number of resistor edges by 1, but it has no effect on the rest of the circuit. The voltage difference between the endpoints of the new current source edge must be equivalent to V_{mn} , i.e. the voltage difference between node pair $\{m, n\}$ before the removal.

By the superposition principle, it is easy to prove that V_{mn} is a linear combination of $\{\mathbb{I}_1, \dots, \mathbb{I}_k, I_{mn}\}$ and $\{\mathbb{V}_1, \dots, \mathbb{V}_l\}$, i.e.

$$V_{mn} = [\mathbb{I}_1 \ \cdots \ \mathbb{I}_k \ I_{mn}] \begin{bmatrix} s_{1,mn}^{\text{III}} \\ \vdots \\ s_{k,mn}^{\text{III}} \\ s_{mn,mn}^{\text{III}} \end{bmatrix} + [\mathbb{V}_1 \ \cdots \ \mathbb{V}_l] \begin{bmatrix} s_{1,mn}^{\text{VI}} \\ \vdots \\ s_{l,mn}^{\text{VI}} \end{bmatrix}$$

where $\{s_{1,mn}^{\text{III}}, \dots, s_{k,mn}^{\text{III}}, s_{mn,mn}^{\text{III}}\}$ and $\{s_{1,mn}^{\text{VI}}, \dots, s_{l,mn}^{\text{VI}}\}$ are source factors. To be more specific, $s_{u,w}^{\text{III}}$ ($u, w = 1, \dots, k, mn$) is the sensitivity of the voltage difference between the w -th current source's endpoints with respect to a change in the value of the u -th current source. $s_{u,w}^{\text{VI}}$ ($u = 1, \dots, l$ and $w = 1, \dots, k, mn$) is the sensitivity of the voltage difference between the w -th current source's endpoints with respect to a change in the value of the u -th voltage source. Similarly, we have

$$V_i = [\mathbb{I}_1 \ \cdots \ \mathbb{I}_k \ I_{mn}] \begin{bmatrix} s_{1,i}^{\text{III}} \\ \vdots \\ s_{k,i}^{\text{III}} \\ s_{mn,i}^{\text{III}} \end{bmatrix} + [\mathbb{V}_1 \ \cdots \ \mathbb{V}_l] \begin{bmatrix} s_{1,i}^{\text{VI}} \\ \vdots \\ s_{l,i}^{\text{VI}} \end{bmatrix}$$

where V_i ($i = 1, \dots, k$) denotes the voltage difference between the endpoints of the i -th

current source, and

$$I_i = [\mathbb{I}_1 \quad \cdots \quad \mathbb{I}_k \quad I_{mn}] \begin{bmatrix} s_{1,i}^{\text{IV}} \\ \vdots \\ s_{k,i}^{\text{IV}} \\ s_{mn,i}^{\text{IV}} \end{bmatrix} + [\mathbb{V}_1 \quad \cdots \quad \mathbb{V}_l] \begin{bmatrix} s_{1,i}^{\text{VV}} \\ \vdots \\ s_{l,i}^{\text{VV}} \end{bmatrix}$$

where I_i ($i = 1, \dots, l$) denotes the current flowing through the i -th voltage source.

Clearly, the removal of the the j -th resistor edge R_j and the removal of the current source I_{mn} have exactly the same effect on the total energy output of the k current sources and l voltage sources. In addition, the removal of the current source I_{mn} doesn't further change the resistance graph. Thus, we have

$$\begin{bmatrix} \Delta V_1 \\ \vdots \\ \Delta V_k \end{bmatrix} = -I_{mn} \begin{bmatrix} s_{mn,1}^{\text{III}} \\ \vdots \\ s_{mn,k}^{\text{III}} \end{bmatrix}$$

$$\begin{bmatrix} \Delta I_1 \\ \vdots \\ \Delta I_l \end{bmatrix} = -I_{mn} \begin{bmatrix} s_{mn,1}^{\text{IV}} \\ \vdots \\ s_{mn,l}^{\text{IV}} \end{bmatrix},$$

and

$$\begin{aligned} & \sum_{i=1}^k \mathbb{I}_i \Delta V_i + \sum_{i=1}^l \mathbb{V}_i \Delta I_i \\ &= -I_{mn} \left\{ [\mathbb{I}_1 \quad \cdots \quad \mathbb{I}_k] \begin{bmatrix} s_{mn,1}^{\text{III}} \\ \vdots \\ s_{mn,k}^{\text{III}} \end{bmatrix} + [\mathbb{V}_1 \quad \cdots \quad \mathbb{V}_l] \begin{bmatrix} s_{mn,1}^{\text{IV}} \\ \vdots \\ s_{mn,l}^{\text{IV}} \end{bmatrix} \right\}. \end{aligned}$$

By (3.18), we have $s_{mn,i}^{\text{III}} = s_{i,mn}^{\text{III}}$ ($i = 1, \dots, k, mn$) and $s_{mn,i}^{\text{IV}} = -s_{i,mn}^{\text{VI}}$ ($i = 1, \dots, l$)

which further gives us

$$\begin{aligned} & \sum_{i=1}^k \mathbb{I}_i \Delta V_i + \sum_{i=1}^l \mathbb{V}_i \Delta I_i \\ &= -I_{mn} \left\{ [\mathbb{I}_1 \ \cdots \ \mathbb{I}_k] \begin{bmatrix} s_{1,mn}^{\text{III}} \\ \vdots \\ s_{k,mn}^{\text{III}} \end{bmatrix} - [\mathbb{V}_1 \ \cdots \ \mathbb{V}_l] \begin{bmatrix} s_{1,mn}^{\text{VI}} \\ \vdots \\ s_{l,mn}^{\text{VI}} \end{bmatrix} \right\}. \end{aligned}$$

By replacing all voltage source edges with short circuits (i.e. setting the value of all voltage sources to zero), we get the current-controlled sub-circuit, C_I . It is easy to prove that ΔP_I , the change of I^2R loss resulting from removing R_j from the current-controlled sub-circuit, is given by

$$\Delta P_I = -I_{mn} [\mathbb{I}_1 \ \cdots \ \mathbb{I}_k] \begin{bmatrix} s_{1,mn}^{\text{III}} \\ \vdots \\ s_{k,mn}^{\text{III}} \end{bmatrix}.$$

Similarly, we have

$$\Delta P_V = I_{mn} [\mathbb{V}_1 \ \cdots \ \mathbb{V}_l] \begin{bmatrix} s_{1,mn}^{\text{VI}} \\ \vdots \\ s_{l,mn}^{\text{VI}} \end{bmatrix}.$$

□

Proposition 13 *The change of total losses, ΔP , resulting from the serial removal (serial attachment) of a resistance link R_j^C from a mixed-source circuit is given by $\Delta P = \Delta P_V + \Delta P_I$, where ΔP_V denotes the change of losses resulting from removing (adding) the link R_j^V from its voltage-controlled sub-circuit, and ΔP_I denotes the change of losses resulting from removing (adding) the link R_j^I from its current-controlled sub-circuit.*

Proof: As in Proposition 12, the proof for the serial removal part of the proposition is logically equivalent to that for the serial attachment part of the proposition. So we just need to prove the serial removal part of the proposition.

Again, we assume there are k current sources $\{\mathbb{I}_1, \dots, \mathbb{I}_k\}$, and l voltage sources $\{\mathbb{V}_1, \dots, \mathbb{V}_l\}$ in the circuit. Suppose we are going to remove the j -th resistor edge R_j

whose endpoint pair is $\{m, n\}$. Since we are doing a serial removal, it will merge node m and node n together. Electrically, it is also equivalent to the parallel attachment of a zero resistance edge to $\{m, n\}$. Proposition 12 states that the change of total I^2R loss resulting from the parallel attachment of a zero resistance edge to $\{m, n\}$ is given by $\Delta P_V + \Delta P_I$. \square

We now state a sequence of corollaries that follow fairly directly from Proposition 12 and Proposition 13.

Corollary 2 *The change of total I^2R loss, ΔP_V , resulting from the parallel removal of a resistor edge with endpoint pair $\{m, n\}$ from a voltage-controlled circuit is given by $\Delta P_V = I_{mn}V'_{mn}$, where I_{mn} denotes the current flowing on the edge before its removal, and V'_{mn} denotes the voltage difference between node pair $\{m, n\}$ after its removal.*

Proof: At the end of the proof for Proposition 12, we know that ΔP_V , the change of I^2R loss resulting from removing R_j from the voltage-controlled sub-circuit, is given by

$$\Delta P_V = I_{mn} [\mathbb{V}_1 \quad \cdots \quad \mathbb{V}_l] \begin{bmatrix} s_{1,mn}^{\text{VI}} \\ \vdots \\ s_{l,mn}^{\text{VI}} \end{bmatrix}.$$

Since there are no current sources in a voltage-controlled circuit, we have

$$V'_{mn} = [\mathbb{V}_1 \quad \cdots \quad \mathbb{V}_l] \begin{bmatrix} s_{1,mn}^{\text{VI}} \\ \vdots \\ s_{l,mn}^{\text{VI}} \end{bmatrix}.$$

Thus $\Delta P_V = I_{mn}V'_{mn}$. \square

Corollary 3 *The change of total I^2R loss, ΔP_I , resulting from the parallel removal of a resistor edge with endpoint pair $\{m, n\}$ from a current-controlled circuit is given by $\Delta P_I = -I_{mn}V'_{mn}$, where I_{mn} denotes the current flowing on the edge before its removal, and V'_{mn} denotes the voltage difference between node pair $\{m, n\}$ after its removal.*

Proof: At the end of the proof for Proposition 12, we know that ΔP_I , the change of I^2R loss resulting from removing R_j from the current-controlled sub-circuit, is given by

$$\Delta P_I = -I_{mn} \begin{bmatrix} \mathbb{I}_1 & \cdots & \mathbb{I}_k \end{bmatrix} \begin{bmatrix} s_{1,mn}^{\text{III}} \\ \vdots \\ s_{k,mn}^{\text{III}} \end{bmatrix}.$$

Since there are no voltage sources in a current-controlled circuit, we have

$$V'_{mn} = \begin{bmatrix} \mathbb{I}_1 & \cdots & \mathbb{I}_k \end{bmatrix} \begin{bmatrix} s_{1,mn}^{\text{III}} \\ \vdots \\ s_{k,mn}^{\text{III}} \end{bmatrix}.$$

Thus $\Delta P_I = -I_{mn}V'_{mn}$. □

Remark 7 *A resistor in the circuit is always a passive element as it consumes power. So I_{mn} and V_{mn} are always of opposite polarity. By Lemma 2 (which is given below), we know V_{mn} and V'_{mn} are always of same polarity. Thus by Corollary 2 and Corollary 3, we know the parallel removal of a resistor edge from a voltage-controlled circuit will always decrease total I^2R loss, and the parallel removal of a resistor edge from a current-controlled circuit will always increase total I^2R loss. It is worth mentioning that this is much deeper than the formulas for serial ($R = R_1 + R_2$) and parallel ($R = \frac{1}{1/R_1 + 1/R_2}$) connection of resistors, as the removal of a resistor not only change the resistance of the graph but also redistribute the currents in the graph. Both the above results are consistent with Proposition 10 and Proposition 11.*

Lemma 2 *The parallel attachment of a resistor edge to endpoint pair $\{m, n\}$ in a mixed-source circuit will always decrease the voltage difference between $\{m, n\}$, and will keep the voltage polarity of $\{m, n\}$ unchanged.*

Proof: Thevenin's theorem states that any linear circuit with voltage and current sources and resistances can be replaced at terminals m - n by an equivalent voltage source V_{mn} in series connection with an equivalent resistor R_{mn} . V_{mn} is the voltage obtained at terminals m - n before we add the new resistor edge. Denoting the new voltage obtained at terminals m - n after we add the new resistor edge as V'_{mn} , it is

easy to prove that V'_{mn} must be smaller than V_{mn} , and the voltage polarity of $\{m, n\}$ must be unchanged. \square

Corollary 4 *The change of total I^2R loss, ΔP_V , resulting from the serial removal of a resistor edge with endpoint pair $\{m, n\}$ from a voltage-controlled circuit is given by $\Delta P_V = -I'_{mn}V_{mn}$, where V_{mn} denotes the voltage difference between node pair $\{m, n\}$ before its removal, and I'_{mn} denotes the current flowing through the short circuit edge connecting the node pair $\{m, n\}$ after the removal.*

Proof: Since we are doing a serial removal, it will merge node m and node n together. Electrically, it is equivalent to the parallel attachment of a zero resistance edge to $\{m, n\}$. Corollary 2 shows that the change of total I^2R loss, ΔP_V , resulting from the parallel removal of a zero resistance edge from $\{m, n\}$ is $I_{mn}V'_{mn}$. In other words, it means the parallel attachment of a zero resistance edge to $\{m, n\}$ will change the total loss by $-I'_{mn}V_{mn}$. \square

Corollary 5 *The change of total I^2R loss, ΔP_I , resulting from the serial removal of a resistor edge with endpoint pair $\{m, n\}$ from a current-controlled circuit is given by $\Delta P_I = I'_{mn}V_{mn}$, where V_{mn} denotes the voltage difference between node pair $\{m, n\}$ before its removal, and I'_{mn} denotes the current flowing through the short circuit edge connecting the node pair $\{m, n\}$ after the removal.*

Proof: Again, the serial removal of a resistor edge from $\{m, n\}$ is equivalent to the parallel attachment of a zero resistance edge to $\{m, n\}$. Corollary 3 shows that the change of total I^2R loss, ΔP_I , resulting from the parallel removal of a zero resistance edge from $\{m, n\}$ is $-I_{mn}V'_{mn}$. In other words, it means the parallel attachment of a zero resistance edge to $\{m, n\}$ will change the total loss by $I'_{mn}V_{mn}$. \square

Remark 8 *Results similar to Corollary 2 through Corollary 5 hold for the removal of multiple resistors together, although the proof becomes more involved.*

Combining the results in Corollary 2 through Corollary 5, we have the following:

Corollary 6 *The change of total loss, ΔP_I , resulting from adding a resistance edge to a current-controlled network is equivalent to the change of total loss resulting from adding the resistance edge to its associated Norton equivalent circuit. The change of total loss, ΔP_V , resulting from adding a resistance edge to a voltage-controlled network is equivalent to the change of total loss resulting from adding the resistance edge to its associated Thevenin equivalent circuit.*

Proof: Based on Corollary 2 through Corollary 5, we know that in a single-source network the change of total loss resulting from the attachment (removal) of a resistor edge is completely determined by

- the current flowing through the link after (before) the change, and
- the voltage difference between the endpoints of the edge before (after) the change.

In other words, the change of total loss is independent of the changes of edges other than the one to be removed or added. This good property enables us to use the Thevenin equivalent circuit or the Norton equivalent circuit to predict the change of total loss in a single-source circuit. Since we know the attachment of a link has opposite effect on the loss of a current-controlled circuit and a voltage-controlled circuit, we'd better use Norton equivalent circuit to replace the current-controlled network and use Thevenin equivalent circuit to replace the voltage-controlled network. Of course, using Thevenin equivalent circuit to replace a current-controlled network is theoretically acceptable, but it requires an additional step to get the right answer, i.e. flipping the sign of the change of total loss. So is using Norton equivalent circuit to replace a voltage-controlled network. □

Corollary 7 *The change of total loss, ΔP , resulting from adding a resistance edge, say R_i , to node pair $\{m, n\}$ in a mixed-source circuit is equivalent to the change of total loss, ΔP_{eq} , resulting from adding the edge R_i to the equivalent circuit of the original mix-source circuit at terminal m - n in Fig. 3-8 where I_{eq} is the current source*

in the Norton equivalent circuit of the current-controlled sub-circuit at terminal m - n , V_{eq} is the voltage source in the Thevenin equivalent circuit of the voltage-controlled sub-circuit at terminal m - n , and R_{eq} is the Thevenin/Norton equivalent resistance at terminal m - n .

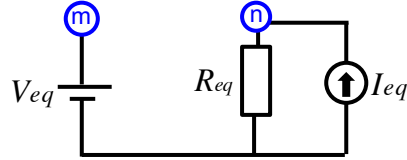


Figure 3-8: The equivalent circuit for a mixed-source network.

Proof: Corollary 6 tells that we can use Norton equivalent circuit to replace the current-controlled sub-circuit and can use Thevenin equivalent circuit to replace the voltage-controlled sub-circuit when calculating the change of total loss in each sub-circuit for a mixed-source one. Moreover, Proposition 12 and Proposition 13 show that the change of total loss in a mixed-source circuit can be completely decomposed into two parts, one for its voltage-controlled sub-circuit and one for its current-controlled sub-circuit. Thus, we just need to “merge” together the Norton equivalent circuit of the current-controlled sub-circuit and Thevenin equivalent circuit of the voltage-controlled sub-circuit for the purposed of calculating the change of total loss for a mixed-source circuit. The idea is visualized in Fig. 3-8. \square

The previous discussion mainly focuses on the effect of adding or removing a resistance edge. We now complete the story by showing the results when a source (either current source or voltage source) edge is added or removed.

Proposition 14 *The change of total losses, ΔP , resulting from the parallel removal (parallel attachment) of a current source \mathbb{I}_j from (to) a mixed-source circuit is given by $\Delta P = \Delta P_I$, where ΔP_I denotes the change of losses resulting from removing (adding) the link \mathbb{I}_j from its current-controlled sub-circuit.*

Proof: As in Proposition 12, we just need to prove the parallel removal part of the proposition.

Again, we assume there are k current sources $\{\mathbb{I}_1, \dots, \mathbb{I}_k\}$, and l voltage sources $\{\mathbb{V}_1, \dots, \mathbb{V}_l\}$, in the circuit. Suppose we are going to remove the last current source \mathbb{I}_k whose endpoint pair is $\{m, n\}$.

By the principle of energy conservation, the change of total I^2R loss must be equivalent to the change of total sources' energy output

$$\sum_{i=1}^{k-1} \mathbb{I}_i \Delta V_i - \mathbb{I}_k V_k + \sum_{i=1}^l \mathbb{V}_i \Delta I_i$$

where ΔV_i denotes the change of voltage difference between the endpoints of the i -th current source, V_k denotes the voltage difference between the endpoints of the k -th current source before the removal, and ΔI_i denotes the change of current flowing through the i -th voltage source.

By Definition 3, we know replacing those short circuits and open circuits created when we generate the initial resistance graph with corresponding voltage and current sources won't change the resistance graph. In addition, the sensitivity of the current flowing through an edge (or of voltage difference between the endpoints of an edge) is completely determined by the resistance graph, i.e. constant resistance graph means constant source factors. Thus by the superposition principle, we know V_k is a linear combination of $\{\mathbb{I}_1, \dots, \mathbb{I}_k\}$ and $\{\mathbb{V}_1, \dots, \mathbb{V}_l\}$, i.e.

$$V_k = [\mathbb{I}_1 \quad \dots \quad \mathbb{I}_k] \begin{bmatrix} s_{1,k}^{\text{III}} \\ \vdots \\ s_{k,k}^{\text{III}} \end{bmatrix} + [\mathbb{V}_1 \quad \dots \quad \mathbb{V}_l] \begin{bmatrix} s_{1,k}^{\text{VI}} \\ \vdots \\ s_{l,k}^{\text{VI}} \end{bmatrix}$$

where $\{s_{1,k}^{\text{III}}, \dots, s_{k,k}^{\text{III}}\}$ and $\{s_{1,k}^{\text{VI}}, \dots, s_{l,k}^{\text{VI}}\}$ are source factors. Following a procedure similar to Proposition 12, we have

$$\begin{bmatrix} \Delta V_1 \\ \vdots \\ \Delta V_{k-1} \end{bmatrix} = -\mathbb{I}_k \begin{bmatrix} s_{k,1}^{\text{III}} \\ \vdots \\ s_{k,k-1}^{\text{III}} \end{bmatrix}$$

$$\begin{bmatrix} \Delta I_1 \\ \vdots \\ \Delta I_l \end{bmatrix} = -\mathbb{I}_k \begin{bmatrix} s_{k,1}^{\text{IV}} \\ \vdots \\ s_{k,l}^{\text{IV}} \end{bmatrix}.$$

By (3.18), we have $s_{k,i}^{\text{III}} = s_{i,k}^{\text{III}}$ ($i = 1, \dots, k$) and $s_{k,i}^{\text{IV}} = -s_{i,k}^{\text{VI}}$ ($i = 1, \dots, l$) which gives us

$$\begin{aligned} & \sum_{i=1}^{k-1} \mathbb{I}_i \Delta V_i - \mathbb{I}_k V_k + \sum_{i=1}^l \mathbb{V}_i \Delta I_i \\ &= -\mathbb{I}_k \left\{ [\mathbb{I}_1 \ \cdots \ \mathbb{I}_{k-1}] \begin{bmatrix} s_{1,k}^{\text{III}} \\ \vdots \\ s_{k-1,k}^{\text{III}} \end{bmatrix} + [\mathbb{I}_1 \ \cdots \ \mathbb{I}_k] \begin{bmatrix} s_{1,k}^{\text{III}} \\ \vdots \\ s_{k,k}^{\text{III}} \end{bmatrix} \right\}. \end{aligned}$$

Thus, the above result is independent of the voltage sources in the mixed-source circuit. By setting the value of all voltage sources to zero, we get the current-controlled sub-circuit. It is easy to prove that ΔP_I , the change of I^2R loss resulting from removing \mathbb{I}_k from the current-controlled sub-circuit, is equivalent to above result. \square

Using the same idea, we can get a similar proposition for the serial removal (serial attachment) of a voltage source from a mixed-source circuit.

Proposition 15 *The change of total losses, ΔP , resulting from the serial removal (serial attachment) of a voltage source \mathbb{V}_j from (to) a mixed-source circuit is given by $\Delta P = \Delta P_V$, where ΔP_V denotes the change of losses resulting from removing (adding) the link \mathbb{V}_j from its voltage-controlled sub-circuit.*

Proof: As in Proposition 12, we just need to prove the serial removal part of the proposition.

Again, we assume there are k current sources $\{\mathbb{I}_1, \dots, \mathbb{I}_k\}$, and l voltage sources $\{\mathbb{V}_1, \dots, \mathbb{V}_l\}$, in the circuit. Suppose we are going to remove the last voltage source \mathbb{V}_l , and its endpoint pair is $\{m, n\}$.

By the principle of energy conservation, the change of total I^2R loss must be equivalent to the change of total sources' energy output

$$\sum_{i=1}^k \mathbb{I}_i \Delta V_i + \sum_{i=1}^{l-1} \mathbb{V}_i \Delta I_i - \mathbb{V}_l I_l$$

where ΔV_i denotes the change of voltage difference between the endpoints of the i -th current source, I_l denotes the current flowing through the l -th voltage source before the removal, and ΔI_i denotes the change of current flowing through the i -th voltage source.

Again, by the superposition principle, we know I_l is a linear combination of $\{\mathbb{I}_1, \dots, \mathbb{I}_k\}$ and $\{\mathbb{V}_1, \dots, \mathbb{V}_l\}$, i.e.

$$I_l = [\mathbb{I}_1 \quad \cdots \quad \mathbb{I}_k] \begin{bmatrix} s_{1,l}^{\text{IV}} \\ \vdots \\ s_{k,l}^{\text{IV}} \end{bmatrix} + [\mathbb{V}_1 \quad \cdots \quad \mathbb{V}_l] \begin{bmatrix} s_{1,l}^{\text{VV}} \\ \vdots \\ s_{l,l}^{\text{VV}} \end{bmatrix}$$

where $\{s_{1,l}^{\text{IV}}, \dots, s_{k,l}^{\text{IV}}\}$ and $\{s_{1,l}^{\text{VV}}, \dots, s_{l,l}^{\text{VV}}\}$ are source factors. Following a procedure similar to Proposition 12, we have

$$\begin{bmatrix} \Delta V_1 \\ \vdots \\ \Delta V_k \end{bmatrix} = -\mathbb{V}_l \begin{bmatrix} s_{l,1}^{\text{VI}} \\ \vdots \\ s_{l,k}^{\text{VI}} \end{bmatrix}$$

$$\begin{bmatrix} \Delta I_1 \\ \vdots \\ \Delta I_{l-1} \end{bmatrix} = -\mathbb{V}_l \begin{bmatrix} s_{l,1}^{\text{VV}} \\ \vdots \\ s_{l,l-1}^{\text{VV}} \end{bmatrix}.$$

By (3.18), we have $s_{l,i}^{\text{VV}} = s_{i,l}^{\text{VV}}$ ($i = 1, \dots, l$) and $s_{l,i}^{\text{VI}} = -s_{i,l}^{\text{IV}}$ ($i = 1, \dots, k$) which gives us

$$\begin{aligned} & \sum_{i=1}^k \mathbb{I}_i \Delta V_i + \sum_{i=1}^{l-1} \mathbb{V}_i \Delta I_i - \mathbb{V}_l I_l \\ &= -\mathbb{V}_l [\mathbb{V}_1 \quad \cdots \quad \mathbb{V}_{l-1}] \begin{bmatrix} s_{1,l}^{\text{VV}} \\ \vdots \\ s_{l-1,l}^{\text{VV}} \end{bmatrix} - \mathbb{V}_l [\mathbb{V}_1 \quad \cdots \quad \mathbb{V}_l] \begin{bmatrix} s_{1,l}^{\text{VV}} \\ \vdots \\ s_{l,l}^{\text{VV}} \end{bmatrix}. \end{aligned}$$

As we can see, the above result is independent of the current sources in the mixed-source circuit. By setting the value of all current sources to zero, we get the voltage-controlled sub-circuit. It is easy to prove that ΔP_V , the change of $I^2 R$ loss

resulting from removing \mathbb{V}_l from the voltage-controlled sub-circuit, is equivalent to above result. \square

By the definition of resistance graph, we know a mixed-source network can be created by the parallel attachment of all current sources and the serial attachment of all voltages to the resistance graph. Thus, combining the result of Proposition 14 and Proposition 15, we can show that the TOTAL I^2R losses of a mixed source circuit are always the sum of TOTAL losses in the voltage controlled sub-circuit and the current controlled sub-circuit.

Proposition 16 (*Additivity of I^2R loss*) *The total I^2R loss, P , of a mixed-source circuit is given by $P = P_I + P_V$, where P_I denotes the total I^2R loss of its current-controlled sub-circuit, and P_V denotes the total I^2R loss of its voltage-controlled sub-circuit.*

When facing the additivity of some squared values, it is natural to wonder if there exists certain form of orthogonality between those values. And we have the follows:

Remark 9 (*Orthogonality between the effects of voltage sources and current sources*) *Suppose there are n resistance edges $\{R_1, \dots, R_n\}$ in the mixed-source circuit, and we denote the currents flowing on the i -th resistance edge as I_i^M in the mixed-source circuit, I_i^V in its voltage-controlled sub-circuit, and I_i^I in its current-controlled sub-circuit, respectively. The diagonal matrix of edge resistances is*

$$\Lambda = \text{diag}\{R_1, \dots, R_n\}$$

Write the vector of currents flowing through each edge as $\vec{I}_M = [I_1^M, \dots, I_n^M]^T$ in the mixed-source circuit, $\vec{I}_V = [I_1^V, \dots, I_n^V]^T$ in the voltage-controlled sub-circuit, and $\vec{I}_I = [I_1^I, \dots, I_n^I]^T$ in the current-controlled sub-circuit, respectively. Then by the superposition principle, we must have

$$\begin{aligned} \vec{I}_M^T \Lambda \vec{I}_M &= (\vec{I}_V^T + \vec{I}_I^T) \Lambda (\vec{I}_V + \vec{I}_I) \\ &= \vec{I}_V^T \Lambda \vec{I}_V + \vec{I}_I^T \Lambda \vec{I}_I + 2\vec{I}_V^T \Lambda \vec{I}_I. \end{aligned}$$

Combining the above result with Proposition 16, we must have

$$\vec{I}_V^T \Lambda \vec{I}_I = 0.$$

We end this section by showing two corollaries that are able to explain the paradoxical behavior happening in Fig. 3-5.

Corollary 8 *The change of total I^2R loss, ΔP_I , resulting from the parallel removal of a current source \mathbb{I} with endpoint pair $\{m, n\}$ from a current-controlled circuit is given by $\Delta P_I = -\mathbb{I}(V_{m,n} + V'_{m,n})$, where $V_{m,n}$ and $V'_{m,n}$ denote the voltage differences between node pair $\{m, n\}$ before and after its removal, respectively.*

Proof: Again, we assume there are k current sources $\{\mathbb{I}_1, \dots, \mathbb{I}_k\}$ in the circuit. Suppose we are going to remove the last current source \mathbb{I}_k , and its endpoint pair is $\{m, n\}$. At the end of the proof of Proposition 14, we know

$$\Delta P_I = -\mathbb{I}_k [\mathbb{I}_1 \quad \dots \quad \mathbb{I}_{k-1}] \begin{bmatrix} s_{1,k}^{\mathbb{I}} \\ \vdots \\ s_{k-1,k}^{\mathbb{I}} \end{bmatrix} - \mathbb{I}_k [\mathbb{I}_1 \quad \dots \quad \mathbb{I}_k] \begin{bmatrix} s_{1,k}^{\mathbb{I}} \\ \vdots \\ s_{k,k}^{\mathbb{I}} \end{bmatrix}.$$

Also we know

$$V_{m,n} = [\mathbb{I}_1 \quad \dots \quad \mathbb{I}_k] \begin{bmatrix} s_{1,k}^{\mathbb{I}} \\ \vdots \\ s_{k,k}^{\mathbb{I}} \end{bmatrix}$$

and

$$V'_{m,n} = [\mathbb{I}_1 \quad \dots \quad \mathbb{I}_{k-1}] \begin{bmatrix} s_{1,k}^{\mathbb{I}} \\ \vdots \\ s_{k-1,k}^{\mathbb{I}} \end{bmatrix}.$$

Thus $\Delta P_I = -\mathbb{I}(V_{m,n} + V'_{m,n})$. □

Corollary 9 *The change of total I^2R loss, ΔP_V , resulting from the serial removal of a voltage source \mathbb{V} with endpoint pair $\{m, n\}$ from a voltage-controlled circuit is given by $\Delta P_V = -\mathbb{V}(I_{m,n} + I'_{m,n})$, where $I_{m,n}$ denotes the current that flowed through the voltage source before the removal, and $I'_{m,n}$ denotes the current flowing through the short circuit edge connecting the node pair $\{m, n\}$ after the removal.*

Proof: Again, we assume there are l voltage sources $\{\mathbb{V}_1, \dots, \mathbb{V}_l\}$, in the circuit. Suppose we are going to remove the last current source \mathbb{V}_l , and its endpoint pair is $\{m, n\}$.

At the end of the proof of Proposition 15, we know

$$\Delta P_V = -\mathbb{V}_l [\mathbb{V}_1 \quad \dots \quad \mathbb{V}_{l-1}] \begin{bmatrix} s_{1,l}^{\mathbb{V}\mathbb{V}} \\ \vdots \\ s_{l-1,l}^{\mathbb{V}\mathbb{V}} \end{bmatrix} - \mathbb{V}_l [\mathbb{V}_1 \quad \dots \quad \mathbb{V}_l] \begin{bmatrix} s_{1,l}^{\mathbb{V}\mathbb{V}} \\ \vdots \\ s_{l,l}^{\mathbb{V}\mathbb{V}} \end{bmatrix}.$$

Also we know

$$I_{mn} = [\mathbb{V}_1 \quad \dots \quad \mathbb{V}_l] \begin{bmatrix} s_{1,l}^{\mathbb{V}\mathbb{V}} \\ \vdots \\ s_{l,l}^{\mathbb{V}\mathbb{V}} \end{bmatrix}$$

and

$$I'_{mn} = [\mathbb{V}_1 \quad \dots \quad \mathbb{V}_{l-1}] \begin{bmatrix} s_{1,l}^{\mathbb{V}\mathbb{V}} \\ \vdots \\ s_{l-1,l}^{\mathbb{V}\mathbb{V}} \end{bmatrix}.$$

Thus $\Delta P_V = -\mathbb{V}(I_{m,n} + I'_{m,n})$. □

Remark 10 *Results similar to Corollary 8 through Corollary 9 hold for the removal of multiple sources together, although the proof becomes more involved.*

Remark 11 *Proposition 14 and Corollary 8 together explain the reason for the paradoxical behavior in Fig. 3.5. After we create the current-controlled sub-circuit of Fig. 3.5(a), we can compute the voltage difference between the node pair from which the 0.25A current source is removed. The voltage difference between this node pair is 0V and 0.125V before and after the removal, respectively. So the total loss will decrease by $0.25(0 + 0.125) = 0.03125$ W.*

3.4 Four Equivalent Loss Computing Methods for Mixed-Source Circuit

Based on the discussion in last section, we can generalize four different methods to calculate the total I^2R loss of an arbitrary mixed-source circuit. To describe and compare them, we assume there are k current sources $\{\mathbb{I}_1, \dots, \mathbb{I}_k\}$, l voltage sources $\{\mathbb{V}_1, \dots, \mathbb{V}_l\}$, and t resistors $\{\mathbb{R}_1, \dots, \mathbb{R}_t\}$ in the circuit.

- (a) The first way is the most traditional one. We calculate either the total power output of all voltage sources and current sources or the total I^2R loss of all resistors which is given by

$$\sum_{i=1}^k \mathbb{I}_i V_i + \sum_{i=1}^l \mathbb{V}_i I_i \quad (\text{or } \sum_{i=1}^t P_{\mathbb{R}_i})$$

(3.19)

s.t. Kirchoff voltage laws

Kirchoff current laws

where V_i denotes the voltage difference between the endpoints of the i -th current source before the removal, I_i denotes the current flowing through the i -th voltage source before the removal, and $P_{\mathbb{R}_i}$ denotes the I^2R loss of the i -th resistor. \mathbb{I}_i and \mathbb{V}_i are the controlling current sources and voltage sources respectively, they remain constant under the considered topology reconfiguration.

- (b) The second way is based on the following idea: a mixed-source circuit can be created by first constructing the current-controlled sub-circuit and then putting back all voltage sources. We've showed that the partial derivative of the cost function P_I described by Equ. (3.5) in the direction I_{e_i} is exactly double the algebraic sum of all voltages on the fundamental cycle defined by e_i . This means we are including the constraints associated with Kirchoff's voltage law and the voltage sources \mathbb{V}_i relative to fundamental cycles in which they appear. The total loss is thus given by minimizing cost function P_I with linear constraints denoting the effect of voltage sources.

$$\min P_I$$

s.t. constraints denoting the effect of voltage sources are satisfied

(3.20)

- (c) The third way is quite similar to the second way: a mixed-source circuit can be created by first constructing the voltage-controlled sub-circuit and then putting back all current sources. Following an idea similar to (b), the total loss can be given by minimizing cost function P_V described in Equ. (3.12) with linear constraints denoting the effect of current sources.

$$\begin{aligned} & \min P_V \\ & \text{s.t. constraints denoting the effect of current sources are satisfied} \end{aligned} \tag{3.21}$$

- (d) The fourth way is based on Proposition 16 and is given by

$$\min P_V + \min P_I \tag{3.22}$$

where P_V is the potential function (described by Equ. (3.12)) of the voltage-controlled sub-circuit, and P_I is the potential function (described by Equ. (3.5)) of the current-controlled sub-circuit.

Although the four methods are of different mathematical forms, they must give us the same result. Specifically, methods (b), (c), and (d) are closely related to each other. In mixed source networks, the operating values of voltages and currents are determined as critical values of P_V (as a quadratic function of fundamental node variables) and P_I (as a quadratic function of fundamental cycle variables) where it is assumed that all voltage sources \mathbb{V}_i and current sources \mathbb{I}_i are present. This is the approach of methods (b) and (c). This approach can be carried out by solving for critical points of P_I (with respect to the fundamental cycle variables) subject to the Kirchhoff voltage constraints that are obtained by adding the \mathbb{V}_i to the resistance graph. Similarly, one can solve for the critical points of P_V (with respect to the fundamental node variables) subject to the Kirchhoff current constraints that are

obtained by adding the \mathbb{I}_i to the resistance graph. Method (d) utilizes the novel decomposition of mixed-source circuit in Proposition 16 and integrates (b) and (c) together. By calculating the loss of the voltage-controlled sub-circuit P_V and the loss of the current-controlled sub-circuit P_I individually, method (d) solves for the loss of a mixed-source circuit in an unconstrained quadratic programming form.

3.5 Summary

In a nutshell, the work in this chapter proves that in a single-source network, although the detailed change of loss is impossible to predict without solving the Kirchhoff's equations, the sign of the overall change in I^2R loss is always certain. Such predictability with respect to total loss is not present in a mixed-source network, and this may result in interesting paradoxes such as fewer sources producing more power. While the demonstrated uncertainty to changes in a mixed-source circuit together with the well recognized complexity in line switching suggests that active control of grid topology in a mixed-source model is a formidable problem, our results nevertheless offer a clean decomposition for the mixed-source circuit that completely separates the effect of current sources and voltage sources on network total loss. As the world's power grids increasingly embrace novel energy sources and new classes of assets associated with storage and demand response, the decomposition concepts we have presented can be used for developing new approaches to resource allocation that appropriately balance generation scheduling, grid topology configuration, and recruitment of demand response.

Chapter 4

Heuristics of Topology Control

A standard and widely adopted approach to modeling topology reconfiguration uses binary variables to indicate the status of candidate lines (in or out of service) in a mixed integer programming (MIP) formulation (Fliscounakis et al., 2007). While Ch. 3 showed that in a voltage-controlled or current-controlled DC circuit, the sign of the overall I^2R congestion change due to topology control is always predictable, the magnitude of change can only be determined by solving Kirchhoff equations, suggesting the necessity of having solution validation in the process of transmission line switching. Such validation involves redoing the OPF problem and therefore is usually the most time consuming part of the problem solving process. To address the combinatorial explosion and to reduce validation times, a lot of recent work focuses on developing fast heuristic algorithms that carefully select the most promising candidate line under a variety of criteria. References (Hedman et al., 2009; Fisher et al., 2008; Fuller et al., 2012; Ruiz et al., 2012a; Ruiz et al., 2017) show the effectiveness of heuristics co-optimizing the generation and the network topology through simulations on different testbed systems. In spite of the seemingly promising simulation results of the heuristic approaches pursued by the research community and a certain level of proven predictability (Baillieul et al., 2015; Wang and Baillieul, 2016; Wang and Baillieul, 2017) of topology control, satisfactory grid-scale solutions are ever-elusive. At the same time, the quest for firmer theoretical foundations of the heuristic approaches continues.

This Chapter first examines fundamental challenges associated with heuristics for topology reconfiguration of power grids. We begin the discussion by exploring a list of paradoxical behaviors associated with greedy heuristics for topology control, and describe examples showing that many plausible heuristic approaches fail to achieve acceptable grid operation. In particular, we define the concepts of *commutativity* which is the ease of creating an optimal sequence of operations out of optimal sub-sequences, and *monotonicity* which is the possibility of continued step-wise improvement on the effects of previous operations, and *consistency* which is the ease of obtaining better operation by increasing the computational complexity. Simulation results, however, discounts the prevalence of the afore mentioned paradoxical behavior by statistically showing the value of locally optimal switch at each stage in reducing generation costs. A theoretical justification is also provided in supporting the value of greedy heuristic in topology control. In order to further reducing the computational cost of greedy heuristic, we propose a fast grid decomposition algorithm based on *vertex cut sets* whose efficiency is then tested and confirmed by simulations on IEEE 118 bus system.

4.1 Paradox in Topology Control Heuristics

In recent years there has been a significant interest in co-optimizing network topology and generation. Hedman et al., 2008, Fisher et al., 2008, Ruiz et al., 2012 and Fuller et al., 2012 show the effectiveness of such co-optimization through simulations on the IEEE 118-bus system and the the WECC 179-bus system. For example, the work reported in Ruiz et al., 2011 finds topology improvements by iteratively solving the linear programming (LP) formulation of the DC optimal power flow (DCOPF) by means of a heuristic algorithm that disconnects the one unprofitable line per iteration while ensuring an N-1 reliable network. Such a heuristic approach is one

way of avoiding the severe computational complexity of the line switching problems, and makes the real time topology control possible. The NP-hardness of the problem, however, makes optimality not guaranteed by any heuristic, and we are led to a set of interesting paradoxical phenomena.

In this section, we focus our attention on several iterative greedy heuristics in which the main idea is to disconnect/connect the line(s) that can reduce the cost most in each iteration. We show paradoxical behaviors associated with the heuristics by using some simple 3-bus power system examples.

Non-commutativity

The first paradoxical behavior is that the most beneficial single line may not be included in the most beneficial pair of lines or the most beneficial set of n ($n > 2$) lines. We call this the *non-commutativity* property of the topology control problem. This problem can be easily illustrated as follows.

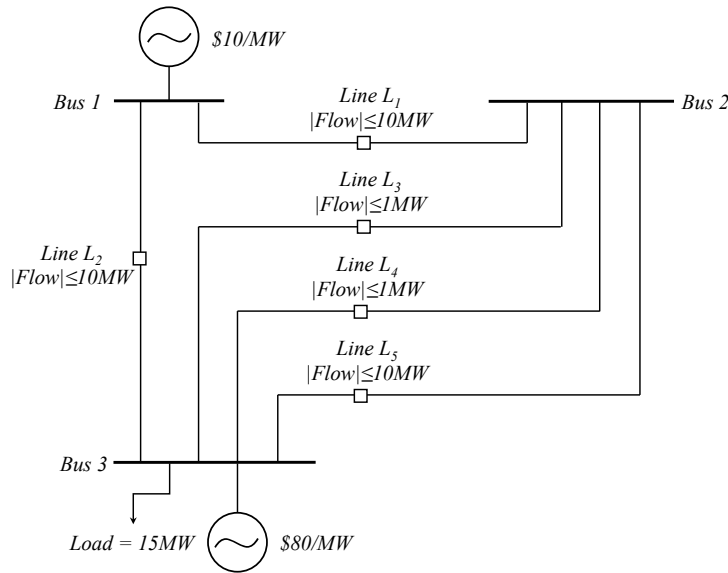


Figure 4.1: The example of non-commutativity problem.

In Fig. 4.1, there are two generators with the cheap one on bus 1 and the expensive one on bus 3 and a 15MW demand on bus 3. We assume that all transmission lines

have the same susceptance, and the line capacities range from 1MW to 10MW as marked in the figure. The original cost before applying topology control is \$710 with the cheap generator supplying 7MW and the expensive generator supplying 8MW.

If we remove the most beneficial line per iteration, then we will remove the line L1 and the cost will be \$500 with the cheap generator supplying 10MW and the expensive generator supplying 5MW. The algorithm will stop here as we can't further reduce the cost by removing another line. However, if we are allowed to remove the most beneficial pair of lines per iteration, then we will keep L1 connected and instead remove the line L3 and L4 together and the cost will be \$150 which equals the cost of unconstrained optimal power flow.

Non-monotonicity

The second paradoxical behavior is that one line which was removed earlier may be reconnected later because keeping it switched off is no longer beneficial. We call this the *non-monotonicity* property of the topology control problem.

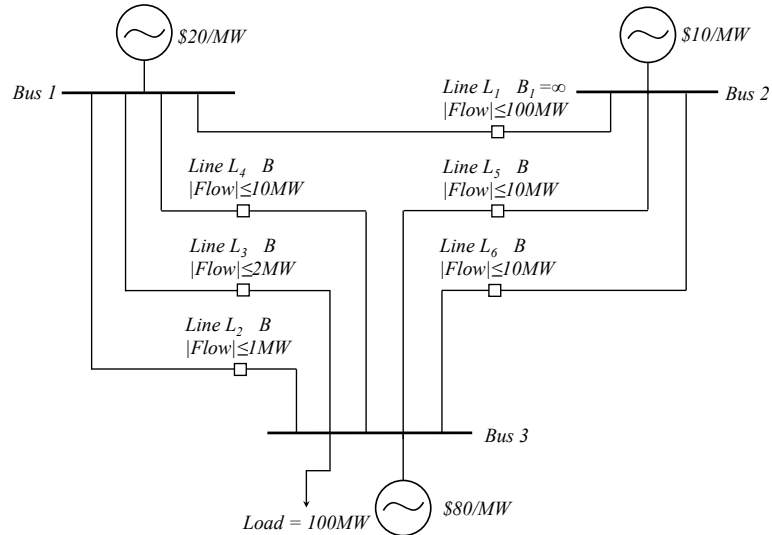


Figure 4.2: The example of non-monotonicity.

This problem is illustrated in Fig. 4.2 which shows a power system with the

cheapest generator on bus 2, a slightly more expensive generator on bus 1, and the most expensive generator on bus 3. We assume that the susceptance of the horizontal transmission line is large enough and all other lines are of the same but limited susceptance. There is a demand of 100MW on bus 3 and the line capacities range from 1MW to 100MW as marked in the figure. The original cost before applying topology control is \$7650 with the cheapest generator supplying 5MW and the most expensive generator supplying 95MW.

Suppose we can either remove or connect the most beneficial line per iteration, then we will remove the line L1 first, line L2 second, and line L3 third. In the fourth iteration, however, we find that having L1 out of service is no longer beneficial and we can reduce the cost by reconnecting L1. After the reconnecting, the cost would be \$5900 with the cheapest generator supplying 30MW and the most expensive generator supplying 70MW. The algorithm will stop here as we can't further reduce the cost by removing or reconnecting another line.

Non-consistency 1

The third example illustrated in in Fig. 4-3 shows that an algorithm that only allows removal of one line per iteration may outperform another algorithm that allows to either remove or reconnect one line per iteration. We call this the *non-consistency* property of the topology control problem. This shows that the increased computational complexity sometimes is not compensated by lower generation cost.

Fig. 4-3 shows a power system with the cheapest generator on bus 2, and the mid-cost generator on bus 1, and the most expensive generator on bus 3. We assume that the susceptance of the horizontal transmission line is large enough and all other lines are of the same but limited susceptance. There is a demand of 100MW on bus 3 and the line capacities range from 1MW to 100MW as marked in the figure. The

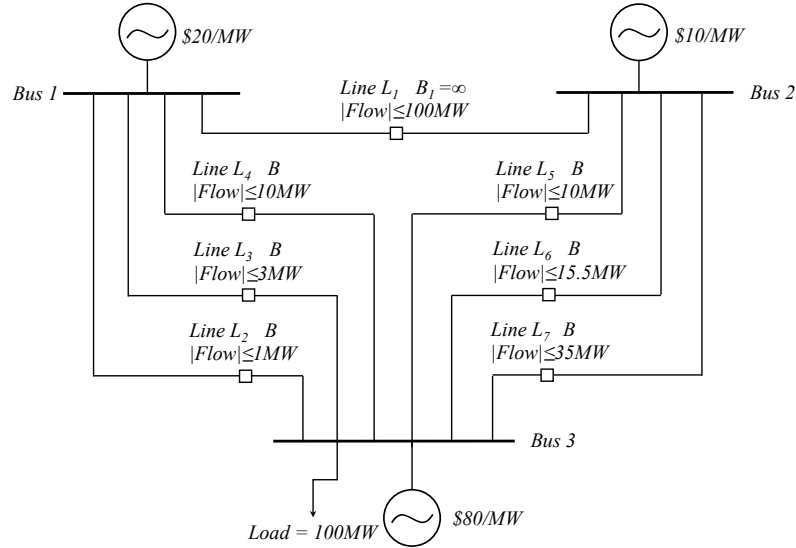


Figure 4-3: The first example of non-consistency problem.

original cost before applying topology control is \$7580 with the cheapest generator supplying 6MW and the most expensive generator supplying 94MW.

Algorithm (1) (only allowing removal of one line per iteration) will remove line L1 first, line L2 second, line L3 third, line L5 fourth, and line L6 last. The final cost will be \$4950 and with the cheapest generator supplying 35MW, and the mid-cost generator supplying 10MW, and the most expensive generator supplying 55MW.

Algorithm (2) (allowing to either remove or reconnect one line per iteration) will remove line L1 first, line L2 second, and line L3 third. In the fourth iteration, line L1 will be reconnected and the algorithm stops. The cost will be \$5200 with the cheapest generator supplying 40MW and the most expensive generator supplying 60MW.

As we can see algorithm (1) outperforms algorithm (2).

Non-consistency 2

The fourth example illustrated in Fig. 4-4 shows another type of non-consistency property: one algorithm that only allows removal of one line per iteration may outperform another algorithm that allows removal of at most 2 lines line per iteration.

Fig. 4.4 shows a power system with the cheap generator on the upper bus and the expensive generator on the lower bus. We assume that the susceptances of L1 through L7 are 8S, 1.1S, 1.1S, 5S, 5S, 5S and 10S, respectively. There is a demand of 100MW on the lower bus and the line capacities of L6 and L7 are both 10MW. The line capacities of other lines are assumed to be sufficiently large. The original cost before applying topology control is \$6775 with the cheap generator supplying 17.5MW and the expensive generator supplying 82.5MW.

Algorithm (1) (only allowing removal of one line per iteration) will remove line L1 first, line L2 second, and line L3 third. The cost will be \$6600 with the cheap generator supplying 20MW and the expensive generator supplying 80MW. The algorithm will stop here as we can't further reduce the cost by removing another line.

Algorithm (3) (allowing to remove at most two lines per iteration) will remove line L4 and L5 in the first iteration, with the resulting cost being \$6607 with the cheap generator supplying 19.9MW and the expensive generator supplying 80.1MW. The algorithm will stop here as we can't further reduce the cost by removing or reconnecting another line or another pair of lines.

As we can see algorithm (1) outperforms algorithm (3).

Mathematically, the Algorithms (1), (2) and (3) described above are of the same level of performance, i.e. no one dominates another. For a general binary programming problem, only when the search space of one heuristic explicitly contains that of the other can it declare dominancy. Thus the paradoxical phenomenon, “*no ‘guaranteed’ extra return for increased computational complexity*”, can be observed in all types of non-brute-force heuristics. This phenomenon, which makes the binary programming problem extremely challenging, is visualized in Fig. 4.5.

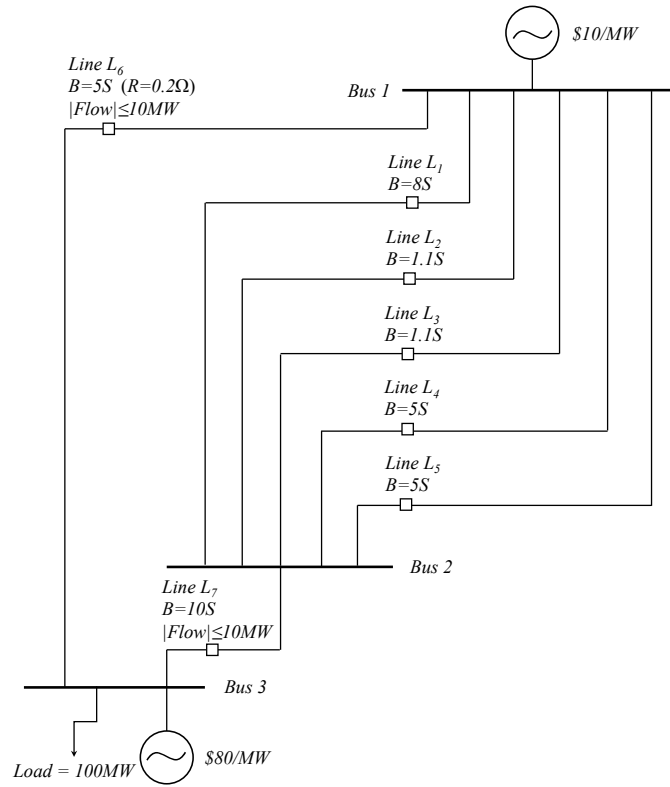


Figure 4.4: The second example of non-consistency problem.

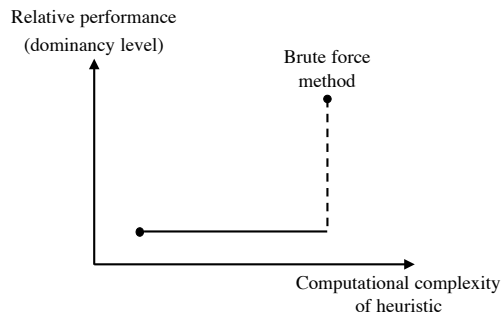


Figure 4.5: Visualization of the paradoxical phenomenon: no extra return for increased computational complexity of heuristics in topology control.

4.2 Paradigm in Topology Control Heuristics

The last section explicitly discounts the value of increased computational effort of heuristics in reducing the generation cost for a *specific* grid scenario. It is natural to ask if the next best thing is true: can the increased computational effort “statistically” reduce more generation cost for a *large set* of scenarios? The result of our simulations suggests the answer is yes.

Test Network Overview

The heuristics were tested on the IEEE 118-bus test system. This test system represents a portion of the Midwestern US Power System as of December, 1962. The version of the test system employed and the generator cost information used in the IEEE 118 network are extracted from Basak et al., 2012. The test system consists of 118 buses, 54 generators, and 194 lines, all of which are assumed to be connected in the initial topology.

Heuristics Overview

Three heuristics were tested and compared in this section. All of them sequentially disconnect transmission lines until no further generation costs can be reduced.

To make this a fair comparison, all heuristics only open closed switches and do not close open switches since the *Line Profits Heuristic* cannot compute potential improvements from reconnecting disconnected lines.

- **Random Heuristic**

The algorithm is specified in Fig. 4-6. This heuristic sequentially solves the DCOPFs. In each iteration, if the DCOPF is feasible, a set of switchable candidate lines is then created. The cardinality of the switchable set is reduced in each iteration after randomly disconnecting a switchable unprofitable line.

In addition, the switchable set enforces a relaxed form of the “N-1” reliability requirement: at no time is a load or generator bus connected by less than TWO lines. The heuristic stops when no switchable unprofitable lines can be found.

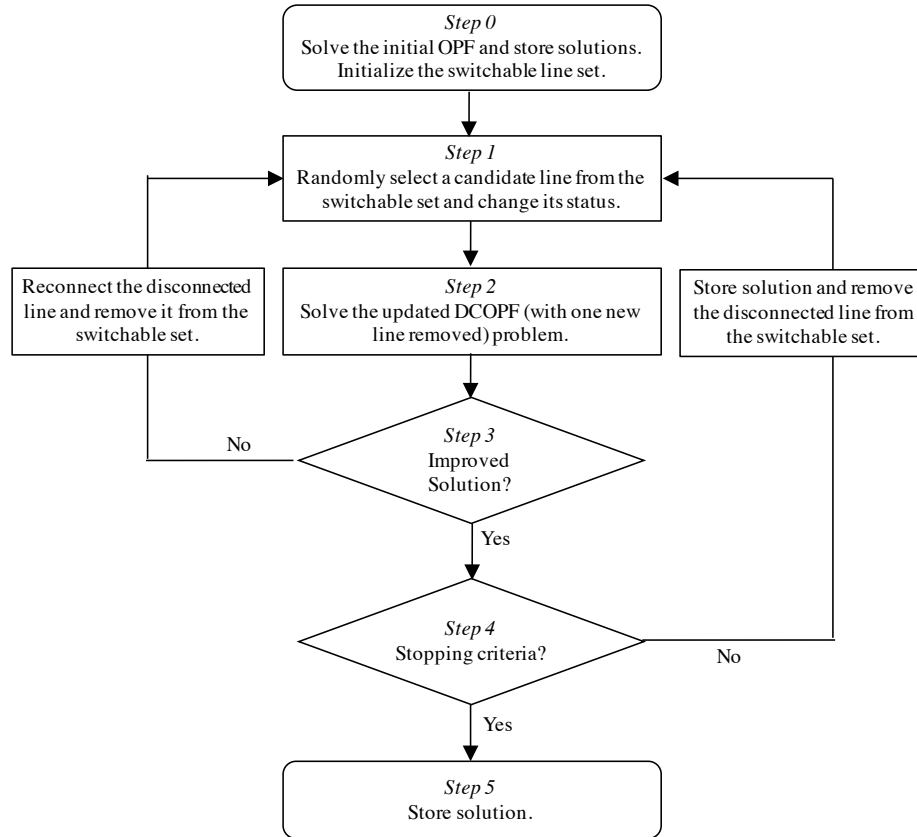


Figure 4-6: Flow chart describing general algorithm structure of the Random Heuristic.

- **Line Profit Heuristic**

This heuristic is proposed in Ruiz et al., 2011, and is named after the metric used in the switching criteria. Its algorithm structure is almost the same as Fig. 4-6 except for Step 1. In the line switching step, the line profits, $f_l(\pi_{n_l} - \pi_{m_l})$, are computed where f_l is the power flow on transmission line l , and $\pi_{n_l} - \pi_{m_l}$ are the *locational marginal price (LMP)* difference between the two ending buses of line l . The most unprofitable line, rather than a random line, is selected as a

candidate for opening. Please refer Ruiz et al., 2011 and Ruiz et al., 2012a for more details.

- **Standard Greedy Heuristic**

The algorithm is specified in Fig. 4.7. Unlike the Line Profit Heuristic that first sorts the candidate lines based on their line profits $f_l(\pi_{n_l} - \pi_{m_l})$ and then selects the first line whose removal leads to savings in the updated DCOPF, the Standard Greedy Heuristic redoes the updated DCOPF for each allowable line removal and then selects the single line to be removed that leads to maximum savings in each iteration.

Clearly, optimality is not guaranteed with any of the heuristics, since the transmission topology is not co-optimized with power dispatch.

Simulation Results and Analysis

To generate the test scenarios for the heuristics, a fixed load is maintained and we perform a Monte Carlo simulation where the generator costs are randomly varied. The sample size used for the Monte Carlo simulation is 50. The percent savings rather than the dollar value are the focus of the comparison.

Two benchmark cases are used to evaluate the savings of the heuristic: Case one considers the initial topology and line constraints whose DCOPF sets an upper bound of the total generation costs, and Case two considers the unconstrained case whose DCOPF provides a lower bound of the generation costs. The cost difference between the two benchmark cases is called the *maximum attainable savings (MAS)*.

The three heuristics are implemented in Matlab, using MATPOWER (Zimmerman et al., 2011) as the DCOPF solver. The performance comparison among the three heuristic is detailed in Table 4.1.

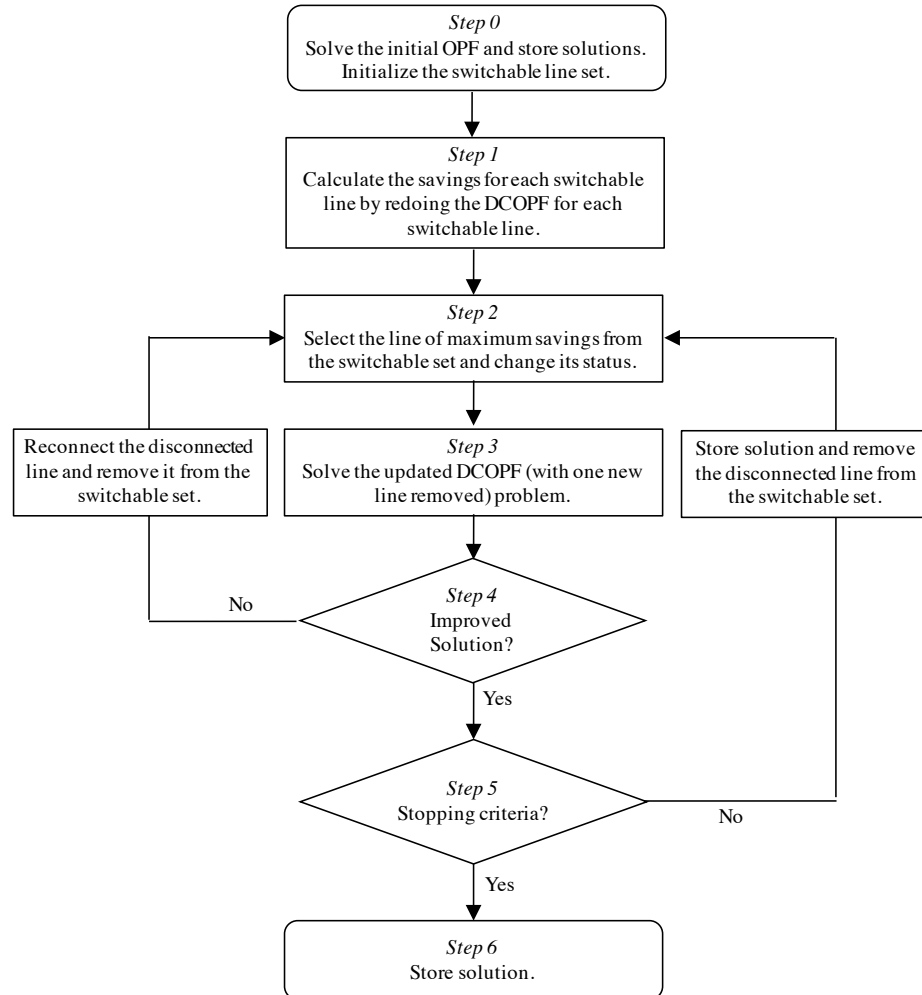


Figure 4-7: Flow chart describing general algorithm structure of the Standard Greedy Heuristic.

Table 4.1: Performance comparison 1.

heuristic	saving/MAS	lines disconnected	mean effort
Random	0.517 ± 0.092	31.22 ± 6.37	0.193
Line Profit	0.631 ± 0.049	14.53 ± 4.12	0.317
Greedy	0.672 ± 0.051	10.18 ± 3.98	1

Strictly speaking, the three heuristics are said to be of the same level computational complexity as they need to redo the DCOPF for each switchable line in the worst case. For example, the Random Heuristic or the Line Profit Heuristic may, though with very low probability, not be able to find a switchable unprofitable line until after redoing the DCOPF for each allowable line removal. In general, the Standard Greedy Heuristic, however, costs much more computational effort than the Random Heuristic and the Line Profit Heuristic especially for a large scale networks. The benefit of the additional computational effort is the increased switching quality, i.e. higher cost reduction achieved at each stage. In general, the switching savings in each iteration is the best in Standard Greedy Heuristic, the worst in the Random Heuristic and better in Line Profit Heuristic. Unlike the paradoxical behaviors for specific scenarios, the better switching quality accumulated in each iteration does lead to more average saving for a set of test scenarios as shown in Table 4.1, which may outweigh the extra computational cost.

It is natural to expect one heuristic may save more if it disconnects more lines. What seems counterintuitive is that, on average, the Standard Greedy Heuristic not only attains maximum savings but also disconnects the fewest lines. This, however, can be well explained by Proposition 10 and Corollary 3.

Recalling the equivalence between the current-controlled circuits and DC power flow models of transmission grids shown in Table 2.1, Proposition 10 tells us that the new transmission network obtained after line switching has fewer lines but has higher total real f^2/B (squared line flow over line susceptance) congestion. Corollary 3 quantifies the increase of the I^2R losses of a circuit due to a disconnected resistor

by using the product of two electrical parameters associated with that disconnected resistor. In the DC power flow models of transmission grids, it is equivalent to say that the increase of total real f^2/B of a transmission grid due to one line removal is given by the product of the power flowing through that transmission line flow before its removal and the phase difference between its ending buses after its removal.

One profitable switching that can greatly reduce the generation cost usually significantly redistributes the power flowing across the network. Such effect is unlikely to be obtained by switching a transmission line with relatively small pre-removal line flow and post-removal phase difference between its ending buses. Since the Standard Greedy Heuristic always executes the line removal leading to maximum savings in each iteration, it is reasonable to expect that the average increase of total real f^2/B in each iteration of the Standard Greedy Heuristic is usually larger than that of the Random Heuristic and Line Profit Heuristic. The combination of the above result together with the ever decreasing total $\overline{f^2}/B$ capacity due to fewer lines in service explain the superior performance of the Standard Greedy Heuristic: not only better approximating the global optimal solution but also better enforcing network connectivity.

4.3 Grid Decomposition Heuristics Based on Vertex Cut Sets

Despite of the superior performance of the Standard Greedy Heuristic, the significant computational cost may limit its application especially for large scale networks. When dealing with the “largest machine in the world” the transmission network, one natural idea is a divide-and-conquer strategy. We ask whether this large and complex system can be usefully decomposed into smaller, more tractable subsystems, thereby reducing the computational effort in optimal power flow (OPF) calculations. Here, we refer the ease of building a system out of subsystems as *composability*, and the ease of

validation of system properties by using the related subsystems as *compositionality* (Kammerer et al., 2013).

In Ch. 2, we proved that the impact of topology control is strictly confined within the biconnected component in which the line switching is applied in a transmission network. The decomposition of a transmission network based on biconnected components is thus “clean” in the sense that if the sizes of all its biconnected components are relatively small, the network will have high level composability and compositionality. Today’s transmission grids, however, can be highly meshed in order to meet reliability standards. Therefore, a large portion of the grid or even the whole grid can be biconnected. What comes with the seemingly ubiquitous opportunities of relieving line congestions provided by a large biconnected component may well be a significantly decreased level of the network composability and compositionality.

While we should not neglect that every switchable line has the potential to alleviate the congestion in a biconnected component of a grid, simulation results in Ruizet al., 2011 showed that a fairly large portion of the switchable lines remained not operated in most samples, and thereby might well go unnoticed. Such observations suggest the possibility that a biconnected component of a grid may still be effectively further decomposed even if the interactions between the sub-grids in the biconnected component are not zero.

Our work thus aims to find an optimal trade off between the size of sub-grids of the biconnected component and the realized composability/compositionality by the grid decomposition. The desired outcome should help us focus attention on a relatively small set of promising switchable lines such that both the computational efforts and the attainable savings can be reasonably controlled.

4.3.1 Vertex Cut Sets & Pseudo Biconnected Components

The initially “clean” decomposition of a transmission grid involves a graph theory term called *cut vertex* which is any single vertex/node whose removal increases the number of connected components of a graph and, by definition, is the only element shared by two or more biconnected components of the graph.

Apparently, further decomposing a biconnected component needs something beyond cut vertex in graph theory, and we have the follows:

Definition 12 *A vertex cut set is a set of vertices of a graph which, if removed together with any incident edges, disconnects the graph. The sub-graphs of a biconnected graph obtained by one or several vertex cut sets are called pseudo biconnected components. The vertices in the vertex cut sets are the only elements shared by two or more pseudo biconnected components. In addition, the union of several vertex cut sets for a given graph is also a vertex cut set.*

Using the concept of vertex cut sets, a two-step construction of pseudo biconnected components can be carried out. Given a graph and a vertex cut set, the disconnected subgraphs remaining when the vertex cut set, together with any incident edges, is removed are called the pre pseudo biconnected components. From these, the pseudo biconnected components are obtained by adjoining the vertex cut set to each pre pseudo biconnected component the entire vertex cut set along with the incident edges that have been removed. Fig. 4-8 shows an example of the decomposition of a biconnected graph where the three red nodes in the middle of graph form the vertex cut set. Note that the decomposition based on one vertex cut set may not be unique. For example, the horizontal black edge in Fig. 4-8(a) can be either assigned to the black-edge sub-graph (Fig. 4-8(c1)) or to the blue-edge sub-graph (Fig. 4-8(c2)). Thus we do have some degree of discretion in decomposing the grid. To reduce the search space of line switching, we will use the convention throughout this paper that, whenever possible, any incident edges of the vertex cut set subject to our discretion

will be assigned to a pseudo biconnected component that is free of congested lines.

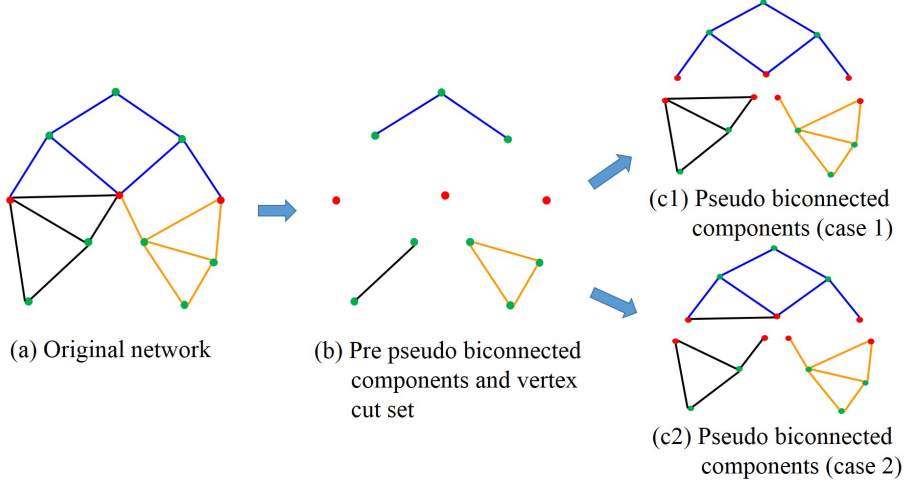


Figure 4-8: One example of the decomposition based on a vertex cut set formed by the three red nodes in the middle.

Ideally, we would expect the decomposition in Fig 4-8 to satisfy the following criteria:

- (1) The interactions between any two lines belonging to two different pseudo biconnected components are insignificant;
- (2) The size of the targeting pseudo biconnected component is large enough to contain all promising switchings;
- (3) The size of the targeting pseudo biconnected components is small enough to be efficiently searched.

4.3.2 Embedded Wheatstone Bridge & LODF

So far, the interactions mentioned in Criterion (1) above are somehow still an abstract notion, therefore requiring some metrics to quantify the effects of line outages.

We recall that the *embedded Wheatstone bridge* between any pair of links in a biconnected component can be created by first applying Kron reduction to the graph

and then getting a simple canonical form of the Wheatstone bridge. In spite of the seemingly ubiquitous interactions in a biconnected component, Lemma 1 proves that the removal of a line has no effect on another line if there is an *embedded balanced Wheatstone bridge* between their pairs of endpoints even when both lines are in the same biconnected component. An embedded balanced Wheatstone bridge in a biconnected component is clearly a singular case with probability zero and thus is trivial for the analysis of any real network. Equ. (2.30), however, points out that the more balanced the embedded balanced Wheatstone bridge is, the weaker the interaction is. This means that if there is a roughly balanced Wheatstone bridge between any two lines that come from two different pseudo biconnected components in a grid, such a decomposition technically works. Although the decomposition based on incompletely balanced Wheatstone bridge is imprecise in the sense that some power will flow between pseudo biconnected components, it offers some hope that it may be possible to isolate congestion effects to a relatively small part of the network, thus effectively reducing the computational complexity.

To quantify the interactions between lines in a transmission grid, we introduce the well-known sensitivity, *line outage distribution factor* or *LODF*, denoted by $\zeta_i^{(j)}$, of the power flowing through line i with respect to the removal of line j . In short, $\zeta_i^{(j)}$ denotes the percentage of line flow on line j that will show up on line i after the outage of line j . Similarly, we can compute another LODF, denoted by $\zeta_j^{(i)}$, of the current flowing through line j with respect to the removal of line i . The pair of LODFs, $\zeta_i^{(j)}$ and $\zeta_j^{(i)}$, are usually different. The interactions between the line pair $\{i, j\}$ are said to be insignificant if $\zeta_i^{(j)}$ and $\zeta_j^{(i)}$ are both small. Similarly, the interactions between two pseudo biconnected components are said to be insignificant if the pair of LODFs for any two lines belonging to two different pseudo biconnected components are small.

In order to quantify the quality of grid decomposition based on vertex cut set,

we need to recalculate the LODFs for each possible line switching which could be computationally intensive for large scale grids.

4.3.3 Shift Factors & LMPs

The computational overhead pushes us to make another trade off between the computational costs and the preciseness of the metrics measuring the interactions in a grid. Such trade off is achieved by introducing another well-know sensitivity, *power transfer distribution factor* or *PTDF*, which gives the sensitivity of the flow on one line with respect to a power transfer between a pair of buses.

The PTDF, by definition, is essentially the difference between a pair of *shift factors*. In the DC power flow model, the *transmission sensitivity matrix* Ψ , also known as the *injection shift factor matrix*, gives the sensitivities in line flows due to changes in the nodal injections, with the reference bus assumed to ensure the power balance. Suppose Ψ_{i,j_1} denotes the sensitivity in power flowing through line i due to one unit increase in the power injection at bus j_1 and one unit decrease in power injection at the reference bus, i.e.

$$\Psi_{i,j_1} = \frac{\Delta \text{flow in line } i}{\Delta \text{injection at bus } j_1},$$

then the shift factor difference $|\Psi_{i,j_1} - \Psi_{i,j_2}|$ gives the PTDF of power flowing through line i with respect to one unit power transfer between bus j_1 and j_2 .

The network LODFs, mathematically, are equivalent to the post-outage network PTDFs. While the pre- and post-outage PTDFs are rarely equivalent, there usually exists a strong correlation between their values. Therefore, although the estimations of the decomposition quality based on pre-outage PTDFs maybe different from those based on LODFs, such differences are reasonably expected to be small.

Here, we would like to remark that the introduction of PTDF does reduce the computation cost associated with the estimations of decomposition quality, but such com-

putation effort is still relatively small compared with solving the updated DCOPFs. The value of the following PTDF analysis, in fact, is more towards a fundamental understanding of some structural properties of the grid decomposition, thus reducing the computational effort spent on finding the optimal vertex cut sets.

We now need to deal with the most challenging step of the decomposition, i.e. minimizing the interactions (PTDFs) between pseudo biconnected components. Though highly desired, such decomposition quality is usually not achievable by just using vertex cut sets as the cushion zones between pseudo biconnected components, due to the unavoidable strong LODFs between those edges belonging to different pseudo biconnected components but incident to same nodes in the vertex cut sets. Instead of complicating the decomposition by expanding the cushion zones to some sub-graphs containing both vertex cut sets and the associated incident edges, we would like to stick to the vertex cut sets, indicating a necessity to modify the criteria. Rather than struggling with the nominal PTDFs between pseudo biconnected components, our decomposition instead aims to minimizing the potentially “useful” portion of those PTDFs, i.e. the portion associated with congestion effect.

When talking about congestion effect, it is natural to wonder about the *locational marginal price* (LMP). In a lossless DC power flow model, the LMP at a given bus, say bus i , is equal to the sum of the LMP at the reference bus and the congestion cost which can be calculated using the following equation:

$$\lambda_i = \lambda_{ref} - \sum_j (\mu_j \times \Psi_{j,i}) \quad (4.1)$$

where

$$\lambda_i = LMP \text{ at bus } i$$

$$\lambda_{ref} = LMP \text{ at the reference bus}$$

$\mu_j = \text{Shadow price of line constraint } j$

$\Psi_{j,i} = \text{Shift factor for real load at bus } i \text{ on line flow } j.$

The sensitivity analysis of DCOPF model suggests that power transfer between buses with close LMPs usually can't change the generation cost as much as that between buses with significantly different LMPs, and similarly line switches in areas with low range LMPs are typically of little usage in reducing overall generation costs. Therefore, the goal of the partition problem based on vertex cuts can reasonably be to decompose the grid into two sets of sub-grids with one set being of high range LMPs and the other being of low range LMPs.

4.3.4 The Optimality of Vertex Cut Sets

In this section, we will show a set of useful properties of vertex cut sets with respect to the decomposition based on LMPs. The discussion starts with the following definition.

Definition 13 *Suppose there is one line congestion in a transmission network and we are able to control certain number of nodal injections, then the smallest set (i.e. of smallest cardinality) of buses that is able to fully alleviate the given line congestion by changing least amount of nodal power injections is defined as the optimal set of buses for that congested line.*

Remark 12 *The optimal set of buses for a given congested line may not be unique.*

We first show that for a given congestion in one pseudo biconnected component, the optimal set of buses in another pseudo biconnected component must be a subset of the vertex cut set used for grid decomposition. The complete proof involves two lemmas and one proposition.

Lemma 3 *If we are allowed to alter all controllable nodal power injections by arbitrary amount and all uncongested lines have enough line capacity, then the cardinality of the optimal set of buses for a given congested line must be 2, i.e. the optimal set of buses is a bus pair.*

Proof. Shift factors do not change if the injection/withdrawal amount increases for any set of buses. Suppose line i is overloaded by Δ_i units of power and the power injections at bus j_1 and j_2 are controllable. In order to alleviate the congestion of line i , the power injections at bus j_1 and j_2 need to be changed by

$$\Delta_{j_1 \& j_2} = \frac{\Delta_i}{|\Psi_{i,j_1} - \Psi_{i,j_2}|}.$$

Thus the pair of controllable buses with the largest shift factor difference associated with the congested line must be the optimal set of buses for that congested line. \square

Lemma 4 *Suppose line i is connected to bus pair $\{i_1, i_2\}$ and line j is connected to bus pair $\{j_1, j_2\}$ in a connected transmission network, and the reference directions of the power flowing through line i and line j are defined as from bus i_2 to bus i_1 and from bus j_2 to bus j_1 , respectively. Then the shift factor differences $\Psi_{i,j_2} - \Psi_{i,j_1}$ and $\Psi_{j,i_2} - \Psi_{j,i_1}$ must be of the same sign.*

Proof. By keeping applying Kron reduction (described in Ch. 2.4) to the original transmission network (shown in the right side of Fig. 4-9) until all nodes but $\{i_1, i_2, j_1, j_2\}$ are eliminated, we can create a 4-terminal equivalent grid with only four buses $\{i_1, i_2, j_1, j_2\}$ which is shown in the left side of Fig. 4-9. Note that the two red lines in Fig. 4-9 may be of different susceptance but the directions of power flowing these line, P_j and $P_{j'}$, must be the same. So do the two blue lines. Thus we just need to focus our attention on the 4-terminal equivalent grid.

By the equivalence in Table 2.1, we can actually treat the 4-terminal equivalent grid as a 4-terminal resistance network and discuss the problem in a circuit environment. Under the circuit environment, we denote the line resistances of the four black lines in the left side of Fig. 4-9 as α , β , γ and δ , respectively, and suppose there is no current injections and withdrawals in the network except one unit nodal injection at node i_2 and one unit nodal withdrawal at node i_1 . If the direction of red line flow

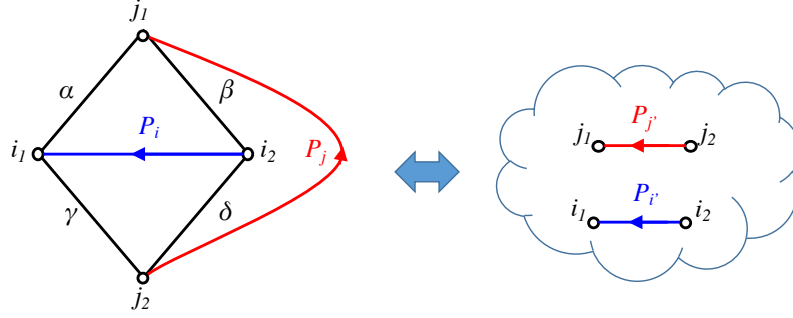


Figure 4-9: The 4-terminal equivalent circuit of the original network.

in the left figure is from node j_2 to node j_1 , we know $\Psi_{j,i_2} - \Psi_{j,i_1} > 0$, indicating

$$\frac{\delta}{\gamma} < \frac{\beta}{\alpha},$$

that we must have $\Psi_{i,j_2} - \Psi_{i,j_1} > 0$. If the direction of red line flow in the left figure is from node j_1 to node j_2 , we know $\Psi_{j,i_2} - \Psi_{j,i_1} < 0$, indicating

$$\frac{\delta}{\gamma} > \frac{\beta}{\alpha},$$

that we must have $\Psi_{i,j_2} - \Psi_{i,j_1} < 0$. □

Proposition 17 *Suppose we use a vertex cut set to decompose a connected transmission network into n ($n \geq 2$) sub-graphs. Assume that we can arbitrarily change the power injection at all buses in the j -th sub-graph to alleviate a given congested line in the i -th sub-graph ($i \neq j$), then one optimal pair of buses must be a subset of the vertex cut set.*

Proof. Although the value of each entry in the injection shift factor matrix varies as the reference bus changes, the PTDF or the difference between a pair of shift factors is independent of the choice of the reference bus. Suppose line i is congested and is connected to bus i_1 and i_2 , and we pick up i_1 as the reference bus and assuming the direction from i_2 to i_1 as the positive power direction, we can get an injection shift factor matrix with all i -th row entries being non-negative.

Suppose there are M buses $\{n_1, \dots, n_M\}$ that are shared by the j -th sub-graph and the rest of the graph. Clearly, $\{n_1, \dots, n_M\}$ is a subset of the vertex cut set. Then in order to prove the proposition, we just need to show that the shift factor differences $\{\Psi_{i,p} - \Psi_{i,n_1}, \dots, \Psi_{i,p} - \Psi_{i,n_M}\}$ cannot be all positive or all negative for any bus p that is owned exclusively by the j -th sub-graph, i.e.

$$\min\{\Psi_{i,n_1}, \dots, \Psi_{i,n_M}\} \leq \Psi_{i,p} \leq \max\{\Psi_{i,n_1}, \dots, \Psi_{i,n_M}\}.$$

We first create two sub-networks to simplify the proof. The first sub-network (shown at the bottom middle of Fig. 4-10) is created from the original network by removing all lines in the j -th sub-graph, and it is called the nearby sub-network. The second sub-network (shown at the top middle of Fig. 4-10) is just the j -th sub-graph, and it is called the remote sub-network. It is easy to see that the two sub-networks share nothing except the buses $\{n_1, \dots, n_M\}$. Buses $\{i_1, i_2\}$ are interior buses of the nearby sub-network, and bus p is interior bus of the remote sub-network.

Then an equivalent sub-network of the remote sub-network can be created by applying Kron reduction to the remote sub-network until all nodes but $\{n_1, \dots, n_M, p\}$ are removed. The equivalent sub-network obtained in this way is a K_{M+1} complete graph as shown at the top right corner of Fig. 4-10. An equivalent network of the original network can then be created by putting together the nearby sub-network and the K_{M+1} equivalent sub-network. The process described above is visualized in Fig. 4-10.

Suppose the reference direction of the power flowing through the line connecting bus p and n_m ($m = 1, \dots, M$) in the equivalent network (shown at the bottom right corner of Fig. 4-10) is defined as from bus p to bus n_m . Then by Lemma 4, we know that the change of power flowing through the line connecting bus p and n_m ($m = 1, \dots, M$) in the equivalent network due to one unit increase in nodal injections

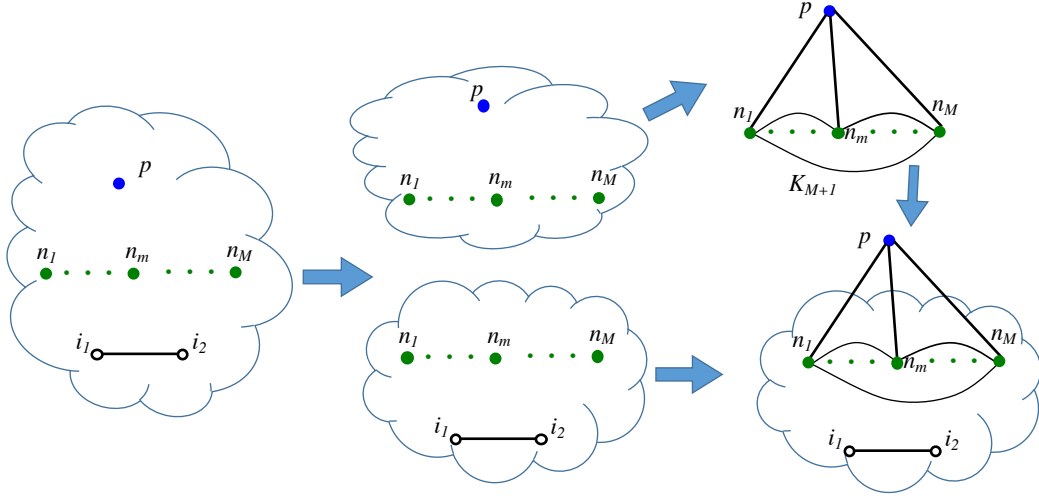


Figure 4.10: The network simplification process.

at bus i_2 and one unit decrease in nodal injections at bus i_1 is of the same sign as that of the shift factor difference $\Psi_{i,p} - \Psi_{i,n_m}$.

Finally, we denote the power flowing through the lines connecting node p and node n_m ($m = 1, \dots, M$) as $\{I_{p,n_1}, \dots, I_{p,n_M}\}$ due to one unit nodal injection at bus i_2 and one unit nodal withdrawal at bus i_1 . By Kirchhoff's current law, we must have

$$\sum_{m=1}^M I_{p,n_m} = 0$$

meaning

$$\sum_{m=1}^M c_m (\Psi_{i,p} - \Psi_{i,n_m}) = 0$$

where $I_{p,n_m} = c_m \Psi_{i,n_m}$ and c_m are some positive coefficient by Lemma 4. Thus $\{\Psi_{i,p} - \Psi_{i,n_1}, \dots, \Psi_{i,p} - \Psi_{i,n_M}\}$ cannot be all positive or all negative. \square

Rather than limiting the discussion to single line congestion, we'd like to know if phenomena similar to Proposition 17 can be found for scenarios with multiple congestions. Things become a little complicated here as the changes of line flows of the congested lines due to the nodal injection regulations may not be all favorable, i.e.

the alleviation of some congestions may come inevitably at the expense of worsening other congestions, requiring all congestions being assigned proper weights to evaluate the overall benefit of the nodal injection regulations. Since our main consideration is to reduce generation cost, the shadow prices of line constraints are naturally used as the weights in the following discussion.

We will show that for multiple given congestions in one pseudo biconnected component, the optimal set of buses in another pseudo biconnected component must also be a subset of the vertex cut sets. The complete proof involves one proposition and two corollaries.

Proposition 18 *Suppose we use a vertex cut set to decompose a connected transmission network into n ($n \geq 2$) sub-graphs. Assume that we can arbitrarily change the power injections at buses in the j -th sub-graph to alter the line flows in the i -th sub-graph ($i \neq j$), then such impact on the i -th sub-graph can be precisely replicated/canceled by regulating the power injections of the buses in the vertex cut set.*

Proof. By the superposition principle in DC power flow model, we just need to prove that all line flows in the i -th sub-graph can always be set to zero if the net power injections at all interior buses of the i -th sub-graph are strictly zero and we can arbitrarily regulate the power injections at the buses in the vertex cut set.

We first show that the reduced nodal susceptance matrix B is positive definite. Since the resistance network is a passive system that consumes energy, and the absorbed power is given by

$$P = v^T G v \quad (4.2)$$

where v is the nodal voltage vector and G is the reduced conductance matrix of the resistance network. It follows that the energy consumption will always be positive only if all eigenvalues of G are positive. Thus, a criterion for passivity is that G be positive definite. Since the DC model of power flow is equivalent to a current driven network as shown in Table 2.1, we know the reduced susceptance matrix B in the DC

power flow model is positive definite, meaning its inverse matrix B^{-1} is also positive definite.

Suppose, in the bus vector, the first l buses are owned exclusively by the i -th sub-graph, the middle m buses are owned by the vertex cut set, and the last $n + 1$ buses containing the reference bus are owned exclusively by other sub-graphs, respectively, we then have the DC power flow equation

$$\theta = B^{-1}p \quad (4.3)$$

where p is the net nodal power injection vector, and θ is the nodal voltage angel vector. Based on the classification of the buses, the reduced voltage angle vector θ can be decomposed into three sub-vectors

$$\theta^T = [\theta_l^T \quad \theta_m^T \quad \theta_n^T],$$

and the positive definite matrix B^{-1} can be decomposed into 9 sub-matrices

$$B^{-1} = \begin{array}{ccc} \begin{array}{ccc} in & at & out \\ \downarrow & \downarrow & \downarrow \end{array} \\ \begin{bmatrix} A_{l \times l} & B_{l \times m} & C_{l \times n} \\ D_{m \times l} & E_{m \times m} & F_{m \times n} \\ G_{n \times l} & H_{n \times m} & I_{n \times n} \end{bmatrix} \begin{array}{l} \leftarrow in \\ \leftarrow at \\ \leftarrow out \end{array} \end{array} \quad (4.4)$$

and we know the sub-matrix $E_{m \times m}$ must have full rank and be positive definite. Thus we have

$$\theta_m = [D_{m \times l} \quad E_{m \times m} \quad F_{m \times n}] p.$$

It follows that we can always set the voltage angles of the vertex cut set θ_m to be equal if we can arbitrarily regulate the power injections of the buses in the vertex cut set.

Next we are going to prove that the line flows in the i -th sub-graph must be all

zero if we set the voltage angles θ_m of the vertex cut set to be equal and if the net power injections at the interior buses of the i -th sub-graph are all zero. If under such scenario there still exist some non-zero line flows in the i -th sub-graph, then we know that the voltage angles of the interior buses of the i -th sub-graph can not be equal, meaning at least one of the interior buses is of non-zero net power injection. This contradicts our assumption. \square

Corollary 10 *Suppose we use a vertex cut set to decompose a connected transmission network into n ($n \geq 2$) connected sub-graphs. We first classify the columns of the injection shift factor matrix into three sets with the first set being associated with the buses owned exclusively by the i -th sub-graph, and the second set being associated with the buses in the vertex cut set, and the third set being associated with the buses owned exclusively by other sub-graphs, and assume their cardinalities are l , m , and n , respectively. We then classify the rows of the injection shift factor matrix into 2 sets with the first set being associated with the lines owned exclusively by the i -th sub-graph, and the second set being associated with the lines owned exclusively by other sub-graphs, and assume their cardinalities are x , and y , respectively. A visualization of the decomposition is shown below.*

$$\Psi = \begin{array}{ccc} & \begin{array}{ccc} in & at & out \\ \downarrow & \downarrow & \downarrow \end{array} & \\ \begin{bmatrix} A_{x \times l} & B_{x \times m} & C_{x \times n} \\ D_{y \times l} & E_{y \times m} & F_{y \times n} \end{bmatrix} & \begin{array}{l} \leftarrow in \\ \leftarrow out \end{array} & \end{array} \quad (4.5)$$

Then the ranks of the sub-matrix

$$[B_{x \times m} \quad C_{x \times n}]$$

and

$$[D_{y \times l} \quad E_{y \times m}]$$

must both be $\leq m$.

Proof: By Proposition 18, we know that the effect of one unit net power injection at a bus in the j -th sub-graph on lines in the i -th sub-graph is a linear combination of the effects of one unit net power injections at the buses in the vertex cut set on

lines in the i -th sub-graph. Thus we know each column of the sub-matrix $[C_{x \times n}]$ is a linear combination of the columns of the sub-matrix $[B_{x \times m}]$, meaning the rank the sub-matrix $[B_{x \times m} \ C_{x \times n}]$ is $\leq m$. Similarly, we can prove that each column of the sub-matrix $[D_{y \times l}]$ is a linear combination of the columns of the sub-matrix $[E_{y \times m}]$, meaning the rank the sub-matrix $[D_{y \times l} \ E_{y \times m}]$ is $\leq m$. \square

Corollary 11 *Suppose we use a vertex cut set to decompose a connected transmission network into n ($n \geq 2$) sub-graphs and all congested lines are contained in the i -th sub-graph (which may be unconnected), then one pair of buses with maximum LMP difference in the j -th sub-graph ($i \neq j$) must be in the vertex cut set.*

Proof: Here, we just need to show that the LMP at any bus in the j -th sub-graph is a convex combination of the LMPs at the buses in the vertex cut set.

Suppose there are m buses in the vertex cut set and their LMPs are $\{\lambda_1, \dots, \lambda_m\}$, and we randomly pick a bus, say bus $j1$ with LMP being λ_{j1} , from the j -th sub-graph. By Proposition 18, we know that the effect of one unit net power injection at a bus $j1$ on lines in the i -th sub-graph is a linear combination of the effect of one unit net power injections at the m buses in the vertex cut set on lines in the i -th sub-graph, and we assume the coefficients of the linear combination are $\{a_1, \dots, a_m\}$, where the power balance equation ensures that $a_1 + a_2 + \dots + a_m = 1$. Thus we have

$$\vec{\Psi}_{i,j1} = [\vec{\Psi}_{i,v_1}, \dots, \vec{\Psi}_{i,v_m}][a_1, \dots, a_m]^T,$$

where $\vec{\Psi}_{i,j1}$ denotes the shift factor vector for read power at bus $j1$ on lines in the i -th sub-graph, $\vec{\Psi}_{i,v_k}$ ($k = 1, \dots, m$) denotes the shift factor vector for read power at the k -th vertex cut set bus on lines in the i -th sub-graph.

Since it assumes all congestions are in the i -th sub-graph, we know the shadow prices for all line constraints that are not in the i -th sub-graph are all zero. Denoting

the shadow price vector for all line constraints in the i -th sub-graph as $[\mu_i]$, we have

$$\begin{aligned}
\lambda_{j1} &= \lambda_{ref} - [\mu_i]^T \vec{\Psi}_{i,j1} \\
&= \lambda_{ref} - [\mu_i]^T [\vec{\Psi}_{i,v_1}, \dots, \vec{\Psi}_{i,v_m}] [a_1, \dots, a_m]^T \\
&= a_1 \lambda_1 + a_2 \lambda_2 + \dots + a_m \lambda_m
\end{aligned} \tag{4.6}$$

Next we will show that $a_i \geq 0$ ($i = 1, \dots, m$), i.e. to cancel the effect of one unit net power injection at bus $j1$ on lines in the i -th sub-graph requires a non-negative net power withdrawn at each bus in the vertex cut set. Suppose we only inject and withdraw power at bus $j1$ (which has one unit net power injection) and the buses in the vertex cut set, and their effects on the i -th sub-graph precisely offset each other. Then the bus with the lowest voltage angle must be one of the buses with positive net power withdrawn (or negative net power injection) and its voltage angle must be strictly lower than any bus with positive net power injection. Apparently, the bus with lowest voltage angle must be in the vertex cut set. If one of the buses in the vertex cut set has positive net power injection, meaning its voltage angle is different from the lowest nodal voltage angle, then there exists a nodal voltage angle difference in the vertex cut set. In such case, the absorbed power in the i -th sub-graph

$$P_i = [\theta_i^T \ \theta_m^T] B_i [\theta_i^T \ \theta_m^T]^T$$

must be positive where θ_i is the voltage angle vector of all interior buses in the i -th sub-graph, θ_m is the voltage angle vector of all bus in the vertex cut set and B_i is the reduced susceptance matrix of the i -th sub-graph. This means some line power flows in the i -th sub-graph must be non-zero, indicating a contradiction to the assumption that the effects of power injections/withdrawals at bus $j1$ and at the buses in the vertex cut set on the i -th sub-graph precisely offset each other. \square

Remark 13 *Corollary 11 points out an useful property of vertex cut set in the trad-*

ing of power or financial transmission rights (FTRs). Essentially, the main task in power trading is to find those pairs of buses between which the LMP differences are significant. If a vertex cut set can decompose the grid such that all congestions are isolated to one or several sub-grids, then the range of the LMPs of buses in the vertex cut that form the boundary of the congested sub-grid(s) will dominate the LMP range of all buses in the non-congested sub-grids. Loosely speaking, the closer the vertex cut gets to the congestions, the higher trading values of the buses in the vertex cut set. Or in other words, if the congested sub-grid(s) defined by the first vertex cut set is a subset of the sub-grid(s) defined by the second vertex cut set, then the buses in the first vertex cut must be of higher or at least equal trading value than that in the second one, suggesting an arbitrage opportunity if violates.

4.3.5 Grid Decomposition Heuristic

This section presents a general algorithm structure for grid decomposition heuristics. The objective of the algorithm is to eliminating the portion(s) of grid with relatively small range of LMPs from the consideration of topology control with little computational effort. The algorithm is specified in Fig. 4-11. This simple algorithm structure first solves an OPF and, given the OPF results, if the OPF is feasible, finds an appropriate vertex cut set to decompose the grid into two parts: one with relatively high range of LMPs and the other with relatively low range of LMPs.

The initial vertex cut set that includes the ending buses of all congested lines forms the boundary of the smallest sub-grid containing all congestions. The algorithm then calculate the LMP absolute deviation for each bus in the initial vertex cut set and “push out” the initial vertex cut from the bus with the largest LMP absolute deviation by swapping out this bus (and therefore the bus becomes an interior bus of the congested sub-grid) and then bringing its neighboring buses into the vertex cut set.

A pre-set LMP range threshold is the characterizing element for the stopping criteria which determine the number of iterations applied, and can include a number of

conditions. The algorithm terminates if the range of the LMP of the vertex cut set falls below the pre-set threshold or if all buses have been brought into the congested sub-grid. Additionally, the algorithm may have a pre-set maximum number of iterations.

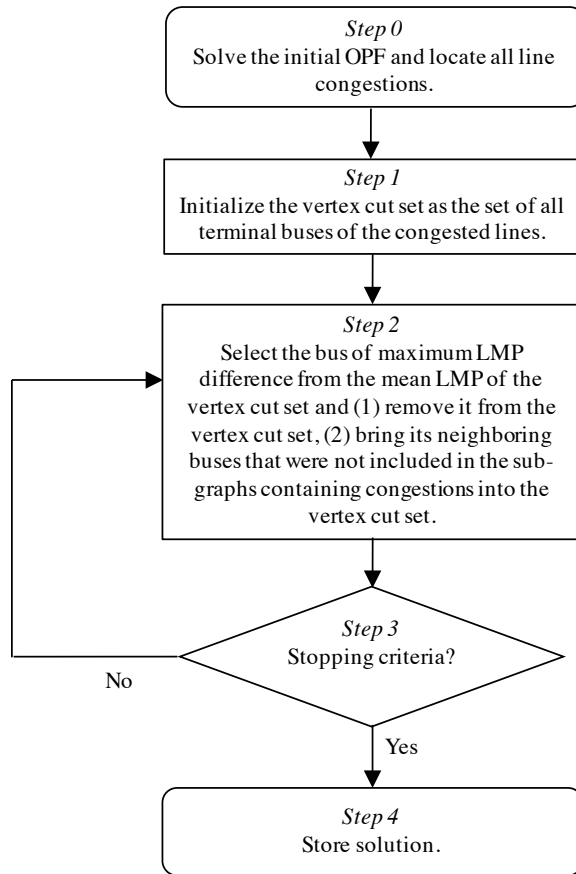


Figure 4-11: Flow chart describing general algorithm structure of grid decomposition based on vertex cut set.

4.3.6 Simulation Results

To test the validity of the grid decomposition based on vertex cut set, a new topology control heuristic is proposed and tested on the IEEE 118-bus test systems introduced in Ch. 4.2. The so called Local Greedy Heuristic is the same as the Standard Greedy Heuristic shown in Fig. 4-7 except that the switchable lines are limited to the neighboring area of the congested line, i.e the congested sub-grid obtained by the grid

decomposition algorithm shown in Fig. 4.11.

Simulation Results and Analysis

To generate the test scenarios for the heuristics, a fixed load is maintained and we perform a Monte Carlo simulation where the generator costs are randomly varied. The sample size used for the Monte Carlo simulation is 50. For the Local Greedy Heuristic based on vertex cut set, the LMP range threshold is set to be 10% of the maximum LMP difference across the grid.

As always, the percent savings rather than the dollar value are the focus of the comparison. The two heuristics are implemented in Matlab, using MATPOWER (Zimmerman et al., 2011) as the DCOPF solver. The performance comparison between the two heuristic is detailed in Table 4.2.

Table 4.2: Performance comparison 2.

heuristic	saving/MAS	lines disconnected	mean effort
Local Greedy	0.653 ± 0.055	12.910 ± 4.312	0.216
Standard Greedy	0.672 ± 0.051	10.18 ± 3.98	1

In the worst case, the two heuristics are of the same level computational complexity if the grid decomposition algorithm brings all buses into the congested sub-grid. In general, the Standard Greedy Heuristic, however, costs much more computational effort especially for a large scale networks. Though the computational costs of the two heuristic differ by almost five times, their attainable savings are quite close, showing the promise in applying grid decomposition to topology control.

4.4 Summary

In spite of the seemingly promising simulation results of the heuristic approaches pursued by the research community and a certain level of proven predictability of topology control, satisfactory grid-scale solutions are ever-elusive. The cautionary

tales associated with our non-commutativity, non-monotonicity, and non-consistency paradoxes leads us to wonder whether other paradox – possibly more problematic – may associated with with as yet untried heuristics. While optimality for NP-hard problems is no obtained, our simulation results based on a set of iterative heuristics nevertheless offer some justification that, with similar searching space, greedy heuristic has a better chance in reducing generation cost and enforcing connectivity. We then focus on further simplifying the problem by developing fast partition algorithms for the decomposition approach. Our approach based on vertex cut set demonstrate that it is indeed possible to design algorithms that isolate a large portion of the congestion effects to a relatively small part of the network.

Chapter 5

Conclusions

5.1 Contributions

Because it uses existing assets to achieve important and timely goals: increased grid flexibility and economic efficiency with no reliability degradation, transmission topology control is an essential part of grid operations.

In Chapter 2, a new electric concept, called *Kirchhoff-Braess Paradox*, has been introduced and proposed for explaining the origin of topology control. Derived from the Braess paradox in transportation network, Kirchhoff-Braess Paradox shows that a grid with fewer transmission lines might be of higher economic efficiency. Based on the well established equivalent relationship between the DC OPF model of transmission network and the current-controlled circuit, the impact of topology control is studied for both the circuit model and the DC OPF model. It is shown that changing the network topology by adding/removing a small link can lead to relatively large power redistribution across the whole network. In particular, we define the concept of *loss cost of a link* (LCL) for the circuit model which is the ratio of the I^2R losses of a circuit after/before adding or removing a link. The widespread influence of topology control is then studied based on the well known Wheatstone bridge and Kron reduction method. The comprehensive analysis of the challenges associated with topology control ends with the proof of the NP-hardness of the switching problem by using the subset sum problem for the reduction.

Chapter 3 focuses on the study of the circuit model with the hope of providing

possible foundations for problem simplification and grid decomposition. The analysis of the loss cost of the link starts from the current-controlled circuits to the voltage-controlled circuits and finally to the mixed-source circuits of arbitrary size. It has been shown that loss cost of a link is frequently greater than one in current-controlled circuit, and this has been studied in detail for simple small networks and in considerable generality for large scale networks. While the results in voltage controlled circuit have qualitative characteristics that are similar to the current-controlled case, there is more subtlety and even a degree of indeterminacy in the mixed-source circuit. It is shown that the effect of removing an edge from a mixed-source circuit can be perfectly decomposed into two sub-effects in its voltage-controlled sub-circuit and current-controlled sub-circuit, respectively. Meanwhile, we give a simple method to calculate the change of total I^2R loss in an arbitrary mixed-source circuit based on the reduced equivalent circuit. Our discussion about the four mathematically equivalent approaches to calculate the total I^2R loss of a mixed-source circuit also points out a way to convert a certain type of constrained linear programming formulation to an unconstrained non-linear programming problem.

The work presented in Chapter 4 commits to integrate simulation results with theoretical results to provide guidance for developing topology control heuristics. Being typically formulated as a mixed integer programming problem, transmission topology control is known to be computationally intractable. By means of some 3-bus microgrids, we show that within a reasonably large class of “greedy” heuristics, none can be found that perform better than the others across all grid topologies, showing the challenges in designing and justifying appropriate heuristics. Our simulations on IEEE 118-bus systems, however, shows that on average 15% additional savings can be achieved through finding the locally optimal switches for an iterative heuristic. Statistical results show that, among all iterative methods, the locally optimal switches

at each iteration have a better change in simultaneously reducing generation cost and preserving reliability. Finally, we propose a fast grid decomposition partition algorithm to overcome the computational complexity of the greedy heuristic while at the same time preserving the superior performance, and its efficiency is confirmed by the simulation results.

5.2 Future Work

Modeling The DC optimal power flow model is consistently used in this thesis. Since the optimal power flow formulation is not an AC optimal power flow, the proposed solution must also pass an AC feasibility test. As a result, the conclusion that the solution is feasible only holds for a DCOPF problem and is not guaranteed for the ACOPF problem, suggesting the potential risks in applying the solution to real grids. Moreover, the location marginal price is traditionally calculated as the sum of system marginal price, congestion component and the marginal loss component. Because the grid decomposition based on vertex cut set proposed in Chapter 4 assumes a lossless grid, the optimal vertex cut set obtained may not dominate the uncongested subgrid in the sense of trading value after the marginal loss components are added back to LMPs. The discrepancy between the ACOPF and DCOPF together with the difference between traditional LMP and lossless LMP, though usually not significant, points out the need for developing more robust topology control algorithms.

Machine Learning The performance of common heuristics of line switching, although time-efficient, may be seriously degraded by the non-commutativity and non-monotonicity property of the topology control problem, and therefore makes a one-size-fits-all heuristic impossible. Future work may focus on handling the line switching problem with a dictionary approach. In such an approach, a dictionary for scenarios of

interest and for common constraints and cost functions is maintained. The algorithm searches the dictionary and finds the closest recorded scenario to current issue based on certain closeness metric. The closest element in the dictionary is then modified to find a new solution that satisfies the constraints of current issue while attempting to achieve a lower generation cost. The new scenario will also be processed by an off-line algorithm engine to figure out the optimal approach which will then be added to the dictionary for future planning. The dictionary can also learn from the “past experience” to reduce the search complexity.

Collision with FTR Markets Financial Transmission Rights (FTRs) are used to hedge congestion risk and are financed by congestion rents collected by ISOs. Since transmission topology control may greatly reshape the LMP profile of the grid, it may undermine the prevailing market mechanisms and cause revenue inadequacy in the FTR market (Hedman et al., 2011a). The potential collision with FTR markets is one of the main obstacles that limits the full utilization of topology control today. As a result, the optimal tradeoff between the economic efficiency and the market surplus (transmission rent) may well be a research topic for future study.

Appendix A

Proof of Remark 1

Remark 1. *For a connected power network, if the optimal power flow solution that minimizes the generation cost does not result in congestion, then the solution is independent of the line susceptances no matter what topological structure the network has.*

Proof. We assume without loss of generality that there are N buses in the power network and the power phase angle at the N -th bus is zero. Then the nodal power injections are related to the power phase angle by

$$\begin{pmatrix} P_1 \\ P_2 \\ \vdots \\ P_{N-1} \end{pmatrix} = B_r \begin{pmatrix} \theta_1 \\ \theta_2 \\ \vdots \\ \theta_{N-1} \end{pmatrix} \quad (\text{A.1})$$

where

$$B_r = \begin{pmatrix} -b_1 & b_{1,2} & \cdots & b_{1,N-1} \\ b_{1,2} & -b_2 & \cdots & b_{2,N-1} \\ \vdots & \vdots & \ddots & \vdots \\ b_{1,N-1} & b_{2,N-1} & \cdots & -b_{N-1} \end{pmatrix} \quad (\text{A.2})$$

is the reduced conductance matrix, $b_{i,j}$ ($i, j = 1, \dots, N$, and $i \neq j$) is the conductance between the i -th bus and the j -th bus and $b_{i,j} = 0$ if there is no connection between i and j , and

$$b_i = \sum_{j=1}^{i-1} b_{i,j} + \sum_{j=i+1}^N b_{i,j} \quad (i = 1, \dots, N-1). \quad (\text{A.3})$$

Next we will show that B_r is always nonsingular if the power network is connected.

Assuming that there exists one non-zero solution $\vartheta_r = (\vartheta_1, \vartheta_2, \dots, \vartheta_{N-1})$ such that $B_r \vartheta_r = 0$. Let $\vartheta = (\vartheta_1, \vartheta_2, \dots, \vartheta_{N-1}, 0)$ and B be the conductance matrix, then we must have $B\vartheta = 0$. This, however, is proved to be impossible. We assume that M ($1 \leq M < N$) elements of ϑ are equal to the maximum of ϑ . Since the network is connected, then at least one of the buses with the maximal phase angle, say the i -th bus, must be connected to one or more buses with lower phase angles. Then the power injection at the i -th bus must be nonzero. This contradicts the assumption $B\vartheta = 0$.

Using the invertible relationship (A.2), we may rewrite the objective function as $\mathbf{C}(P_1, \dots, P_N) = \hat{\mathbf{C}}(\theta_1, \dots, \theta_N)$ whose optimal solution must be the same as what would have been obtained by minimizing $\mathbf{C}(P_1, \dots, P_N)$ directly. \square

References

- Arghandeh, R., Gahr, M., von Meier, A., Cavraro, G., Ruh, M., and Andersson, G. (2015). Topology detection in microgrids with micro-synchrophasors. In *2015 IEEE Power & Energy Society General Meeting*, pages 1–5. IEEE.
- Arya, L., Choube, S., and Kothari, D. (2000). Line switching for alleviating overloads under line outage condition taking bus voltage limits into account. *International Journal of Electrical Power & Energy Systems*, 22(3):213–221.
- Bacher, R. and Glavitsch, H. (1986). Network topology optimization with security constraints. *IEEE Transactions on Power Systems*, 1(4):103–111.
- Bacher, R. and Glavitsch, H. (1988). Loss reduction by network switching. *IEEE Transactions on Power Systems*, 3(2):447–454.
- Baillieul, J., Zhang, B., and Wang, S. (2015). The Kirchhoff-Braess paradox and its implications for smart microgrids. In *2015 IEEE 54th Annual Conference on Decision and Control*, pages 6556–6563. IEEE.
- Bakirtzis, A. and Meliopoulos, A. S. (1987). Incorporation of switching operations in power system corrective control computations. *IEEE Transactions on Power Systems*, 2(3):669–675.
- Basak, P., Chowdhury, S., nee Dey, S. H., and Chowdhury, S. (2012). A literature review on integration of distributed energy resources in the perspective of control, protection and stability of microgrid. *Renewable and Sustainable Energy Reviews*, 16(8):5545–5556.
- Bean, N., Kelly, F., and Taylor, P. (1997). Braess’s paradox in a loss network. *Journal of Applied Probability*, 34(1):155–159.
- Behzad, M. and Chartrand, G. (1972). *Introduction to the Theory of Graphs*. Allyn and Bacon.
- Bertram, T. J., Demaree, K. D., and Dangelmaier, L. C. (1990). An integrated package for real-time security enhancement. *IEEE Transactions on Power Systems*, 5(2):592–600.

- Bijwe, P., Kothari, D., and Arya, L. (1993). Alleviation of line overloads and voltage violations by corrective rescheduling. *IEEE Proceedings C (Generation, Transmission and Distribution)*, 140(4):249–255.
- Blumsack, S., Lave, L. B., and Ilić, M. (2007). A quantitative analysis of the relationship between congestion and reliability in electric power networks. *The Energy Journal*, pages 73–100.
- Calvert, B. and Keady, G. (1993). Braess’s paradox and power-law nonlinearities in networks. *The ANZIAM Journal*, 35(1):1–22.
- Capitanescu, F., Ramos, J. M., Panciatici, P., Kirschen, D., Marcolini, A. M., Platbrood, L., and Wehenkel, L. (2011). State-of-the-art, challenges, and future trends in security constrained optimal power flow. *Electric Power Systems Research*, 81(8):1731–1741.
- Chowdhury, S., Chowdhury, S., and Crossley, P. (2009). Islanding protection of active distribution networks with renewable distributed generators: A comprehensive survey. *Electric Power Systems Research*, 79(6):984–992.
- Cohen, J. E. and Horowitz, P. (1991). Paradoxical behaviour of mechanical and electrical networks. *Nature*, 352(6337):699–701.
- Dobson, I. (2012). Voltages across an area of a network. *IEEE Transactions on Power Systems*, 27(2):993–1002.
- Feng, Z., Ajarapu, V., and Maratukulam, D. J. (2000). A comprehensive approach for preventive and corrective control to mitigate voltage collapse. *IEEE Transactions on Power Systems*, 15(2):791–797.
- Fincke, U. and Pohst, M. (1985). Improved methods for calculating vectors of short length in a lattice, including a complexity analysis. *Mathematics of computation*, 44(170):463–471.
- Fisher, E. B., O’Neill, R. P., and Ferris, M. C. (2008). Optimal transmission switching. *IEEE Transactions on Power Systems*, 23(3):1346–1355.
- Fliscounakis, S., Zaoui, F., Houry, M.-P., and Milin, E. (2009). Loss reduction as a mixed integer optimization problem. In *2009 IEEE Bucharest PowerTech*, pages 1–6. IEEE.
- Fliscounakis, S., Zaoui, F., Siméant, G., and Gonzalez, R. (2007). Topology influence on loss reduction as a mixed integer linear programming problem. In *2007 IEEE Lausanne PowerTech*, pages 1987–1990. IEEE.
- Fuller, J. D., Ramasra, R., and Cha, A. (2012). Fast heuristics for transmission-line switching. *IEEE Transactions on Power Systems*, 27(3):1377–1386.

- Glavitsch, H. (1993). Power system security enhanced by post-contingency switching and rescheduling. In *1993 IEEE Athens PowerTech*, pages 16–21. IEEE.
- Gómez-Expósito, A., Conejo, A. J., and Cañizares, C. (2016). *Electric energy systems: analysis and operation*. CRC Press.
- Granelli, G., Montagna, M., Zanellini, F., Bresesti, P., Vailati, R., and Innorta, M. (2006). Optimal network reconfiguration for congestion management by deterministic and genetic algorithms. *Electric power systems research*, 76(6-7):549–556.
- Hedman, K. W., O’Neill, R. P., Fisher, E. B., and Oren, S. S. (2008). Optimal transmission switchingsensitivity analysis and extensions. *IEEE Transactions on Power Systems*, 23(3):1469–1479.
- Hedman, K. W., O’Neill, R. P., Fisher, E. B., and Oren, S. S. (2009). Optimal transmission switching with contingency analysis. *IEEE Transactions on Power Systems*, 24(3):1577–1586.
- Hedman, K. W., Oren, S. S., and O’Neill, R. P. (2011a). Revenue adequacy constrained optimal transmission switching. In *2011 44th Hawaii International Conference on System Sciences (HICSS)*, pages 1–10. IEEE.
- Hedman, K. W., Oren, S. S., and O’Neill, R. P. (2011b). A review of transmission switching and network topology optimization. In *2011 IEEE Power and Energy Society General Meeting*, pages 1–7. IEEE.
- Hsu, Y.-Y., Ho, K.-L., Liang, C.-C., Lai, T.-S., Chen, K.-K., and Chang, B.-S. (1992). Voltage control using a combined integer linear programming and rule-based approach. *IEEE Transactions on Power Systems*, 7(2):744–752.
- Kammerer, R., Frömel, B., Obermaisser, R., and Milbredt, P. (2013). Composability and compositionality in CAN-based automotive systems based on bus and star topologies. In *2013 11th IEEE International Conference on Industrial Informatics (INDIN)*, pages 116–122. IEEE.
- Kellerer, H., Pferschy, U., and Pisinger, D. (2004). Introduction to NP-completeness of knapsack problems. In *Knapsack problems*, pages 483–493. Springer.
- Koglin, H. and Muller, H. (1980). Overload reduction through corrective switching actions. In *1980 IEEE International Conference on Power System Monitoring and Control*, pages 159–164. IEEE.
- Korilis, Y. A., Lazar, A. A., and Orda, A. (1999). Avoiding the Braess paradox in non-cooperative networks. *Journal of Applied Probability*, 36(1):211–222.
- Liebchen, C. and Rizzi, R. (2007). Classes of cycle bases. *Discrete Applied Mathematics*, 155(3):337–355.

- Lobato, E., Echavarren, F., Rouco, L., Navarrete, M., Casanova, R., and Lopez, G. (2003). A mixed-integer LP based network topology optimization algorithm for overload alleviation. In *2003 IEEE Bologna PowerTech*, pages 5–9. IEEE.
- Mazi, A., Wollenberg, B., and Hesse, M. (1986). Corrective control of power system flows by line and bus-bar switching. *IEEE Transactions on Power Systems*, 1(3):258–264.
- Medina, J., Muller, N., and Roytelman, I. (2010). Demand response and distribution grid operations: Opportunities and challenges. *IEEE Transactions on Smart Grid*, 1(2):193–198.
- Murty, K. G. and Kabadi, S. N. (1987). Some NP-complete problems in quadratic and nonlinear programming. *Mathematical programming*, 39(2):117–129.
- Papadimitriou, C. H. and Steiglitz, K. (1998). *Combinatorial optimization: algorithms and complexity*. Courier Corporation.
- Rolim, J. G. and Machado, L. J. B. (1999). A study of the use of corrective switching in transmission systems. *IEEE Transactions on Power Systems*, 14(1):336–341.
- Rossier, C. and Germond, A. (1983). Network topology optimization for power system security enhancement. In *1983 CIGRE-IFAC Symposium on Control Application for Power System Security*, paper 206-01.
- Ruiz, P., Goldis, E., Rudkevich, A. M., Caramanis, M. C., Philbrick, C. R., and Foster, J. M. (2017). Security-constrained transmission topology control MILP formulation using sensitivity factors. *IEEE Transactions on Power Systems*, 32(2):1597–1605.
- Ruiz, P. A., Foster, J. M., Rudkevich, A., and Caramanis, M. C. (2011). On fast transmission topology control heuristics. In *2011 IEEE Power and Energy Society General Meeting*, pages 1–8. IEEE.
- Ruiz, P. A., Foster, J. M., Rudkevich, A., and Caramanis, M. C. (2012a). Tractable transmission topology control using sensitivity analysis. *IEEE Transactions on Power Systems*, 27(3):1550–1559.
- Ruiz, P. A., Rudkevich, A., Caramanis, M. C., Goldis, E., Ntakou, E., and Philbrick, C. R. (2012b). Reduced MIP formulation for transmission topology control. In *2012 50th Annual Conference on Communication, Control, and Computing (Allerton)*, pages 1073–1079. IEEE.
- Sahraei-Ardakani, M., Li, X., Balasubramanian, P., Hedman, K., and Abdi-Khorsand, M. (2016). Real-time contingency analysis with transmission switching on real power system data. *IEEE Transactions on Power Systems*, 31(3):2501–2502.

- Schnyder, G. and Glavitsch, H. (1988). Integrated security control using an optimal power flow and switching concepts. *IEEE Transactions on Power Systems*, 3(2):782–790.
- Schnyder, G. and Glavitsch, H. (1990). Security enhancement using an optimal switching power flow. *IEEE Transactions on Power Systems*, 5(2):674–681.
- Shao, W. and Vittal, V. (2005). Corrective switching algorithm for relieving overloads and voltage violations. *IEEE Transactions on Power Systems*, 20(4):1877–1885.
- Steinberg, R. and Zangwill, W. I. (1983). The prevalence of Braess’ paradox. *Transportation Science*, 17(3):301–318.
- Vajjhala, S. P. and Fischbeck, P. S. (2007). Quantifying siting difficulty: A case study of US transmission line siting. *Energy Policy*, 35(1):650–671.
- Vartabedian, R. (2012). Rise in renewable energy will require more use of fossil fuels. *Delta*, 7:54–57.
- Wang, S. and Baillieul, J. (2016). Kirchhoff-Braess phenomena in DC electric networks. In *2016 IEEE 55th Conference on Decision and Control*, pages 3286–3293. IEEE.
- Wang, S. and Baillieul, J. (2017). A novel decomposition for control of DC circuits and grid models with heterogeneous energy sources. *arXiv:1709.07569*.
- Wrubel, J., Rapcienski, P., Lee, K., Gisin, B., and Woodzell, G. (1995). Practical experience with corrective switching algorithm for on-line applications. In *1995 IEEE Power Industry Computer Application Conference*, pages 365–371. IEEE.
- Zhang, B. and Baillieul, J. (2016). Control and communication protocols based on packetized direct load control in smart building microgrids. *Proceedings of the IEEE*, 104(4):837–857.
- Zhang, B., Caramanis, M. C., and Baillieul, J. (2014). Optimal provision of regulation service reserves under dynamic energy service preferences. *arXiv:1403.4828*.
- Zimmerman, R. D., Murillo-Sánchez, C. E., and Thomas, R. J. (2011). Matpower: Steady-state operations, planning, and analysis tools for power systems research and education. *IEEE Transactions on power systems*, 26(1):12–19.

CURRICULUM VITAE

